



THESIS

2  
2008

LIBRARY  
Michigan State  
University

This is to certify that the  
dissertation entitled

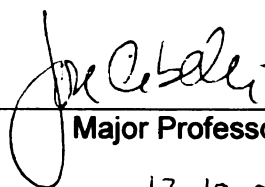
**PLCZ mRNA INJECTION: A NATURAL APPROACH TO  
ACTIVATE BOVINE SOMATIC CELL NUCLEAR TRANSFER  
EMBRYOS**

presented by

Pablo Juan Ross

has been accepted towards fulfillment  
of the requirements for the

Ph.D. degree in Animal Science



Major Professor's Signature

12.10.07

Date

*MSU is an affirmative-action, equal-opportunity employer*

**PLACE IN RETURN BOX** to remove this checkout from your record.  
**TO AVOID FINES** return on or before date due.  
**MAY BE RECALLED** with earlier due date if requested.

DATE DUE	DATE DUE	DATE DUE

**PLCZ mRNA INJECTION: A NATURAL APPROACH TO ACTIVATE BOVINE  
SOMATIC CELL NUCLEAR TRANSFER EMBRYOS**

**By**

**Pablo Juan Ross**

**A DISSERTATION**

**Submitted to  
Michigan State University  
in partial fulfillment of the requirements  
for the degree of**

**DOCTOR OF PHILOSOPHY**

**Department of Animal Science**

**2007**



## **ABSTRACT**

### **PLCZ mRNA INJECTION: A NATURAL APPROACH TO ACTIVATE BOVINE SOMATIC CELL NUCLEAR TRANSFER EMBRYOS**

**By**

**Pablo Juan Ross**

Somatic cell nuclear transfer (SCNT), whereby a somatic cell nucleus is transplanted into an enucleated oocyte, has been successfully used in various mammalian species to derive live cloned offspring. A broad variety of applications that range from agriculture to biomedicine have been envisioned for SCNT; however, its efficiency remains very low. Activation of embryonic development is triggered by the sperm upon fertilization and it involves repetitive increases in intracellular free- $\text{Ca}^{2+}$  ( $[\text{Ca}^{2+}]_i$ ). Upon fusion with the oocyte, the sperm delivers a factor (phospholipase C-zeta; PLCZ) which induces long-lasting  $[\text{Ca}^{2+}]_i$  oscillations. During SCNT, the activation stimulus must be provided artificially. In cattle SCNT, the most common activation protocols induce a single  $[\text{Ca}^{2+}]_i$  increase and treatment with protein synthesis or kinase inhibitors, which may have detrimental consequences for embryonic development. The hypothesis that an activation protocol that closely mimics the mechanism of activation initiated by the sperm has the potential to improve nuclear reprogramming after SCNT was tested. The activity of bovine- and mouse-derived PLCZ cRNA on bovine oocytes was characterized. Mouse and bovine PLCZ activated development of bovine oocytes in a concentration dependent fashion. At its most effective concentrations, PLCZ induced parthenogenetic development at rates

similar to those observed after using common chemical activation protocols. Moreover, PLCZ cRNA injection induced sperm-like  $[Ca^{2+}]_i$  oscillations and IP<sub>3</sub>R downregulation. Then PLCZ was implemented as an activation agent for SCNT embryos. SCNT embryos generated by PLCZ cRNA injection were compared with those produced by standard chemical activation protocols (Ionomycin/DMAP and Ionomycin/CHX), and to IVF-derived embryos as controls. PLCZ cRNA injection induced  $[Ca^{2+}]_i$  oscillations similar to those observed after fertilization and induced blastocyst development at rates similar to IVF embryos. Gene expression analysis at 8-cell and blastocyst stages revealed that some abnormalities observed in SCNT embryos activated by chemical means were not found in SCNT embryos activated using PLCZ cRNA injection. Finally, chromatin modifications were analyzed at the blastocyst stage. The levels of trimethylated lysine 27 at histone H3 were higher in bovine SCNT embryos activated using CHX and DMAP than in those activated using PLCZ or derived from IVF. In summary, this dissertation shows that PLCZ cRNA injection can; 1) induce sperm-like calcium oscillations, 2) be effectively used to trigger the initiation of development in SCNT embryos, and 3) produce cloned embryos that have more similar characteristics to their IVF counterpart than chemically activated cloned embryos.

**To Laura**

## **ACKNOWLEDGEMENTS**

I would like to thank Jose Cibelli for his guidance and support during my years as graduate student. I am deeply grateful for the opportunity he gave me to fulfill my dream of completing my PhD.

I would also like to extend my thanks to the members of my committee; George Smith, Richard Pursley, Guilherme Rosa, William Spielman, and Rafael Fissore. Special thanks go to Rafael Fissore for allowing me to perform experiments at his lab, for providing us with PLCZ cRNA, and for his valuable feedback and suggestions.

To all the members of the CRL lab, thanks for your continuous support. I would like to especially thank Amy Lager, Zeki Beyhan, Akiko Yabuuchi, Kai Wang, Kerriane Cunniff, German Kaiser, and Ricardo Felmer for their help with nuclear transfer experiments. I would like to recognize Anil Bettgowda for his help and training on gene expression analysis and Sook-Young Yoon for her help with oocyte injections and calcium measurements at UMass. I also recognize Ramon Rodriguez's contribution and assistance with immunofluorescence analysis, Neli Ragina for her help with RT-PCR, and Juan Pedro Steibel for his assistance with statistical analysis. To Steve Suhr, Jason Knott, and Angela Busta; thank you for your input on the manuscript. I would also like to recognize the efforts of all the undergraduate students who collected ovaries for my experiments. To Theresa Doerr, big thanks for your

help and support, and for always being there to address my last minute urgent requests.

Also, I would like to thank my “old” friends as well as the many “new” friends that I have made during my time here at MSU for their support. Special thanks to my fishing buddies, hunting partners and beer-brewing friends for all the nice moments we shared.

My sincerest appreciation goes to my family. I cannot thank my parents, sisters, and brothers enough who have encouraged me along the way and have never doubted the ambitions that I have set forth for myself. Also to my father- and sisters-in-law, thank you for your support. Most of all, to my wife Laura, who has endured the burdens and tribulations of a graduate student’s wife, while giving me the most precious thing in my life, my daughter, Luisa. I love you with all my heart.

## TABLES OF CONTENTS

LIST OF TABLES.....	x
LIST OF FIGURES.....	xi
ABBREVIATIONS.....	xv
<b>CHAPTER 1</b> .....	<b>1</b>
INTRODUCTION AND LITERATURE REVIEW.....	1
Introduction.....	2
Cloning by somatic cell nuclear transfer.....	7
Applications of SCNT: Why clone mammals?.....	9
Abnormalities associated with somatic cell nuclear transfer.....	10
Epigenetic modifications and nuclear reprogramming after fertilization and SCNT.....	12
Gene expression in cloned preimplantation embryos.....	14
Paternal contribution to the embryo: what is missing in SCNT?.....	16
Oocyte activation.....	18
Role of Ca <sup>2+</sup> during oocyte activation and early development.....	19
Phosphoinositide (PI) signaling pathway and oocyte activation.....	25
PLCZ: the putative sperm factor.....	27
Oocyte activation after SCNT - the artificial way.....	30
<b>CHAPTER 2</b> .....	<b>36</b>
FULL DEVELOPMENTAL POTENTIAL OF MAMMALIAN PREIMPLANTATION EMBRYOS IS MAINTAINED AFTER IMAGING USING A SPINNING-DISK CONFOCAL MICROSCOPE.....	37
Abstract .....	38
Introduction.....	39
Materials and methods.....	42
Chemicals.....	42
Animals and embryos.....	42
Mitochondria imaging.....	44
Measurement of reactive oxygen species.....	44
Caspase 3 activity assay.....	45
Pancaspase activity assay.....	46
Comet assay.....	46

Somatic cell nuclear transfer.....	47
Plasmid vector construction.....	48
Differential staining for inner cell mass and trophectoderm cell number determination of bovine blastocysts .....	49
Confocal imaging for ICM and TE cell number determination of bovine blastocysts.....	49
Statistical analysis.....	50
Results .....	51
Viability of preimplantation embryos following confocal imaging.....	51
Live visualization and quantification of nuclei in bovine embryos.....	59
Discussion.....	61
Acknowledgments.....	66
Competing interest statement.....	67
<b>CHAPTER 3.....</b>	<b>72</b>
<b>PARTHENOGENETIC ACTIVATION OF BOVINE OOCYTES USING BOVINE AND MURINE PHOSPHOLIPASE C ZETA.....</b>	<b>73</b>
Abstract.....	74
Background.....	75
Results.....	78
Validation of the intracytoplasmic injection technique for bovine oocytes.....	78
Activation and parthenogenetic development of bovine oocytes injected with PLCZ cRNA.....	81
Injection of PLCZ cRNAs induces $[Ca^{2+}]_i$ oscillations and IP <sub>3</sub> R-1 down regulation in bovine oocytes.....	85
PLCZ cRNA-activated bovine embryos exhibit high degree of normal chromosomal composition.....	92
Discussion.....	95
PLCZ and parthenogenetic development.....	96
PLCZ and $[Ca^{2+}]_i$ oscillations in bovine oocytes.....	98
Conclusions.....	101
Methods.....	101
Oocyte collection and maturation.....	102
PLCZ complementary RNA (cRNA) preparation.....	102
cRNA microinjection.....	103
Intracellular calcium monitoring.....	104
Western blot of IP <sub>3</sub> R-1.....	104
In vitro fertilization.....	105
Parthenogenetic activation.....	106
Chromosomal analysis.....	106
Statistical analysis.....	107

Acknowledgments.....	107
<b>CHAPTER 4.....</b>	<b>109</b>
ACTIVATION OF BOVINE SOMATIC CELL NUCLEAR TRANSFER EMBRYOS BY PLCZ cRNA INJECTION.....	109
Abstract.....	110
Introduction.....	111
Materials and methods.....	113
PLCZ complementary RNA (cRNA) preparation.....	113
Somatic cell nuclear transfer.....	114
Activation and embryo culture.....	114
Intracellular calcium monitoring.....	115
Blastocysts differential staining and TUNEL assay.....	116
Blastocyst chromosomal analysis.....	117
Cell number determination of live embryos.....	117
Quantitative RT-PCR.....	118
Immunostaining of embryos.....	121
Statistical analysis.....	122
Results and discussion.....	122
PLCZ triggers fertilization-like $[Ca^{2+}]_i$ oscillations in bovine oocyte reconstructed by SCNT.....	122
Embryonic development of cloned embryos activated by PLCZ cRNA injection.....	125
Effect of oocyte activation method on nuclear reprogramming after somatic cell nuclear transfer.....	131
<b>CHAPTER 5.....</b>	<b>141</b>
SUMMARY AND FUTURE DIRECTIONS.....	141
<b>APPENDIX.....</b>	<b>148</b>
<b>REFERENCES.....</b>	<b>155</b>



## LIST OF TABLES

### CHAPTER 2

Table 2.1: Embryonic development after confocal fluorescence imaging. Mouse embryos were tested at the 2-cell stage while bovine embryos were evaluated at the 8- and 16-cell stage. All embryos were stained with Mitotracker Red CMXRos and imaged using the CARV system.....	52
---	----

### CHAPTER 3

Table 3.1: Parthenogenetic embryo development induced by injection of mouse PLCZ cRNA into bovine oocytes.....	83
Table 3.2: Optimization of bovine PLCZ cRNA concentration to activate bovine oocytes.....	83
Table 3.3: Optimization of mouse PLCZ cRNA concentration to activate bovine oocytes.....	84
Table 3.4: Chromosomal composition of parthenogenetic 8-cell embryos activated using different protocols.....	93

### CHAPTER 4

Table 4.1: Primers used for quantitative real time RT-PCR.....	120
Table 4.2: Time interval between $[Ca^{2+}]_i$ oscillations in SCNT embryos activated using PLCZ cRNA injection.....	124
Table 4.3: Preimplantation development of IVF and SCNT derived embryos activated using different protocols.....	126
Table 4.4: Chromosomal composition of blastocysts activated using different protocols.....	130

## LIST OF FIGURES

Images in this dissertation are presented in color

### CHAPTER 1

Figure 1.1: Contributions of gametes/somatic cell to fertilization and somatic cell nuclear transfer (SCNT).....	17
Figure 1.2: a) Schematic model of the molecular events that encompass mammalian fertilization.....	21
Figure 1.3: $\text{Ca}^{2+}$ response after incubation of MII oocytes with Ionophore (a) or after fertilization (b).....	32

### CHAPTER 2

Figure 2.1: Embryos stained with MitoTracker Red and imaged using the CARV system. (A) Mouse two-cell embryo and (B) bovine eight-cell embryo....	53
Figure 2.2: Effect of imaging mouse embryos using a spinning-disk confocal microscope. (A) Brightfield image of embryos at indicated times after imaging. (B) Brightfield and fluorescent images of embryos labeled with DHF for determination of ROS production. (C) Quantitation of ROS production. (D) Mean comet length (open bar) and caspase activity of embryos after imaging using the CARV system. ....	54
Figure 2.3: Effect of imaging bovine embryos using a spinning-disk confocal microscope. (A) Brightfield image of blastocysts and expanded blastocysts. (B) Brightfield and fluorescent images of embryos labeled with DHF for determination of ROS production. (C) Quantitation of ROS production. Bars indicate mean fluorescent intensity of each embryo relative to the intensity before imaging. (D) Mean comet length (open bar) and caspase activity (gray bar) of embryos after imaging using the CARV system.....	57
Figure 2.4: Comparison between live imaging and differential staining techniques for counting ICM, TE, and total cell numbers in bovine embryos.....	60
Figure 2.5: Comparison between HcRed and Syto 16 live imaging technique for counting ICM, TE, and total cells in transgenic SCNT embryos.....	62

Supplementary Figure S1: Caspase 3 activity in bovine and mouse embryos following exposure to fluorescent imaging using the CARV system. Quantitation of caspase activity in (A) mouse and (B) bovine embryos. (C) Brightfield and fluorescent images of bovine and mouse embryos after imaging. Caspase 3 activity is determined by fluorescent intensity.....	68
---	----

Supplementary Figure S2: DNA damage in imaged embryos determined by comet assay. Mean comet fluorescent intensity of individual (A) mouse and (B) bovine embryos measured 1.5 hours after imaging using the CARV system. (C) Representative images of comet tails observed after imaging mouse embryos using the CARV system.....	70
---	----

### CHAPTER 3

Figure 3.1: Validation of intracytoplasmic injection technique. a, b, c: Sequence of injection. d) Schematic representation of the microscope reticulum used as guide to control the injected volume. e) An oil drop of the same size as the injected volume is shown next to an oocyte. f) Oocytes injected using Texas Red dextran. g) From left to right, oocyte injected 2X and 1X the normal volume of Texas Red dextran. h) Fluorescent intensity profile of the line shown in f. i) Fluorescent intensity profile of the line shown in g. j) Developmental rates of injected and uninjected bovine oocytes after activation using ionomycin/DMAP.....	79
--	----

Figure 3.2: PLCZ cRNA injection induces bovine parthenogenetic development at similar rates to common chemical activation protocols. a) Mean cleavage (open bars) and blastocyst (black bars) rates after IVF or parthenogenetic activation using different methods. b) Cleavage of embryos after IVF or parthenogenetic activation using different methods.....	86
--	----

Figure 3.3: PLCZ cRNA injection induces sperm-like calcium oscillations. a) Representative $[Ca^{2+}]_i$ profiles. b) Minutes after injection at which the $[Ca^{2+}]_i$ pattern changed from interspike intervals of > 3 minutes to < 3 minutes for each treatment.....	88
--	----

Figure 3.4: PLCZ cRNA injection induces IP <sub>3</sub> R-1 downregulation. a) Immunoblot. b) Quantification of IP <sub>3</sub> R-1 mass relative to the levels observed in MII oocytes.....	91
--	----

Figure 3.5: Representative chromosomal spreads from 8-cell stage bovine embryos (1000X). a) Diploid cell, b) triploid cell, and c) tetraploid cell.....	94
---	----

## CHAPTER 4

Figure 4.1: Representative $[Ca^{2+}]_i$ profiles observed in SCNT embryos from 1 to 14 hours after mPLCZ cRNA injection.....	124
Figure 4.2: Representative pictures of blastocysts generated by IVF and SCNT using different activation protocols.....	126
Figure 4.3: Cell number, allocation, and apoptosis in IVF and SCNT embryos produced using different activation methods. a) Representative images of analyzed embryos. b) Quantification of TUNEL positive cells per embryo. c) Comparison of cell number and allocation among groups.....	128
Figure 4.4: Representative blastocyst chromosomal spreads. a, b: diploid chromosome complements, c, d: tetraploid chromosome complements.....	130
Figure 4.5: Quantification of mRNA abundance in 8-cell embryos generated by IVF or SCNT using different activation protocols.....	132
Figure 4.6: Quantification of mRNA abundance in blastocysts generated by IVF or SCNT using different activation protocols.....	134
Figure 4.7: Immunofluorescence analyses of IVF and SCNT embryos activated by using different protocols. a) Representative pictures of immunostained embryos. Semi-quantitative evaluation of b) H4K5Ac and c) H3K27me3 immunostaining.....	138

## APPENDIX

Figure A1: Cytogenetic analysis of donor cell line used for SCNT. The analysis was performed on G-banded cells by Cell Line Genetics (Madison, WI) resulting in an apparently normal Female Bovine Karyotype (60,XX).....	149
Figure A2: Confocal imaging of bovine embryos does not affect the level of GAPDH transcript abundance.....	150
Figure A3: Immunofluorescence staining for trimethylated Histone 3 lysine 27 (H3K27me3) of bovine embryos of different origins at different stages of preimplantation development.....	151
Figure A4: Level of Histone H3 lysine 27 trimethylation (H3K27me3) in embryos derived from in vitro fertilization, SCNT, and parthenogenesis.....	153

Figure A5: Cytochalasin B (CB) is required to avoid extrusion of a polar body after injection of PLCZ cRNA into bovine SCNT oocytes.....	154
---	-----

## ABBREVIATIONS

- [Ca<sup>2+</sup>]<sub>i</sub>**: Intracytoplasmic free-Ca<sup>2+</sup> concentration
- APC/C**: Anaphase promoting complex/cyclosome
- BSA**: Bovine serum albumin
- CaMKII**: Calcium/calmodulin-dependent protein kinase II
- CDK1**: Cyclin dependent kinase 1
- CDX2**: Caudal-related homeobox 2
- CHX**: Cycloheximide
- CN&A**: Cell number and allocation
- COC**: Cumulus oocyte complex
- CPEB**: Cytoplasmic polyadenylation element binding protein
- cRNA**: Complementary RNA
- DAG**: 1,2-diacylglycerol
- DAPI**: Diamidino-2-phenylindole
- DMAP**: 6-dimethylaminopurine
- DSC2**: Desmocollin 2
- EC<sub>50</sub>**: Half maximal effective concentration
- EMI1**: Early mitotic inhibitor 1
- EMI2**: Early mitotic inhibitor 2
- ER**: Endoplasmic reticulum
- ERP**: EMI1 related protein
- ES**: Embryonic stem

**FBS:** Fetal bovine serum

**FGFr2:** Fibroblast growth factor receptor type 2

**FSH:** Follicle-stimulating hormone

**GAPDH:** Glyceraldehyde 3-phosphate dehydrogenase

**GLUT1:** Glucose transporter 1

**H<sub>2</sub>DCFDA:** 2', 7'-dichlorodihydrofluorescein diacetate

**H3K27me<sub>3</sub>:** Trimethylated lysine 27 of histone H3

**H3K4me:** Histone 3 lysine 4 methylation

**H4K5Ac:** Acetylated lysine 5 of histone H4

**HECM:** Hamster embryo culture medium

**HH:** Hepes buffered HECM

**ICM:** Inner cell mass

**ICSI:** Intracytoplasmic sperm injection

**IETS:** International embryo transfer society

**IP<sub>3</sub>:** Inositol-1,4,5-tri-phosphate

**IP<sub>3</sub>R:** IP<sub>3</sub> receptor

**IVF:** In vitro fertilization

**KSOM:** Potassium simplex optimized medium

**LH:** Luteinizing hormone

**MCS:** Multiple cloning site

**MII:** Metaphase II stage

**MPF:** Maturation promoting factor

**NA:** Numerical aperture

**PCR:** Polymerase chain reaction

**PH:** Pleckstrin homology

**PI(3)P:** Phosphatidylinositol-3-phosphate

**PI(5)P:** Phosphatidylinositol-5-phosphate

**PI:** Phosphoinositide

**PIP<sub>2</sub>:** Phosphatidylinositol-4,5-bisphosphate

**PKC:** Protein kinase C

**PLC:** Phospholipase C

**PLCZ:** Phospholipase C-zeta

**PVA:** Polyvinyl alcohol

**ROS:** Reactive oxygen species

**RT:** Reverse transcription

**SOX2:** SRY-box containing gene 2

**TALP:** Tyrodes albumin lactate pyruvate

**TE:** Trophectoderm

**TRYP8:** Pancreatic anionic trypsinogen

**TUNEL:** Terminal deoxynucleotidyl transferase-mediated dUTP nick-end  
labeling

**U2AF1L2:** U2 small nuclear ribonucleoprotein auxiliary factor small subunit  
related protein 2



## **CHAPTER 1**

### **INTRODUCTION AND LITERATURE REVIEW**

## **Introduction**

Somatic cell nuclear transfer (SCNT) is a technique by which the nucleus of a somatic cell is introduced into an enucleated oocyte. As a result, the somatic nucleus is modified by the recipient oocyte cytoplasm allowing the development of the reconstructed embryo into a whole individual. The result is a genetic clone of the animal from which the donor cell was derived. Several species were successfully cloned using this methodology [1] and a broad variety of applications were envisioned for SCNT-cloning [2]. The ability to produce offspring from cultured somatic cells allows the production of biopharmaceuticals and nutraceuticals by cloned animals, organs for xenotransplantation, genetically engineered animal models of human diseases, derivation of isogenic embryonic stem (ES) cells for cell therapies, preservation of endangered species, genetic improvement of domestic species, as well as propagation of superior genotypes [2].

The most important limitation of SCNT is the inefficiency of producing healthy offspring in all species studied so far [3]. The frequency of development to term of SCNT-derived embryos is well below that observed after in vivo and in vitro fertilization. Overall, the efficiency of producing offspring after SCNT was lower than 5% [3]. Less than 50% of embryos reached the blastocyst stage in vitro. Then, after transferring blastocysts to surrogate mothers, about 50% established a pregnancy [4-6], but most of them failed to develop past the first trimester of gestation [5-7]. The remaining pregnancies were gradually lost at different stages [6], with only a small proportion reaching full term development.

This is in great contrast to pregnancies derived from fertilized embryos, in which pregnancy losses were rare after the first trimester. Moreover, perinatal mortality was high for cloned offspring [8]. Among the common abnormalities associated with mortality of cloned embryos were placental insufficiencies and malformations, fetal abnormalities, prolonged gestations, parturition difficulties, musculoskeletal problems, and respiratory problems [8]. The basis for these abnormalities are poorly understood, but are generally attributed to faulty or incomplete nuclear reprogramming [9-11]. Nuclear reprogramming involves silencing of somatic specific genes and reactivation of embryonic genes through erasure of the epigenetic cell memory and establishment of an epigenetic pattern that is suitable for embryonic development [12]. However little is known about the mechanisms that promote these changes.

The initiation of embryonic development is triggered by the sperm upon fertilization. Oocytes of most mammalian species are arrested at the metaphase stage of the second meiotic division (MII) at ovulation, and only complete meiosis upon fertilization. The sperm activating stimulus not only released the oocyte from its meiotic arrest but also induced a series of orderly processes that are referred to as oocyte activation [13, 14]. These include oocyte exit from meiosis, cortical granule exocytosis, recruitment of maternal mRNA, and pronuclear formation [13, 14]. In all mammals studied so far, a series of elevations in intracellular free calcium concentration ( $[Ca^{2+}]_i$ ) was observed upon sperm entry [15]. This  $Ca^{2+}$  signal was indispensable and sufficient to induce oocyte activation [16]. Moreover, a different number of  $[Ca^{2+}]_i$  oscillations was required

to initiate the different events of oocyte activation [13]. This gives credence to the notion that  $[Ca^{2+}]_i$  oscillations are not only needed to induce the events of oocyte activation but also to ensure the orderly completion of these events leading to the normal initiation of embryonic development [13].

In recent years, a sperm-specific PLC isoform, PLCZ, was suggested to be the factor that the sperm introduces into the oocyte to induce its activation [17, 18]. This PLC variant was sperm specific [17] and, when introduced into mouse oocytes, induced sperm-like  $[Ca^{2+}]_i$  oscillations [19]. When cRNA coding for PLCZ was introduced into mouse [17], human [20], and pig [21] matured oocytes, it induced  $[Ca^{2+}]_i$  oscillations and oocyte activation. In mouse sperm, PLCZ was localized to the postacrosomal region [19], the area thought to first interact with the oocyte membrane [22]. Functional studies using RNAi to reduce the level of PLCZ in sperm showed that  $[Ca^{2+}]_i$  oscillations were reduced after intracytoplasmic sperm injection (ICSI), and a lower number of progeny was obtained after natural mating [23]. Also, in fractionation studies, the presence of immunoreactive PLCZ correlated with the ability of fractions to induce oocyte activation [19], and immunodepletion of PLCZ from sperm extracts suppressed its  $[Ca^{2+}]_i$  oscillation-inducing ability [17]. Altogether, this evidence indicates that PLCZ delivered into the oocyte upon sperm-oocyte fusion is the factor responsible for oocyte activation.

The pattern of  $[Ca^{2+}]_i$  oscillations is species-specific and is observed over a relatively long period (3-4 hours in mice; 16-18 hours in cattle). The importance of the  $[Ca^{2+}]_i$  oscillatory pattern was well studied in mice and rabbits [24, 25]. It

was shown that alterations in  $\text{Ca}^{2+}$  signaling not only affected the early events of embryonic development [13, 26], but also 8-cell [27] and blastocyst stage embryonic gene expression [28], peri-implantation phenotype [24, 28], and even development to term [28]. It is possible that the long-lasting effect of  $[\text{Ca}^{2+}]_i$  oscillations was mediated by alterations in chromatin structure and reprogramming of gene expression that occur after fertilization [24, 27, 28]. For instance, perturbations of the pattern of  $[\text{Ca}^{2+}]_i$  oscillations were shown to affect oocyte mRNA recruitment [13], thus probably affecting zygotic genome activation [13].

Activation protocols commonly used in SCNT rely on chemicals that not only induce a non-physiological  $[\text{Ca}^{2+}]_i$  oscillation pattern, but also affect other cellular processes, with possible negative consequences for embryonic development [29]. Thus, an activation protocol that closely mimics the mechanism of activation initiated by the sperm has the potential to improve the developmental capacity of cloned embryos.

Thus, the hypothesize that bovine preimplantation embryos produced by SCNT and activated using PLCZ mRNA recapitulate developmental events observed in fertilized embryos when compared to chemically activated SCNT embryos was tested. The following objectives were proposed:

- Test different sources and concentrations of PLCZ on the capacity to induce parthenogenetic activation of bovine oocytes.
- Compare embryonic development of SCNT embryos activated by

PLCZ, ionomycin/6-dimethylaminopurine (DMAP), ionomycin/cycloheximide (CHX), and in vitro fertilization (IVF) derived embryos.

- Determine the effect of activation stimuli on SCNT embryo ploidy, apoptosis, gene expression, and chromatin modifications.

It is expected that this novel activation protocol will improve the reprogramming of the somatic cell leading to a more efficient SCNT technique.

## **Cloning by somatic cell nuclear transfer**

In the 19<sup>th</sup> century, August Weisman proposed a theory for the phenomena of cell differentiation during development of an individual from a zygote. He theorized that cell differentiation results from the differential and sequential partitioning of the genome. Roux provided evidence toward that hypothesis in 1888, when he was not able to obtain development after destroying one blastomere with a hot needle from a two-cell frog embryo. However, he did not realize that the destroyed blastomere prevented the complete development due to the positional effect it had on the intact blastomere.

In 1894, Dreisch repeated the experiment using a two-cell and four-cell sea urchin embryo separated into individual blastomeres by shaking. He found that each blastomere developed into a complete larva, suggesting that the entire genetic information was present in each blastomere during cell division, in contrast to Weismann's theory. In 1914, Hans Spemann further extended these results by partially constricting a salamander zygote with a baby hair and forcing the nucleus of the embryo to one side [30]. The part containing the nucleus started to divide and develop, and at the 16-cell stage the ligature was loosened allowing one nucleus to enter the unnucleated portion. Finally the ligature was completely tightened cutting the embryo in two. The result was the development of two larvae, suggesting that a nucleus from a 16-cell embryo was able to direct the development and differentiation of a complete amphibian. In his report, Spemann proposed what he called a "fantastic experiment", where a nucleus

from a somatic adult cell would be transplanted into an enucleated zygote or oocyte to test the genomic potential of older nuclei [31].

The required technology to perform Spemann's proposed experiment was developed in the 1950's. In 1952, Briggs and King injected blastula nuclei into enucleated oocytes obtaining tadpoles, and later adult animals [32]. However, all the attempts to generate adult animals from adult differentiated cells were unsuccessful [33, 34], leading to the conclusion that the genetic potential of a cell declined as it differentiated.

In mammals, the technology of nuclear transfer was developed several decades later. The transfer of a blastocyst-cell nucleus into an enucleated mouse zygote was reported by Illmensee and Hoppe in 1981, with the development of adult animals [35]. However, controversy surrounded these results, as other groups were unable to repeat the experiment. McGrath and Solter developed a more efficient technique by which the donor cell was fused with the enucleated zygote [36]. However, these and other authors were not able to obtain offspring after embryonic cell nuclear transfer. Only pronuclear transfer in mouse-enucleated zygotes resulted in viable offspring [37].

In contrast to the mouse, Willadsen obtained offspring after fusing sheep MII oocytes with 8 or 16-cell embryonic blastomeres [38]. Later this procedure was successfully repeated in several species including cattle [39], rabbits [40], pigs [41], mice [42], and monkeys [43]. Cloning from morula and blastocyst cells was soon achieved [44, 45].



In 1996, Campbell et al. reported the production of offspring from sheep embryonic disc cells cultured for 6 to 13 passages [46], opening the possibility of introducing genomic modification during cell culture. A year later, Wilmut et al. announced a great breakthrough when they reported the birth of Dolly, a sheep obtained after the transfer of an adult mammary cell into an enucleated oocyte [47]. Dolly was the only cloned animal resulting from 277 attempts (0.3 % efficiency). Many other mammals have been cloned from an adult donor cell nucleus. These include cattle [48], mouse [49], goat [50], pig [51], gaur [52], mouflon [53], rabbit [54], cat [55], rat [56], mule [57], horse [58], african wildcat [59], dog [60], ferret [61], wolf [62], buffalo [63], and red deer [64]. In each of these species, the efficiency has remained very low, with less than 1 % of all nuclear transfers from adult cells developing into normal offspring. Nevertheless, the success of SCNT cloning in several species has demonstrated that the cytoplasm of the MII oocyte has the potential to reprogram a somatic cell nucleus to an embryonic stage, capable of generating a complete individual.

### **Applications of SCNT: Why clone mammals?**

Cloning by nuclear transfer has the potential to contribute substantially to animal agriculture, biotechnology, biomedicine, preservation of endangered species and basic research. The success of adult SCNT with almost all agriculturally important species [47, 48, 50, 54, 65] confirms its usefulness for the clonal expansion of animals with superior genotypes. Moreover, SCNT makes possible germline genetic modifications in domestic species [48]. Traits which

have been considered for genetic modification include feed utilization, resistance to diseases (thus reducing drug/antibiotic use), reduction of animal waste, and diversification of agricultural products, i.e., providing new economic opportunities in rural areas, and generation of new consumer products [66]. SCNT can also be used for gene targeting, making additions or deletions in the genome feasible. Using this approach, cattle that lack the prion gene responsible for bovine spongiform encephalopathy were recently produced [67]. Targeted modifications have also been successfully achieved in sheep [68] and pigs [69]. Farm animals carrying genetic modifications have great potential in biotechnology. Engineered animals are being used as bioreactors for the production of pharmaceuticals and as potential organ donors for the human population. Further, SCNT offers alternative means to preserve endangered, and even to recover extinct species. Wells et al. reported the use of SCNT to clone the last surviving animal of the Enderby Island cattle breed [70], and Lanza et al., using interspecies nuclear transfer, were able to clone an endangered species (*Bos gaurus*) [71]. The same approach was used to clone Mouflons (an endangered breed of sheep) with tissue collected from dead animals [53]. Although all of the above-described applications for SCNT are far-reaching, its broad implementation has been hindered by low efficiency.

### **Abnormalities associated with somatic cell nuclear transfer**

From the first successful attempt in 1997 to date, the efficiency of producing live offspring from nuclear transfer using somatic cells remains low.

Surprisingly, the development of SCNT embryos to the blastocyst stage was similar to that attained by IVF. Moreover, after embryo transfer, a similar pregnancy rate was observed between SCNT- and IVF- or in vivo-derived bovine embryos [4-6]. However, high incidence of pregnancy losses occurred during the first trimester of gestation [5-7]. Also, late gestation losses increased in SCNT pregnancies as compared with IVF and in vivo derived pregnancies [6]. Fetal and placental abnormalities are often reported. Abnormal development of the placenta, with defects in vasculature formation, was a principal contributor to the early losses observed in cattle [5]. Examination of the placenta of embryos between days 40 and 50 of gestation revealed hypoplastic placentas with partially developed cotyledons or completely normal placentas [5]. Late losses were usually associated with hydroallantois, a rare defect observed in artificial insemination or IVF pregnancies [6]. Moreover, high proportion of cloned offspring was larger than normal and often died soon after birth.

A comprehensive analysis of the health profiles of cloned animals indicated that 32% of cattle exhibited some form of abnormality [8]. Various abnormalities were manifested in animals derived from SCNT including "Large Offspring Syndrome", diabetes, pulmonary hypertension, viral infection, dystocia, kidney problems, leg malformations, pneumonia, heart defects, liver fibrosis, osteoporosis, joint defects, anemia, and placental abnormalities. However, all the abnormalities seen in clones disappeared in the clone's offspring, leading to the conclusion that the abnormalities must be of epigenetic rather than of genetic origin. This also indicated that even though cloned embryos develop to the

blastocyst stage at similar rates as fertilized embryos, their developmental capacity is severely hampered. This was interpreted to be the result of incomplete or aberrant chromatin reprogramming.

### **Epigenetic modifications and nuclear reprogramming after fertilization and SCNT**

As two highly differentiated cells meet at fertilization to generate a new individual, their genomes must be combined and rendered amenable to direct embryonic and fetal development. Cell identity is established during differentiation by epigenetic modifications of the genome, which are heritable changes in chromatin that control/establish gene expression patterns without affecting the underlying DNA sequence. After SCNT, the epigenetic profile of the donor cell has to be modified; erasing the epigenetic memory of the somatic cell and establishing the epigenetic program of the early embryo. Although the mechanism of reprogramming is not well understood it involves changes in DNA methylation and histone tail modifications. DNA methylation in the promoter region of gene is associated with gene silencing. Histone tail modifications include acetylation, methylation, phosphorylation, and ubiquitination among others [72]. Among these modifications, histone acetylation and methylation are better characterized. Histone acetylation was associated with transcriptional permissiveness, while histone methylation can indicate repression or activation of transcription depending on which residue was modified [72]. Moreover, histone tail residues can be mono-, di-, or tri-methylated, and the number of methyl

groups can have different consequences for transcription. In general, Histone 3 Lysine 4 methylation (H3K4me) was associated with transcriptional activation and H3K9me indicated gene silencing [72]. Another methylation mark that is well characterized in terms of its function is H3K27me3 [72]. This mark is established by Polycomb group proteins and is generally associated with stable repression of gene expression [72].

Global DNA methylation patterns undergo marked changes during early development of mammalian embryos [73, 74]. Initially, DNA methylation levels were high in sperm and oocyte chromatin. After fertilization, paternal DNA was actively and rapidly demethylated by still unknown factors [75]. In contrast, maternal DNA was passively demethylated within the subsequent cell divisions, mainly by lack of maintenance of DNA methylation [75]. In bovine embryos, remethylation of DNA started at the 8-16 cell stage, and at the blastocyst stage the inner cell mass (ICM) was hypermethylated compared to the trophectoderm (TE) [73]. These events were somewhat recapitulated after SCNT, albeit with errors [73, 74]. The somatic cell chromatin had a high degree of DNA methylation and after nuclear transfer demethylation was observed although not to the extent observed in IVF embryos [73]. Interestingly, in cloned blastocysts the methylation levels at the ICM appeared normal while the TE cells presented increased methylation [74]. In fertilized embryos, histone acetylation increased at the 8-cell stage coincident with embryonic genome activation [74, 76]. In bovine SCNT embryos, acetylation of lysine 9 and 18 at histone H3 was higher than control IVF embryos [74, 77], while histone H4 lysine 5 acetylation was lower in cloned

embryos at the 8-cell stage and similar to fertilized embryos at all other stages [76]. Methylation of H3K9 followed a pattern similar to DNA methylation in fertilized embryos [78]. In blastocysts, methylation levels of H3K9 were higher at the TE in SCNT than in IVF-derived embryos [74].

As the roles that different histone modifications play in establishing and maintaining cell identity and the enzymes that induce such modifications are uncovered, it will be important investigating their involvement in reprogramming the embryonic genome after fertilization and SCNT, as they are likely to play a critical role during nuclear reprogramming.

### **Gene expression in cloned preimplantation embryos**

Because epigenetic changes underlie changes in gene transcription, a number of studies analyzed gene expression in SCNT embryos. Microarray studies which evaluated gene expression at a global scale found that less than 3 % of the genes were differentially expressed between cattle SCNT and fertilized embryos [79-83]. Curiously, although all microarray studies suggested that the proportion of misregulated genes was low, there was no agreement on the identities of the aberrantly expressed genes. Candidate gene approaches such as RT-PCR [84-87] and quantitative real time PCR [88-90] were also used to evaluate differences in gene expression between SCNT versus fertilized embryos. To date, no clear picture has yet emerged as to which genes are consistently misexpressed in cloned preimplantation embryos. This is not surprising considering that several aspects of the nuclear transfer procedure,

including donor cell type, type of recipient cytoplasm, enucleation and transfer procedures, activation method, and embryo culture environment differed among the various studies, and some of these factors affected gene expression of cloned embryos [80, 83, 84, 86, 87, 89]. Alternatively, discrepancies among studies may indicate the stochastic nature of the reprogramming errors [82]. Furthermore, technical aspects of gene expression analysis in embryos can confound the interpretation of results. For instance, the low amount of material obtained from preimplantation embryos pushed available techniques to their sensitivity limits. Of particular concern is the use of appropriate controls to correct gene expression levels for differences in input mRNA, mRNA extraction efficiency, and reverse transcription. Housekeeping genes that show no differences in gene expression among the treatments to be compared represent the best control; however, it is very difficult to validate this assumption. Alternatively, external controls can be used to normalize gene expression levels, which when introduced before RNA extraction can reliably control for RNA extraction and reverse transcription efficiency [91]. Nonetheless, they can not control for the amount of input sample. This factor can be precisely determined when using early stage preimplantation embryos. When analyzing blastocyst gene expression however, the number of cells in the embryo may influence the amount of input RNA, thus a system that accounts for the number of cells in the embryo is required to correctly interpret blastocyst gene expression results.

### **Paternal contribution to the embryo: what is missing in SCNT?**

The union of a sperm and oocyte initiates the development of a whole new individual. Through gametogenesis, these cells acquire unique characteristics that combined upon fertilization allow the development of the zygote into all the cell types that constitute an organism. The most basic information that the gametes contribute is the DNA complement that each carry. However, the information contained in the reconstituted zygotic DNA is not used until zygotic genome activation which occurs at different times after fertilization (up to 3 days after fertilization in cattle [92]). The molecular contributions of the oocyte at fertilization have long been recognized [93]. The oocyte is equipped with a large pool of proteins and RNAs that will facilitate the transition from gametes into an embryo and drive the initial stages of embryonic development [94]. In contrast, the sperm has been regarded as a mere vehicle for the paternal genetic complement [95]. In recent years, the contribution of the sperm towards the embryo is being reconsidered [96]. It is now well known that the sperm contributes centrioles, the oocyte activation stimulus, genetic imprints and mRNAs [96]. SCNT offers a unique opportunity to test the functional relevance of these factors (**Figure 1.1**). The low efficiency of cloning by nuclear transfer could be reasonably attributed to the lack of sperm contribution. The somatic cell nucleus introduced into an enucleated oocyte replaces both male and female DNA complements. Also, provided that the information has been successfully maintained, both maternal and paternal imprints are supplied by the somatic cell.



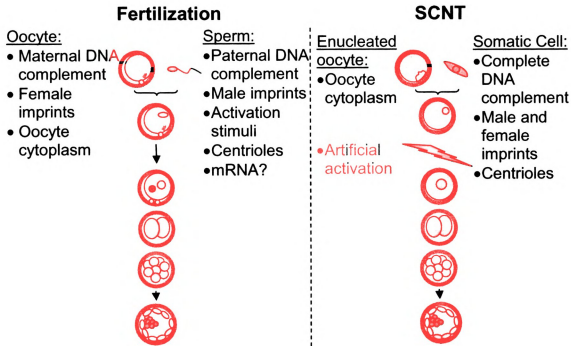


Figure 1.1: Contributions of gametes/somatic cell to fertilization and somatic cell nuclear transfer (SCNT).

In most mammalian species, the sperm also contributes the centriole, which in combination with oocyte derived proteins, will form the microtubule organizing center of the cell, known as the zygotic centrosome [97]. After SCNT, the centrosome was provided by the somatic cell [97]. The activation stimulus that the sperm delivers upon fusion with the oocyte is lacking in somatic cells, and thus artificial activation has to be performed [98]. Artificial protocols used to activate the oocyte failed to completely recapitulate the effects the sperm induces upon fertilization. The recent identification of the sperm factor that induces oocyte activation offers a unique opportunity to test its function in the absence of other factors derived from the sperm.

### **Oocyte activation**

Most mammalian oocytes are ovulated arrested at the MII stage of meiosis. The meiotic arrest is released upon fertilization which also triggers a series of events that lead to initiation of early embryonic development. These events included cortical granule exocytosis, pronuclear formation, and mRNA translation which collectively are referred to as oocyte activation [13, 14]. It was suggested that the activation process is initiated by a soluble factor that diffuses from the sperm cytoplasm into the oocyte upon fusion [99]. A different hypothesis was based on the activation of an oocyte membrane receptor upon sperm-oocyte contact. Evidence supporting the former hypothesis includes the observation that normal oocyte activation and embryonic development was achieved after injecting the sperm into the oocyte [100], without allowing gamete membrane

interaction. Moreover, microinjection of sperm extract into MII oocytes was capable of inducing oocyte activation. Oocyte activation did not occur when extracts from other tissues were used, or when the sperm extract was added to the medium containing the oocytes [101-105].

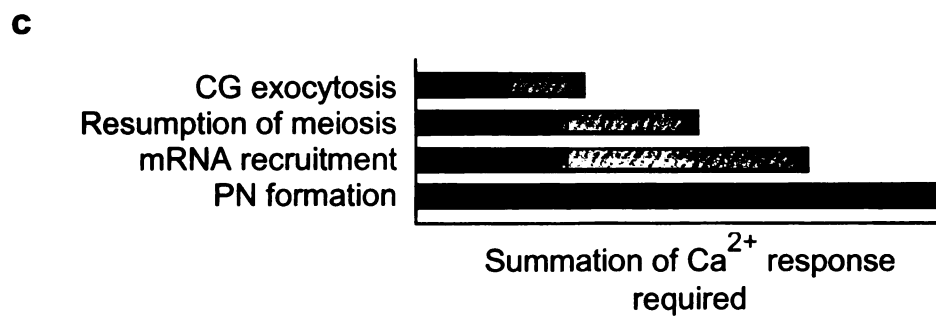
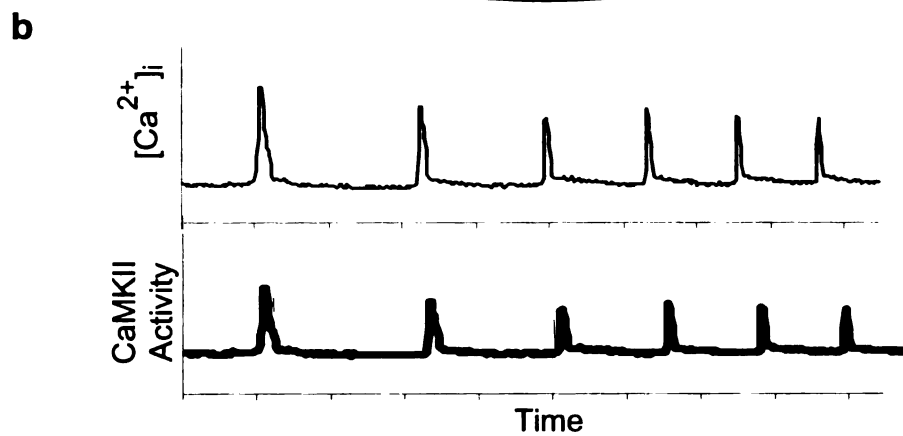
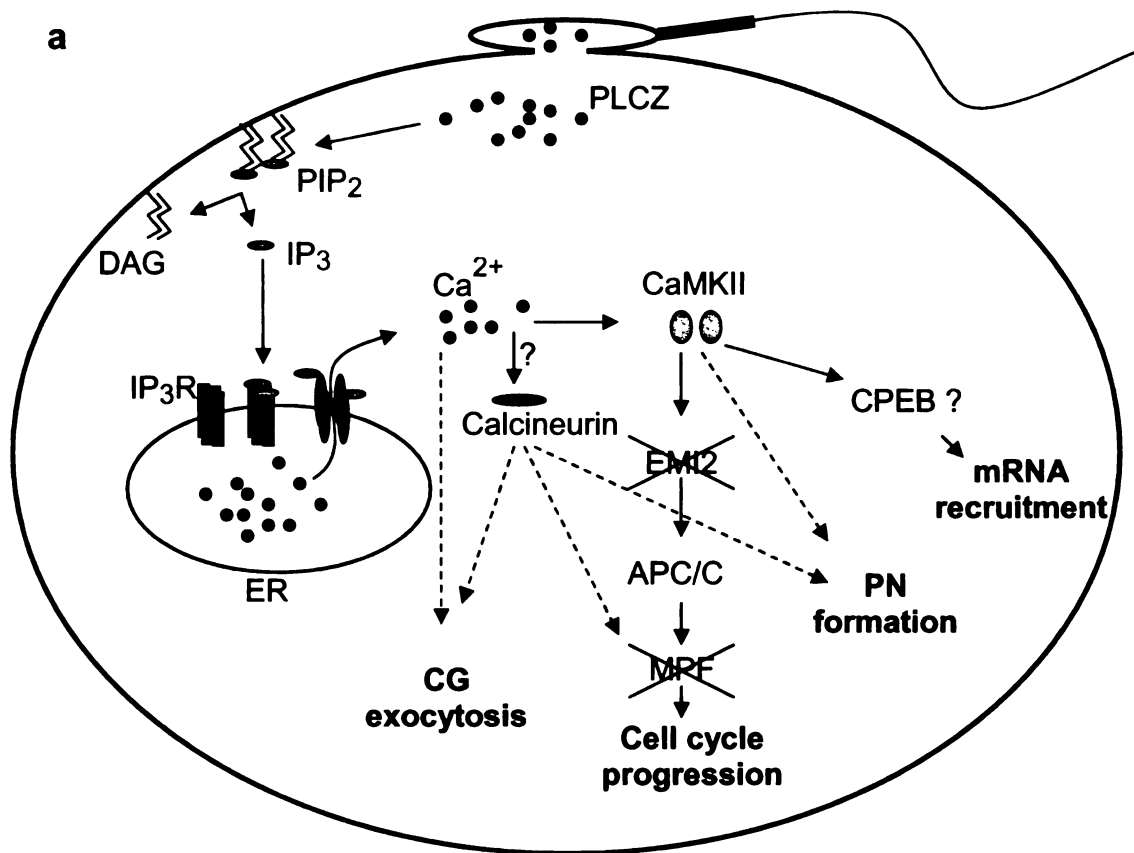
### **Role of $\text{Ca}^{2+}$ during oocyte activation and early development**

The involvement of  $\text{Ca}^{2+}$  in the signaling events leading to oocyte activation was suggested in the early 1930s (cited by [106]). This idea was first substantiated 40 year later by the finding that the  $\text{Ca}^{2+}$  ionophore A23187 was capable of activating sea urchin, starfish and hamster oocytes [107]. Later, the rise in calcium that immediately follows gamete fusion was recorded using the  $\text{Ca}^{2+}$ -binding bioluminescent protein aequorin. Furthermore, activation was induced by injecting  $\text{Ca}^{2+}$  into oocytes and was prevented when EGTA, a  $\text{Ca}^{2+}$  chelator, was preinjected into oocytes. This evidence indicated that  $[\text{Ca}^{2+}]_i$  increase is necessary and sufficient to induce oocyte activation after fertilization and thus initiate embryonic development [106]. Later experiments in hamster oocytes showed that a series of hyperpolarizations followed fertilization, indicating repetitive increases in  $[\text{Ca}^{2+}]_i$  occur, as each hyperpolarization was due to a  $\text{Ca}^{2+}$ -activated  $\text{K}^+$  conductance increase [108]. Using  $\text{Ca}^{2+}$  sensitive electrodes and aequorin bioluminescence the repetitive nature of the  $\text{Ca}^{2+}$  signal was confirmed [106]. Thereafter, with the use of fluorescent reporters of  $[\text{Ca}^{2+}]_i$ , it was established that the  $\text{Ca}^{2+}$  signal in all mammals studied so far adopts an

oscillatory pattern that persists for several hours after fertilization [109]. Curiously, the pattern of  $[Ca^{2+}]_i$  oscillations is largely species specific [110].

The role of the oscillatory  $Ca^{2+}$  signal was extensively studied using a system that permits a precise control of  $[Ca^{2+}]_i$  elevations in oocytes without compromising their developmental ability [24]. This system consists of an electroporation chamber that allows for the rapid exchange of buffers and culture media [24]. Using this methodology, it was shown that the  $Ca^{2+}$  stimulus is more efficient to activate oocytes when it is applied in a repetitive manner [24]. Moreover, the temporal modulation of the  $Ca^{2+}$  signal during oocyte activation affected the developmental performance and morphology of rabbit parthenogenetic conceptuses at day 11.5 of pregnancy [24]. Also, a different number of  $[Ca^{2+}]_i$  oscillations was required to initiate different oocyte activation events and a higher number was required to complete all these events [13] (**Figure 1.2**). Specifically, cortical granule exocytosis was initiated by only 1-4  $[Ca^{2+}]_i$  elevations, resumption of meiosis required 4-8, and maternal mRNA recruitment was initiated by 8  $[Ca^{2+}]_i$  rises but became more apparent after 24  $[Ca^{2+}]_i$  elevations [13]. More important, altering the pattern of  $[Ca^{2+}]_i$  oscillations in fertilized mouse embryos resulted in gene expression alterations at the blastocyst stage and although no differences in blastocyst production were observed, fewer offspring were born after embryo transfer [28]. When  $[Ca^{2+}]_i$  oscillations were precociously interrupted, the incidence of implantation decreased, whereas extending the  $Ca^{2+}$  signal resulted in

Figure 1.2: a) Schematic model of the molecular events that encompass mammalian fertilization. Upon sperm oocyte fusion, phospholipase C-zeta (PLCZ) diffuses into the oocyte's cytoplasm where it catalyzes the conversion of phosphatidylinositol-4,5-bisphosphate (PIP<sub>2</sub>) into 1,2-diacylglycerol (DAG) and inositol-1,4,5-tri-phosphate (IP<sub>3</sub>). IP<sub>3</sub> binds to its receptor (IP<sub>3</sub>R) in the endoplasmic reticulum (ER) inducing a conformational change that allows Ca<sup>2+</sup> to freely diffuse into the oocyte's cytoplasm. Ca<sup>2+</sup> activates Ca<sup>2+</sup>/calmodulin-dependent protein kinase II (CaMKII) and possibly Calcineurin which then act at different targets inducing the events of oocyte activation. Continuous arrows indicate direct relation, dashed arrows represent indirect relations (Adapted from Malcuit et al. [111]). b) Representative temporal profile of intracellular free-Ca<sup>2+</sup> concentration ([Ca<sup>2+</sup>]<sub>i</sub>) and CaMKII activity observed after fertilization. c) Graph representing the persistence of [Ca<sup>2+</sup>]<sub>i</sub> oscillations required to complete the different events of oocyte activation as indicated by Ducibella et al. and Ozil et al. [13, 26]. Solid bars represent the level of [Ca<sup>2+</sup>]<sub>i</sub> required to initiate the events and grey bars represent the amount required to complete the events.



postimplantation abnormalities and the offspring born showed a greater variability in weight compared to controls [28]. The mechanism by which the  $\text{Ca}^{2+}$  signal that persists for only a few hours after fertilization influenced long-term development is not yet understood; however, a role for  $[\text{Ca}^{2+}]_i$  oscillations in chromatin remodeling and reprogramming of gene expression following fertilization is possible.

Some of the downstream effectors of  $\text{Ca}^{2+}$  were elucidated (**Figure 1.2**). Calcium/calmodulin-dependent protein kinase II (CaMKII) plays an important role, as its activity oscillated in parallel with  $[\text{Ca}^{2+}]_i$  oscillations [112]. Introducing constitutively active CaMKII into MII oocytes triggered several activation-related events including cell cycle resumption, recruitment of maternal mRNAs, and development to blastocyst stage, in the absence of  $[\text{Ca}^{2+}]_i$  increase [113-115]. However, cortical granule exocytosis and the membrane block of polyspermy did not occur normally after CaMKII injection [113, 115], indicating that mechanisms independent of CaMKII are also involved in translating the  $\text{Ca}^{2+}$  signal at fertilization.

MI arrest is characterized by high levels of maturation promoting factor (MPF) activity, which rapidly fall at fertilization. MPF is composed of a catalytic subunit (CDK1) and a regulatory subunit (cyclin B). For meiosis to progress, MPF activity has to decrease. This is accomplished by inducing the destruction of cyclin B by the anaphase promoting complex/cyclosome (APC/C). To prevent premature APC/C activity as cells enter mitosis, an inhibitor (EMI1) holds APC/C inactive [116, 117]. An EMI1 related protein (ERP1/EMI2) was identified to be





oocyte and testis specific [118-120]. Knock-down of EMI2 in mouse MII oocytes induced parthenogenetic activation [121], and when EMI2 synthesis was prevented during oocyte maturation, oocytes failed to arrest at MII [122]. Such results indicate that EMI2 is necessary to achieve meiotic arrest. It was shown that CaMKII phosphorylated and thus inactivated EMI2 [118-120], which released the inhibition of APC/C which in turn degrades cyclin B and thus decreases MPF activity releasing the MII arrest (**Figure 1.2**).

Protein expression following fertilization was coupled to  $[Ca^{2+}]_i$  oscillations in mouse oocytes [13]. Because there was no transcription during this period of embryonic development, these changes were attributed to translation of maternal mRNA. It was shown in hippocampal neurons that CaMKII can phosphorylate and activate cytoplasmic polyadenylation element binding protein (CPEB) [123]. In turn, CPEB played an important role in mRNA polyadenylation and expression in oocytes [124]. Thus it can be speculated that  $Ca^{2+}$ -activated CaMKII can induce recruitment of maternal mRNA and affect protein expression through activation of CPEB in oocytes (**Figure 1.2**). Furthermore, recruitment of maternal mRNA was required for subsequent embryonic genome activation, thus representing a possible mechanism by which  $Ca^{2+}$  signaling may affect embryonic development in the short and long term.

Recently, studies in xenopus indicated that calcineurin, a  $Ca^{2+}$ -dependent protein phosphatase, functions as a  $Ca^{2+}$  second messenger during oocyte activation [125, 126] (**Figure 1.2**). After  $Ca^{2+}$  was released in frog oocytes, calcineurin was transiently activated independently of CaMKII. Also, inhibition of



calcineurin impaired cyclin-B degradation, dephosphorylation of proteins phosphorylated during metaphase II stage, migration of pronuclei, and rearrangement of the cytoskeleton in the cortical areas of the oocyte [125, 126]. So, two pathways that usually act in opposition (CaMKII and calcineurin) are coordinated after fertilization to synergistically elicit the same final effect, oocyte activation.

### **Phosphoinositide (PI) signaling pathway and oocyte activation**

Overwhelming evidence indicates that inositol-1,4,5-tri-phosphate (IP<sub>3</sub>) is involved in the generation of  $[Ca^{2+}]_i$  oscillations at fertilization. Activation of the PI pathway results in the hydrolysis of phosphatidylinositol-4,5-bisphosphate (PIP<sub>2</sub>), producing IP<sub>3</sub> and 1,2-diacylglycerol (DAG). The elevation in IP<sub>3</sub> concentration is responsible for inducing  $[Ca^{2+}]_i$  release from the endoplasmic reticulum (ER) in response to IP<sub>3</sub> receptor (IP<sub>3</sub>R) binding. Also, production of DAG via activation of protein kinase C (PKC) was involved in regulating  $Ca^{2+}$  influx [127]. The most compelling evidence for an involvement of this pathway in oocyte activation is that injection of IP<sub>3</sub>R competing functional inhibitor, heparin, or a blocking antibody, prevented fertilization-induced  $[Ca^{2+}]_i$  oscillations [15]. Similarly, experimentally induced downregulation of IP<sub>3</sub>R before fertilization blocked sperm-induced  $[Ca^{2+}]_i$  oscillations [128]. Moreover, all three known IP<sub>3</sub>R types are expressed in mammalian oocytes, although type 1 is more abundant. IP<sub>3</sub>R-1 is localized to the cortex of the oocyte's cytoplasm, where  $[Ca^{2+}]_i$  release first takes place, and is degraded shortly after fertilization [128, 129]. IP<sub>3</sub>R

degradation can be considered evidence of IP<sub>3</sub> production, because in somatic cells IP<sub>3</sub>R degradation only occurred as a consequence of IP<sub>3</sub> binding [111]. IP<sub>3</sub>R-1 is believed to play an important role in controlling the duration of [Ca<sup>2+</sup>]<sub>i</sub> oscillations in mammalian oocytes [111, 130]. Following fertilization, IP<sub>3</sub>R-1 was degraded to about 50 percent of that present in MII stage oocytes [128, 129], which was believed to contribute to the decreased responsiveness to IP<sub>3</sub> observed after fertilization [131]. Moreover, post-translational modifications of IP<sub>3</sub>R-1 by cell-cycle-dependent kinases also played an important role in reducing IP<sub>3</sub>R-1 activity [132].

Unfortunately, IP<sub>3</sub> determination in single oocytes/zygotes is not possible. However, direct evidence that the sperm induces IP<sub>3</sub> production came from experiments using sea urchin egg homogenates. In such studies sperm extracts induced [Ca<sup>2+</sup>]<sub>i</sub> release by IP<sub>3</sub> production and the activity that generated IP<sub>3</sub> was in the sperm rather than in the oocyte [133, 134].

Involvement of the PI signaling pathway indicated the participation of a phosphoinositide-specific phospholipase C (PLC) activity. PLCs, catalyze the hydrolysis of PIP<sub>2</sub>, producing IP<sub>3</sub> and DAG. PLCβ1, γ1, γ2, γ3, δ1, and δ4 are known to be present in mammalian sperm [109]. However most of the above enzymes were regarded improbable players since they do not correlated with [Ca<sup>2+</sup>]<sub>i</sub> oscillating activity in chromatographically separated fractions of sperm extract [135]. Also, microinjection of recombinant proteins coding for active PLCβ, γ, and δ at levels similar to those found in sperm failed to induce oocyte activation [136]. Recombinant PLCγ1 was able to induce [Ca<sup>2+</sup>]<sub>i</sub> oscillation in

mouse oocytes only when injected at levels 500-900 times greater than those found in a single sperm [136, 137]. Recently, a novel PLC isoform, PLC-zeta (PLCZ) was discovered and shown to be expressed in sperm. Further evidence indicates that PLCZ may represent the long sought after sperm factor responsible for oocyte activation [17].

### **PLCZ: the putative sperm factor**

In 2002, using bioinformatics and cDNA library screening, Saunders et al. identified a novel PLC isozyme, PLCZ [17]. They showed that PLCZ was specifically expressed in sperm and injection of PLCZ cRNA into mouse MII oocytes induced sperm-like  $[Ca^{2+}]_i$  oscillation. Furthermore, they showed that injection of PLCZ cRNA induced oocyte activation and early embryonic development and PLCZ immunodepletion from sperm extracts abolished the ability of the extracts to induce  $[Ca^{2+}]_i$  oscillations [17].

Further studies supported the notion that PLCZ is the long sought after sperm factor. Injection of cRNA coding for PLCZ into mouse [17], human [20], and pig [21] oocytes, induced  $[Ca^{2+}]_i$  oscillations and oocyte activation. Furthermore, injection of recombinant PLCZ into mouse oocytes was sufficient to induce sperm-like  $[Ca^{2+}]_i$  oscillations [138]. PLCZ localized to the postacrosomal region in mouse sperm [19], the area thought to first interact with the oocyte membrane [22], and to the equatorial region in bull sperm [139], also an area expected to come in contact with the ooplasm rapidly after gamete fusion [22]. Accordingly, 90 minutes after ICSI, PLCZ was completely released into the



ooplasm and the sperm head lost its ability to induce further  $[Ca^{2+}]_i$  oscillations [139]. In fractionation studies, the presence of immunoreactive PLCZ correlated with the ability of the fractions to induce oocyte activation [19], and immunodepletion of PLCZ from sperm extracts suppressed its  $[Ca^{2+}]_i$  oscillation-inducing ability [17].

In vitro assays of PIP<sub>2</sub> hydrolysis activity at various  $Ca^{2+}$  concentrations revealed significant PLCZ activity at  $Ca^{2+}$  concentrations as low as 10 nM, and 70% maximal activity at 100 nM, corresponding to the basal  $[Ca^{2+}]_i$  in oocytes [138]. A PLC activity with similar characteristics was previously described in boar sperm extracts [134]. Comparatively, the half maximal effective concentration (EC<sub>50</sub>) of PLCZ was 52 nM while that of PLCδ1 was 5.7 μM [138]. The potent activity of PLCZ is critical to oocyte activation because upon entry into the oocyte the sperm factor triggers  $Ca^{2+}$  release without any previous  $[Ca^{2+}]_i$  rise, and must maintain long lasting  $[Ca^{2+}]_i$  oscillations.

Functional studies using a transgenic RNAi approach to reduce PLCZ in sperm showed that reduced  $[Ca^{2+}]_i$  transients were observed after intracytoplasmic injection of PLCZ depleted sperm [23]. Also, a lower number of progeny were obtained when the transgenic males were mated to wildtype females [23]. More significantly, no transgenic offspring were produced, suggesting mosaicism was likely and that sperm with decreased PLCZ content were not able to induce full term development [23].

PLC isozymes are characterized by the presence of distinct domains. PLCZ contains EF, X, Y and C2 domains, common to other PLCs. However,

PLCZ lacks the PH domain (pleckstrin homology) found in all other PLC isoforms. The PH domain is the major determinant of PLC binding to phosphoinositol-containing lipids and thus of PLC localization to the membrane. The catalytic domain of PLC is divided in two parts named X and Y domains, separated by the X-Y linker region. The X-Y linker region may be important for PLCZ binding to lipid membranes by electrostatic interactions [140]. The EF-hands are domains that change their conformation upon  $\text{Ca}^{2+}$  binding. PLCZ has four EF-hands, and EF1 and EF2 were important for PLCZ activity and EF3 was responsible for its high  $[\text{Ca}^{2+}]_i$  sensitivity [141]. The C2 domain binds phospholipid headgroups, and PLCZ's C2 domain bound preferentially to phosphatidylinositol-3-phosphate (PI(3)P) and phosphatidylinositol-5-phosphate (PI(5)P). Such binding suppressed PLCZ activity, possibly by reducing access of PLCZ to its substrate  $\text{PIP}_2$  [141]. Deletion of the EF domains of PLCZ or of the C2 domain resulted in complete loss of PLC activity [141],  $[\text{Ca}^{2+}]_i$  oscillation induction and oocyte activation potential of PLCZ [141, 142].

The PLCZ locus was identified in several species including human, monkey, mouse, rat, chicken, cow, pig, and dog [143]. A high degree of conservation was observed at the characteristic domains, but the inter-domain regions differed significantly among the different transcripts. For example human PLCZ had the shortest X-Y linker region of all PLCZs, which may be important considering that PLCZs from different species displayed different potency to induce  $[\text{Ca}^{2+}]_i$  oscillations [144]. For instance, human PLCZ cRNA was able to induce  $[\text{Ca}^{2+}]_i$  oscillations in mouse oocytes at much lower concentrations than





mouse PLCZ cRNA did [144]. Whether the interdomain regions play a role in PLCZ activity remains to be elucidated [142].

The involvement of other PLCs in modulating/supplementing PLCZ at fertilization has recently been investigated. Transgenic RNAi studies indicated that oocyte-derived PLC $\beta$ 1 helped in modulating the  $[Ca^{2+}]_i$  response initiated by PLCZ [145]. Considering that only a 30% reduction in PLC $\beta$ 1 protein was achieved it would be interesting to see if a conditional knockout approach reveals a greater involvement of this isoform on modulating/supplementing the oscillation generating activity of PLCZ.

Taken together, the above evidence suggests that PLCZ is the sole factor provided by the sperm that is required to induce oocyte activation.

### **Oocyte activation after SCNT – the artificial way**

Activation of mammalian oocytes after SCNT is absolutely required, as somatic cells do not carry the activity required to induce this event. Thus, numerous procedures have been developed to artificially activate mammalian oocytes [146]. These artificial stimuli were design to induce oocyte activation and early embryonic development. The development of oocytes without the contribution of the sperm is defined as parthenogenesis, and this model has been extensively used to study artificial activation protocols and early embryonic development.

As  $Ca^{2+}$  is a key regulator of oocyte activation, several approaches to artificial oocyte activation rely on inducing a single or repetitive  $[Ca^{2+}]_i$  rise. In

cattle, oocyte activation was successfully achieved through a variety of protocols [146]. The most prevalent protocols induced a single  $[Ca^{2+}]_i$  rise, which can be achieved by physical or chemical ways [29]. Electrical stimulation by administration of direct current (DC) pulses in the presence of exogenous  $Ca^{2+}$  induced  $Ca^{2+}$  influx through pores formed in the plasma membrane [147]. This activation method was successfully used in cloning the first sheep and goats [47, 50]. Treatment of oocytes with ethanol also resulted in  $[Ca^{2+}]_i$  increase and oocyte activation [148]. The most commonly used activation protocols in bovine SCNT utilize a  $Ca^{2+}$  ionophore such as A23187 or Ionomycin [146]. Ionophores allow passive diffusion of  $Ca^{2+}$  through the plasma membrane and the ER and thus induce a single large increase in  $[Ca^{2+}]_i$  [148] (**Figure 1.3**). Because a single  $[Ca^{2+}]_i$  rise is not enough to completely downregulate MPF activity and initiate embryonic development, the  $Ca^{2+}$  stimulus was supplemented with protein kinase or protein synthesis inhibitors [29]. Among them, DMAP, a broad serine/threonine kinase inhibitor, was used after ionomycin treatment to induce high rates of bovine parthenogenetic development [149]. Moreover, this activation treatment was used in production of the first cloned calves [48] and is widely used today. DMAP acts by inhibiting phosphorylation at cdc25 [29]. Cdc25 is required for MPF activation from its inactive form pre-MPF. By inhibiting cdc25, pre-MPF fails to become activated and meiosis arrest is terminated. In spite of the successful use of DMAP, its broad-spectrum of targets may have adverse consequences [29]. For instance, parthenogenetic embryos activated with

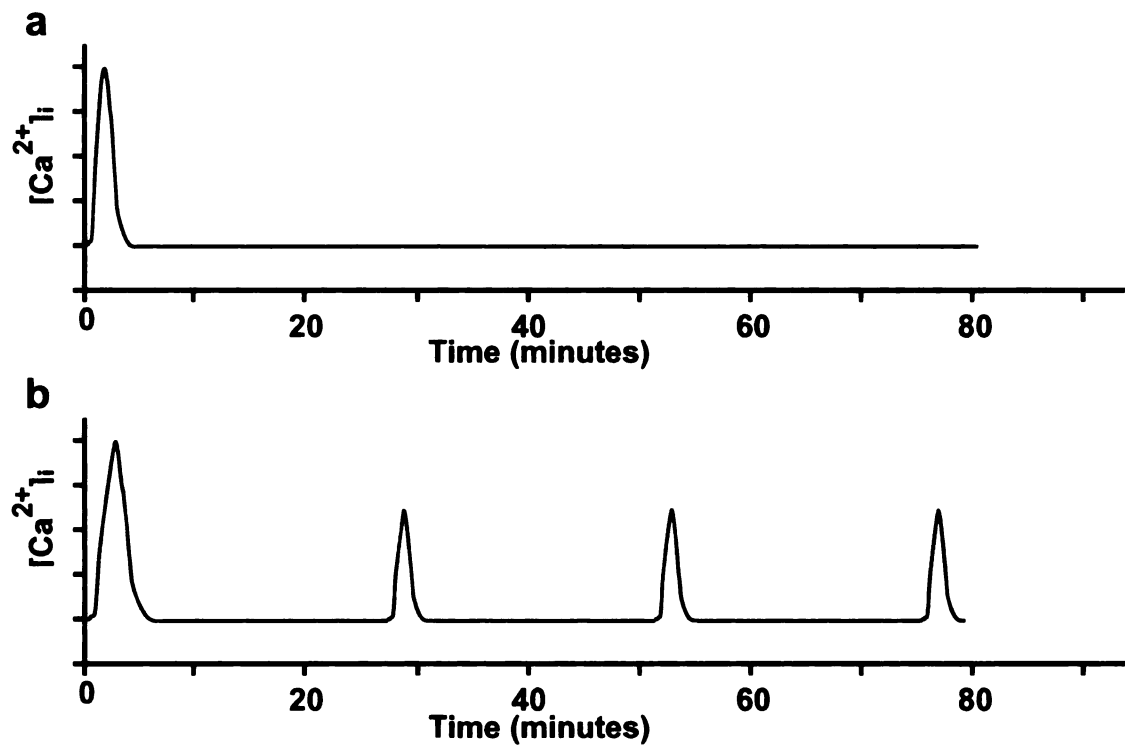


Figure 1.3:  $Ca^{2+}$  response after incubation of MII oocytes with ionophore (a) or after fertilization (b) (data from Nakada and Mizuno [148]).

ionomycin and DMAP often displayed chromosomal abnormalities, with an abnormal pattern of karyokinesis described during the first cell cycle [150]. More specific compounds to target CDKs were also used to activate bovine oocytes. Butyrolactone 1, a natural inhibitor of CDK1, the catalytic unit of MPF, was successfully incorporated in cloning procedures [151]. Other inhibitors were synthesized using combinatorial chemistry [152]. These small molecules, like roscovitine, olomoucine and bohemine, are purine analogs that compete for the ATP-binding site of CDKs, including CDK1 [152]. Incubation with bohemine after ionomycin treatment induced parthenogenetic activation [153] activated SCNT embryos at high rates [154]. However, the derivation of live offspring after activating SCNT embryos using these specific inhibitors was not reported.

Another possible way to inhibit MPF activity is by using protein synthesis inhibitors. Their utility is based on the fact that cyclin B concentrations oscillate during the cell cycle and levels of MPF molecules are dependent on the continued synthesis and degradation of cyclin B. Thus, inhibiting protein synthesis leads to depletion of MPF. CHX is a widely used protein synthesis inhibitor used in activation protocols for mouse, human, pig and bovine oocytes. Moreover, cloned bovine offspring was produced by activating oocytes after SCNT using CHX [155]. However, inhibition of protein synthesis in the early zygote may have adverse consequences. Indeed, initiation of DNA synthesis was delayed in SCNT embryos activated using CHX [156].

Among the systems that induce repetitive  $[Ca^{2+}]_i$  transients,  $SrCl_2$  is routinely used to clone mice [49]. Some evidence indicated that  $SrCl_2$  acts by

sensitizing IP<sub>3</sub>R to low IP<sub>3</sub> concentrations causing the gating of IP<sub>3</sub>R and Ca<sup>2+</sup> release [157]. Unfortunately, SrCl<sub>2</sub> did not elicit [Ca<sup>2+</sup>]<sub>i</sub> oscillations in bovine oocytes [98]. Moreover, in mice the oscillations induced by SrCl<sub>2</sub> treatment were of longer duration than those induced by fertilization and IP<sub>3</sub>R downregulation was not achieved following SrCl<sub>2</sub> treatment, which indicated that the PI pathway was not completely activated [128].

[Ca<sup>2+</sup>]<sub>i</sub> oscillations were also induced by repetitive electrical stimulations. The administration of DC pulses allowed for very precise regulation of [Ca<sup>2+</sup>]<sub>i</sub> transients [24]. Using this system, efficient parthenogenetic development was achieved by mimicking the sperm induced [Ca<sup>2+</sup>]<sub>i</sub> oscillations in mouse and rabbit oocytes [13, 24]. Unfortunately, the delivery of repetitive DC pulses is technically challenging and thus this method has not been implemented to activate cloned embryos.

Other methods to induce repetitive [Ca<sup>2+</sup>]<sub>i</sub> rises include injection of sperm extracts. Activation of SCNT embryos after boar sperm extract injection and production of live offspring was reported. However, [Ca<sup>2+</sup>]<sub>i</sub> oscillations generated from this protocol were short lived and did not induce downregulation of IP<sub>3</sub>R-1, as observed after fertilization [158], and thus incompletely mimicked the fertilization-induced activation stimulus.

Several factors may be implicated in the alterations observed in SCNT derived embryos. However, the activation stimulus should not be ignored as a potential cause of failure in the production of normal cloned animals. The non-physiological pattern of calcium oscillations and the use of non-specific inhibitors

of several metabolic pathways in early zygotes may have negative consequences for embryonic development by inhibiting important uncharacterized processes or by failing to correctly initiate them. Therefore, a method that consistently recapitulates the events taking place after fertilization is needed for the activation of SCNT embryos.

## **CHAPTER 2**

**Pablo J Ross, Gloria I Perez, Tak Ko, Myung-Sik Yoo, and Jose B Cibelli. Full  
Developmental Potential of Mammalian Preimplantation Embryos Is Maintained  
After Imaging Using a Spinning-Disk Confocal Microscope.**

**Biotechniques 2006; 41:741-750<sup>1</sup>.**

<sup>1</sup>Reprinted with permission from Biotechniques



## **CHAPTER 2**

**FULL DEVELOPMENTAL POTENTIAL OF MAMMALIAN PREIMPLANTATION  
EMBRYOS IS MAINTAINED AFTER IMAGING USING A SPINNING-DISK  
CONFOCAL MICROSCOPE**

## **ABSTRACT**

Fluorescent live imaging of cells and embryos at subcellular resolution poses significant challenges for biologists due to morbidity and mortality ensuing from phototoxicity. Here we report the use of a spinning-disk confocal microscope to image mouse and bovine preimplantation embryos without impairing their developmental potential. We also present data indicating that this imaging technique does not affect the functionality of subcellular components as assessed by ROS production, caspase activity and DNA integrity. Spinning-disk confocal microscopy was also useful in determining cell number and allocation in transgenic bovine blastocysts. We conclude that this imaging method is suitable for monitoring preimplantation embryos.

## INTRODUCTION

Fluorescent probes are being used extensively in developmental biology for various imaging techniques, including nontoxic live staining and visualization of expressed fluorescent proteins. These techniques have enabled the identification and tracing of numerous cellular and subcellular structures and molecules. Nonetheless, a number of limitations are associated with the use of existing microscopy techniques. For instance, live cell fluorescence microscopy using laser-scanning confocal microscopy (LSCM) induces embryo damage, as the cells are exposed to high-intensity light [159]. A couple of microscopic techniques that are less toxic to cells lend themselves to exploitation. Two-photon fluorescence microscopy has proven less toxic for live samples and was used by Squirrell and colleagues to image hamster preimplantation embryos with no signs of developmental damage [159]. However, despite its lower phototoxicity, the use of two-photon fluorescence microscopy has been hindered by its high cost and demand for technical expertise. In contrast, spinning-disk confocal microscopy is significantly more affordable and causes no discernable cellular damage and, as a consequence, is becoming the method of choice for dynamic imaging of living cells [160, 161].

The spinning-disk technology uses a Nipkow disk, which was invented in 1884 [162] and adapted for optical microscopy in 1968 [163]. In essence, the spinning-disk apparatus uses the same principle as LSCM to obtain confocal images, i.e., the excitation light goes through a small pinhole and then the fluorescence emission passes back through a pinhole, thus eliminating out-of-

focus light. The main difference of the spinning-disk systems is that they rely on several confocal pinholes mounted on a perforated disc that rotates at high speed, thus merging the fluorescence into one uniform two-dimensional image. As a result, photobleaching and damage to the living cells are minimal. This technology is particularly useful in biological studies that require a high rate of microscopic imaging [160]. Applications of the technique include, among other things, monitoring cytokinesis regulation [164], microtubules dynamics [165],  $\text{Ca}^{2+}$  and cAMP signaling [166] calcium dynamics [167], membrane receptor internalization [168], and microvasculature physiology [169].

We have extended the use of the spinning-disk confocal technology to image live mammalian embryos (mouse and bovine) without compromising their developmental potential. We hypothesize that by using fluorescent markers during preimplantation development, it should be possible to capture high-resolution images that can later be correlated with the developmental competence of the embryos. Such a procedure could be useful for monitoring embryos of certain species, particularly under experimental conditions in which few embryos develop into normal individuals. For instance, only about 20 to 30 percent of bovine two-cell embryos produced by *in vitro* fertilization (IVF) reach the blastocyst stage, and barely half of these generate a pregnancy when transferred into a synchronized recipient [170]. In contrast, ~70 percent of *in vivo*-produced bovine embryos, when transferred to the uterus of a recipient cow, give rise to healthy calves. Likewise, a dramatically lower developmental efficiency is seen in somatic-cell-nuclear-transfer- (SCNT-)derived embryos, in which only 1

to 10 percent of the embryos transferred into the uterus develop into healthy offspring [171]. This implies that most of the *in vitro*-produced embryos are destined to die; yet it remains very difficult to identify the phenotype of a developmentally competent embryo. Therefore, there is an imminent need for an affordable and reliable method to assess preimplantation embryos before they are transferred into surrogate mothers.

Similarly, despite the fact that SCNT has been successfully implemented in several mammalian species, attempts to improve its efficiency are hindered by the lack of reliable markers to indicate when the somatic nucleus transferred into the oocyte has undergone complete genome reprogramming and when the resulting embryo is able to generate a live offspring once transferred into the uterus of a surrogate mother. To date, the only reliable marker for success of complete reprogramming is the birth of a healthy offspring. This implies a long waiting period — at least nine months in cattle — to determine the health status of the cloned offspring; it is therefore of utmost importance to find alternative markers for determining the developmental competence of a cloned preimplantation embryo. Each marker should be easily detectable by noninvasive methods and must be nontoxic to the embryo.

Among traits that have been suggested as potential markers for reprogramming are gene expression and cell number and their allocation (CN&A) to embryonic cell lineages at the blastocyst stage. Gene expression can be also monitored using fluorescent reporters driven by gene-specific promoters. Such an approach has been used in the mouse to identify cloned embryos with higher

chances of generating embryonic stem cells [172]. CN&A are determined, so far, by techniques that require the destruction of the embryos [173] and are inherently limited in terms of correlating any trait with developmental potential. Therefore, we have devised a methodology based on confocal resolution in order to determine blastocyst CN&A without destroying the embryo. This method emanated from our hypothesis that the spinning-disk technology, coupled with standard fluorescent illumination, could provide the required spatial resolution without compromising the viability of the embryo.

Here, we present data on the use of spinning-disk confocal microscopy to image bovine and mouse preimplantation embryos without compromising their *in vitro* development and functionality. In addition, imaged mouse embryos gave rise to healthy offspring. Moreover, this imaging technique allowed us to determine cell number and allocation in live bovine blastocysts, thus facilitating the association of preimplantation phenotypes (e.g., CN&A) with developmental potential.

## **MATERIALS AND METHODS**

### **Chemicals**

All materials were obtained from Sigma Aldrich (Saint Louis, MO) unless otherwise specified.

### **Animals and embryos**

CD1 mouse two-cell embryos were collected from superovulated females

40 to 45 hours after hCG. The embryos were stained with 300 nM Mitotracker Red CMXRos (Molecular Probes, Eugene, OR) for 15 minutes. Outside the incubator and during imaging, embryos were maintained in HEPES-buffered HECM medium [174] (HH; 114 mM NaCl, 3.2 mM KCl, 2 mM CaCl<sub>2</sub>, 0.5 mM MgCl<sub>2</sub>, 0.1 mM Na pyruvate, 2 mM NaHCO<sub>3</sub>, 10 mM HEPES, 17 mM Na lactate, 1X MEM nonessential amino acids, 100 IU/ml penicillin G, 100 µg/ml streptomycin, 3 mg/ml BSA). After imaging, embryos were cultured in KSOM medium (Specialty Media, Phillipsburg, NJ) at 37°C and 5% CO<sub>2</sub>. Blastocyst development was assessed on day 4 after fertilization, and embryos were surgically transferred into the uterus of day 2-3 pseudopregnant CD1 recipients. The pregnancies were allowed to proceed to term, and the number of pups born was recorded.

Bovine embryos were produced by *in vitro* fertilization of oocytes collected from slaughterhouse ovaries. The oocytes were matured in Medium 199 supplemented with 10% FBS (HyClone, Logan, UT), 1 µg/ml of FSH (Sioux Biochem, Sioux, IA), 1 µg/ml of LH (Sioux Biochem, Sioux City, IA), 2.3 mM of sodium pyruvate, and 25 µg/ml of gentamicin sulphate (Gibco, Grand Island, NY) and fertilized *in vitro* using TALP-based medium [175]. Embryo culture was performed in KSOM medium supplemented with 3 mg/ml of BSA, but all manipulations outside the incubator were performed in HH medium. Eight- to 16-cell embryos were collected for staining on day 3 after fertilization. After imaging, the embryos were cultured in KSOM medium supplemented with 3 mg/ml of BSA

and 10% FBS at 38.5°C and 5% CO<sub>2</sub>.

All procedures involving animals were approved by the Michigan State University IACUC (East Lansing, Michigan, USA).

### **Mitochondria imaging**

*In vitro*-generated bovine eight-cell embryos and *in vivo*-produced mouse two-cell embryos were stained with Mitotracker Red CMXRos (300 nM in HH medium for 15 minutes; Molecular Probes, Eugene, Oregon) and individually imaged using a spinning-disc confocal module (CARV, Atto Bioscience, Inc., Rockville, MD) attached to a Nikon TE2000-U microscope and a 40X Plan Fluor oil objective (1.3 NA). The sample was excited with a 120-W metal halide lamp (X-Cite 120, Fluorescence Illumination System; EXFO, Quebec, Montreal, Canada) at full intensity, using a fluorescent filter set (Exciter HQ575/50x, Dichroic Q610LP, Emitter HQ640/50m; Chroma Technology Corp., Rockingham, VT). Images were captured with an EMCCD camera fitted with on-chip multiplication gain (Cascade 512B, Roper Scientific, Tucson, AZ), using MetaMorph software. Sets of exposures of different durations were taken.

### **Measurement of reactive oxygen species**

Reactive oxygen species (ROS) formation was determined through the use of 2', 7'-dichlorodihydrofluorescein diacetate (H<sub>2</sub>DCFDA, Molecular Probes, Eugene, OR). The H<sub>2</sub>DCFDA dye is membrane permeant; upon entering the cell,



the acetate groups are hydrolyzed, creating a membrane impermeant form of the dye (H<sub>2</sub>DCF). When present, endogenous reactive oxygen species will oxidize this polar form of the dye to a quantifiable fluorogenic compound (DCF); by proxy, this represents the level of ROS present in the cell, which can be detected by fluorescent microscopy with excitation and emission settings at 488 and 525 nm, respectively. ROS content was evaluated before and after confocal imaging to determine the amount of ROS generated, and the average fluorescence intensity was measured using MetaMorph software. Embryos were pretreated with 10 nM DCHFDA for 15 minutes prior to imaging. ROS production was calculated as the proportion of fluorescence intensity observed after imaging compared to the level registered just before imaging. To corroborate that the substrate was activating properly, a positive control was included that involved exposing the embryos to epifluorescence for 5 to 10 seconds, which has been previously shown to increase ROS content in embryos [159].

### **Caspase 3 activity assay**

Caspase 3 activity was measured using the cell-permeable fluorogenic substrate (PhiPhiLux-G1D2) according to the manufacturer's recommendations (OncoImmunin, Inc., Gaithersburg, MD). Briefly, after imaging, the embryos were incubated in 10  $\mu$ l of 10  $\mu$ M PhiPhiLux-G1D2 substrate solution in RPMI 1640. After incubation for 1 hour at 37°C in the dark, the embryos were rinsed once in HH medium and imaged using epifluorescence microscopy fitted with FITC fluorescence filters. Average fluorescence intensity was measured using

MetaMorph software (Universal Imaging Corp., Downingtown, PA). As a positive control, embryos were incubated in 100  $\mu$ M H<sub>2</sub>O<sub>2</sub> in HH medium for 1 hour.

### **Pancaspase activity assay**

Active caspases were measured using the Caspatag Pan-Caspase *In Situ* Assay Kit (CHEMICON International, Temecula, CA), following the manufacturer's specific protocol. This reagent is based on the use of a caspase inhibitor that is labeled with carboxyfluorescein (FAM-VAD-FMK). The inhibitor is cell permeable and noncytotoxic; once inside the cell, it binds covalently to active caspases and becomes sequestered in the cytoplasm. Unbound reagent will diffuse out of the cell during the washing steps. The green fluorescent signal is a direct measure of the amount of active caspase(s) present in the cell at the time the reagent was added. After labeling for 1 hour, the embryos were imaged using epifluorescence microscopy fitted with FITC fluorescence filters. Average fluorescence intensity was measured using MetaMorph software. Positive (embryos incubated in 500 mM H<sub>2</sub>O<sub>2</sub> for 1 hour) and negative controls (nonimaged embryos) were included in all assays.

### **Comet assay**

The comet assay was performed to determine the effect of confocal imaging using the CARV system on embryonic DNA integrity. DNA damage was analyzed in whole embryos. The comet assay kit from Trevigen Inc. (Gaithersburg, MD) was used according to the manufacturer's protocol. Briefly,

the embryos were rinsed in PBS solution and placed on the supplied slides. Then, 75 µl of low-melting-point agarose was added. The slide was left at 4°C for 30 minutes for the agarose to solidify. Next, the embryos were lysed in cold buffer and their DNA denatured in alkaline solution (PH > 13). Electrophoresis was performed in neutral buffer (TBE), and finally DNA was stained using SYBR-green. The comets were imaged using a standard epifluorescence microscope with the appropriate excitation and emission filters. The comet length and total intensity were determined using MetaMorph software.

A group of treated embryos and a group of negative controls were loaded separately on each slide. As a positive control, embryos were treated with 500 µM H<sub>2</sub>O<sub>2</sub> in HH medium for 30 minutes.

### **Somatic cell nuclear transfer**

Oocytes that had matured for 16-18 hours were separated from the surrounding cumulus cells by vortexing in HH medium containing hyaluronidase (1 mg/ml) for 5 minutes. All micromanipulations were carried out in HH medium supplemented with 7.5 µg/ml cytochalasin B and 20% FBS (HyClone, Logan, UT). Oocyte enucleation was performed, using a 15-µm (internal diameter) glass pipette, by aspirating the MII plate in a small volume of surrounding cytoplasm. Oocytes were previously stained in KSOM medium containing 5 µg/ml of bisbenzidine for 10 minutes. Enucleation was performed under ultraviolet light to ensure the removal of the oocyte's DNA. Donor cells were dissociated by treatment with 10 IU/ml of pronase in HH media for 5 minutes. A single cell was

inserted into the perivitelline space of the enucleated oocyte using a 20- $\mu$ m (internal diameter) glass pipette. Bovine skin fibroblasts expressing nuclear-targeted HcRed1 protein driven by chicken-beta-actin promoter and CMV enhancer were used as donor cells. Oocyte-cell couplets were fused in sorbitol fusion medium (250mM D-sorbitol, 0.5 mM MgOAc and 1 mg/ml BSA). Oocytes were placed in a fusion chamber with a 0.5-mm gap between electrodes, mechanically aligned, and fused with a single direct current pulse of 200 volts/mm for 15  $\mu$ s.

Activation of the NT units was performed 2-4 hours after fusion by treatment with 5  $\mu$ M ionomycin (Calbiochem, San Diego, CA) for 4 minutes followed by incubation in KSOM media containing 2 mM DMAP for 4 hours. After activation, the NT units were rinsed several times in HH medium and cultured in 400- $\mu$ l drops of KSOM media supplemented with 3 mg/ml of BSA under mineral oil at 38.5°C and 5% CO<sup>2</sup> in air. On day 3 (NT=day 0), the embryo culture drops were supplemented with 10% FBS and cultured under the same conditions until day 7, when blastocysts were recovered for imaging.

### **Plasmid vector construction**

We used a plasmid vector containing a chicken beta-actin promoter and a CMV enhancer driving expression of nuclear localized HcRed1 protein. The CMV promoter of pHcRed1-Nuc plasmid (Clontech, Mountain View, CA) was excised by digesting with AseI and Eco47III restriction enzymes and replaced with a multiple cloning site (MCS) from pBluescript II KS+ plasmid (Stratagene, La Jolla,

CA) which was previously amplified by PCR using T3 and T7 primers. Then, the chicken beta-actin promoter and cytomegalovirus IE enhancer combination (Sal1 to EcoR1) from the pCX-EGFP vector [176] was subcloned into the MCS upstream of HcRed1 protein sequence.

#### **Differential staining for inner cell mass and trophectoderm cell number determination of bovine blastocysts**

The zona pellucida of each blastocyst was removed by incubation in 0.5% pronase for 1 minute. Embryos were exposed to a 1:5 dilution of rabbit anti-pig whole serum for 1 hour, rinsed three times for 5 minutes each in HH media, and placed into a 1:5 dilution of guinea pig complement containing 10 µg/ml of propidium iodide and 10 µg/ml of bisbenzimidazole for 1 hour. After a short rinse in HH media, embryos were mounted in 70 percent glycerol solution on a glass slide under a coverslip. Total cell count and allocation of cells to trophectoderm (TE) and inner cell mass (ICM) lineages were determined using an epifluorescence microscope. TE cells were observed as red nuclei and ICM cells as blue nuclei.

#### **Confocal imaging for ICM and TE cell number determination of bovine blastocysts**

Bovine blastocysts produced by IVF, parthenogenesis, and SCNT were imaged to determine their cell number and allocation using a spinning-disk confocal microscope followed by three-dimensional deconvolution. Imaging was

performed in embryos stained with Syto 16, a cell-permeant nuclear stain (Molecular Probes, Eugene, OR; 5  $\mu$ M in HH medium for 15 minutes) and in transgenic embryos expressing HcRed1 fluorescent protein targeted to the nucleus. Embryos were placed with the ICM facing the objective lens in between two coverslips separated from each other by 150  $\mu$ m. The sample was excited with a 120-W metal halide lamp (X-Cite 120, Fluorescence Illumination System; EXFO, Quebec, Montreal, Canada) using a fluorescent filter set specific for the fluorophores (Syto-16: Exciter HQ470/40x, Dichroic Q495LP, Emitter HQ525/50m; HcRed: Exciter HQ575/50x, Dichroic Q610LP, Emitter HQ640/50m; Chroma Technology Corp, Rockingham, VT). A Z-stack of the embryo was acquired every 5  $\mu$ m using a spinning-disk confocal system, and the images were processed using AutoQuant and MetaMorph software. All nuclei were marked by drawing a contour on the image for each focal plane and were then counted. Nuclei in the periphery of the embryo were assigned to the TE, with the remaining nuclei assigned to the ICM.

### **Statistical analysis**

Fluorescence intensity data and comet length were analyzed by ANOVA, using the MIXED procedure of SAS considering different variances (i.e., heteroskedasticity). Multiple mean comparisons were performed using the Tukey adjustment. Means and standard error of means were used to plot the data. Embryo and pup development were analyzed by chi square test.

## RESULTS

### Viability of preimplantation embryos following confocal imaging

Following imaging using the CARV system (**Figure 2.1**), mouse two-cell embryos did not differ in blastocyst rate formation from stained, nonimaged controls when subjected to a series of 5, 10 or 20 fluorescence exposures taken along the z-axis of the embryo at 50-ms exposures. Surprisingly, embryos stained with MitoTracker had a greater rate of development to blastocysts compared to nonstained embryos. Transferring these embryos to pseudopregnant females did not affect the proportion of pups born (**Table 2.1**). However, there was a tendency for the 20-z, 50-ms exposures to decrease pup rate ( $P=0.085$ ). All pups born reached adulthood and generated healthy offspring.

We found that a set of 20 exposures of 50 ms each is the maximum tolerated by mouse embryos. Beyond this threshold, blastocyst development decreased abruptly and embryos were incapable of generating offspring (**Table 2.1, Figure 2.2A**).

Bovine embryos imaged at the eight- to 16-cell stage showed no differences in blastocyst development (d7.5; day 0=IVF) or number of hatched blastocysts (d11) in comparison with nonimaged embryos (**Table 2.1, Figure 2.3A**). Despite numerous attempts, we were unable to find a level of exposure that disturbed embryonic development in the bovine embryo.

Table 2.1. Embryonic development after confocal fluorescence imaging. Mouse embryos were tested at the 2-cell stage while bovine embryos were evaluated at the 8- and 16-cell stage. All embryos were stained with Mitotracker Red CMXRos and imaged using the CARV system.

Experiment	Treatment	Z planes (n)	Exposure time (ms)	n	BI rate <sup>1</sup>	Hatched BI rate <sup>2</sup>
Bovine 1	Control	-	-	63	36%	36%
	Stained	-	-	49	39%	26%
	30Z-50ms	30	50	56	37%	26%
Bovine 2	Stained	-	-	69	31%	16%
	30Z100ms	30	100	67	33%	18%
	60z100ms	60	100	68	32%	21%
	90z100ms	90	100	68	37%	19%
Bovine 3	Stained	-	-	55	25%	22%
	60z100ms	60	100	56	23%	23%
	60z250ms	60	250	56	29%	25%
	60z500ms	60	500	56	25%	20%
						Pups born <sup>3</sup>
Mouse	Control	-	-	87	79% <sup>a</sup>	17/28 (57%)
	Stained	-	-	106	91% <sup>b</sup>	22/36 (61%)
	5z50ms	5	50	122	96% <sup>b</sup>	37/66 (56%)
	10z50ms	10	50	55	93% <sup>b</sup>	19/39 (49%)
	20z50ms	20	50	54	89% <sup>ab</sup>	11/29 (38%)
	30z50ms	30	50	97	30% <sup>c</sup>	0/27

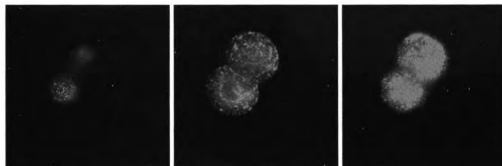
<sup>1,2</sup> Percentage of embryos developing to the indicated stage over embryos imaged. BI = blastocyst

<sup>3</sup> Pups born/embryos transferred. Only pregnant recipients considered.

<sup>a, b, c</sup> Groups with different superscripts were significantly different (P<0.05)



**A**



**B**

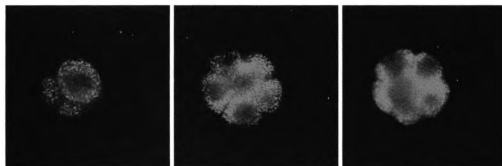
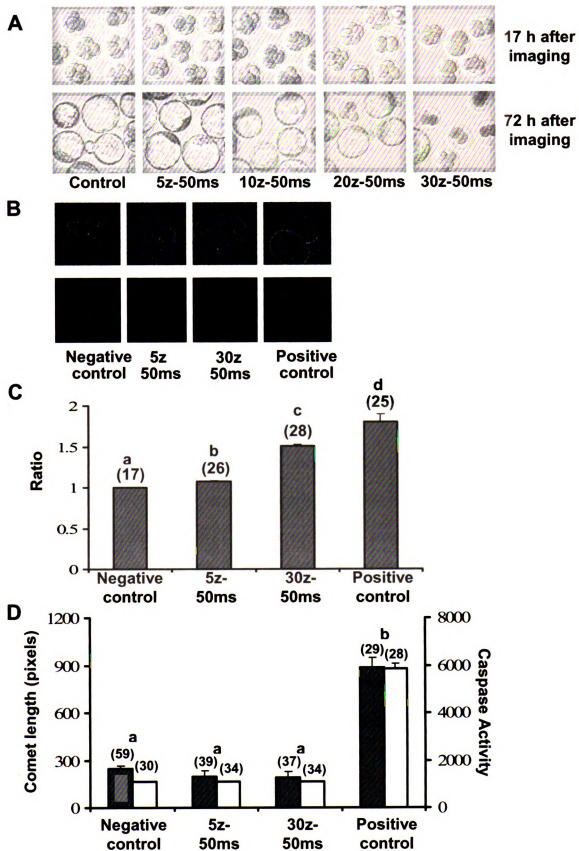


Figure 2.1: Embryos stained with MitoTracker Red and imaged using the CARV system. (A) Mouse two-cell embryo and (B) bovine eight-cell embryo. Different Z-planes of the same embryo are shown.

Figure 2.2: Effect of imaging mouse embryos using a spinning-disk confocal microscope. (A) Brightfield image of embryos at indicated times after imaging. (B) Brightfield and fluorescent images of embryos labeled with DHF for determination of ROS production. (C) Quantitation of ROS production. Bars indicate mean fluorescent intensity of each embryo relative to the intensity before imaging. Positive control = exposure to 5 seconds of epifluorescence. (D) Mean comet length (open bar) and caspase activity (gray bar) of embryos after imaging using the CARV system. Positive control: incubation in 100 mM H<sub>2</sub>O<sub>2</sub> for 1 hour. Different letters indicate statistical differences between treatments (P<0.05).

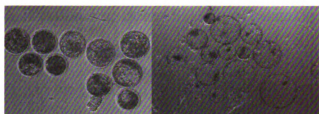
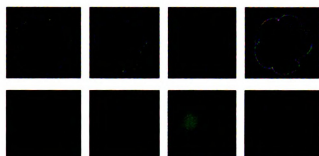
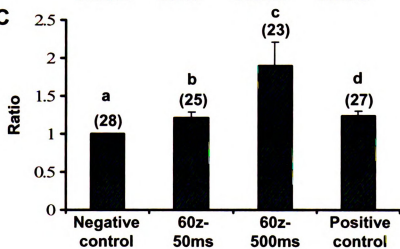
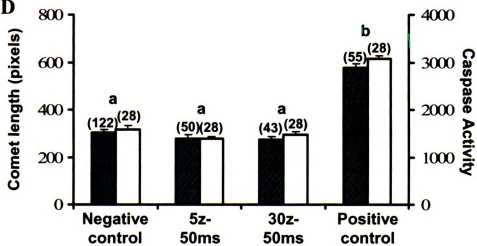


ROS content was evaluated immediately before and after confocal imaging to determine the amount of ROS generated. Mouse embryos exposed to imaging significantly increased their ROS content when compared with nonimaged controls. When the embryos were subjected to 5 or 30 consecutive 50-ms exposures, the increase in ROS content was 7 and 50 percent, respectively, over the levels registered before imaging (**Figure 2.2B,C**). Similarly, a significant increase was observed in bovine embryos after exposure (**Figure 2.3B,C**).

We also evaluated whether high exposure to fluorescent light induces caspase activation directly or following accumulation of ROS. The data revealed that pancaspases (**Figures 2.2D and 2.3D**) and caspase 3 (**Supplementary Figure S1**) were not activated when measured 1.5 hours after imaging.

Since DNA damage could also be induced by fluorescent light or by the accumulation of ROS in imaged embryos, we decided to evaluate DNA integrity using the comet assay [177, 178]. When we evaluated bovine and murine embryos subjected to different exposure conditions, we did not find any differences in the length or intensities of DNA tails (**Figure 2.2D, 2.3D and Supplementary Figure S2**) compared with nonexposed controls. DNA damage was not different among embryos exposed to different levels of imaging.

Figure 2.3: Effect of imaging bovine embryos using a spinning-disk confocal microscope. (A) Brightfield image of blastocysts and expanded blastocysts. (B) Brightfield and fluorescent images of embryos labeled with DHF for determination of ROS production. (C) Quantitation of ROS production. Bars indicate mean fluorescent intensity of each embryo relative to the intensity before imaging. Positive control = exposure to 10 seconds of epifluorescence. (D) Mean comet length (open bar) and caspase activity (gray bar) of embryos after imaging using the CARV system. Positive control: incubation in 500 mM H<sub>2</sub>O<sub>2</sub> for 1 hour. Different letters indicate statistical differences between treatments (P<0.05).

**A****B**Negative  
control60z  
50ms60z  
500msPositive  
control**C****D**

### **Live visualization and quantification of nuclei in bovine embryos**

Currently, 'differential staining' is the only reliable method to differentiate cells that belong to the ICM from those that are TE [173, 179]. Using our spinning-disc confocal microscope, we set out to compare the results obtained using the traditional differential staining with our live staining in the same embryo (**Figure 2.4**). We stained IVF and parthenogenetically activated day 7 bovine blastocysts using Syto16. Z-stack pictures were taken using a spinning-disc confocal microscope. This system produces a good spatial separation, both in XY and Z planes, allowing visualization of individual nuclei in the blastocyst-stage embryo. Complete Z series of optical sections at 5- $\mu$ m intervals were acquired from each embryo. The images stack was then subjected to three-dimensional deconvolution using AutoQuant software, and the nuclei were manually counted. Allocation of nuclei to ICM or TE was based on their position in the embryo. Nuclei located at the periphery of the embryo were considered TE, while the cells in the interior of the blastocyst were considered ICM. Subsequently we performed standard differential staining in the same embryo and correlated the results using both methods. Both techniques for cell counting and allocation agreed greatly. We observed a very high correlation and a slope no different than 1 ( $P > 0.1$ ) for the number of ICM, TE and total cells, and for the ICM:TE cell ratio with regression analysis (**Figure 2.4**). This data indicate that cell number and allocation can be precisely determined in bovine blastocysts using a live imaging system, without destroying the embryo.

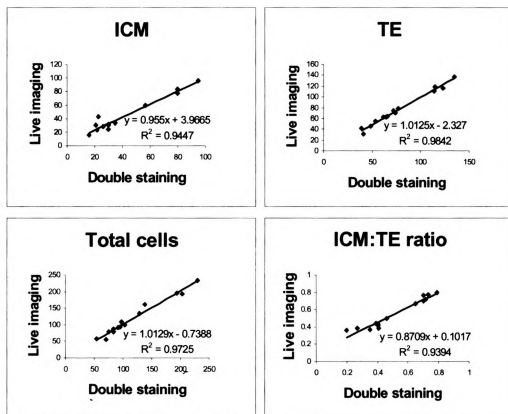
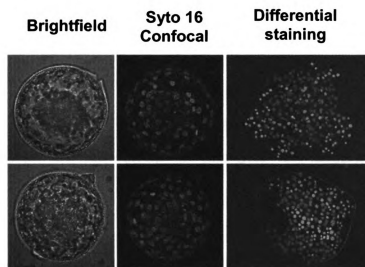


Figure 2.4: Comparison between live imaging and differential staining techniques for counting ICM, TE, and total cell numbers in bovine embryos.



To determine the accuracy of our *in vivo* cell counting method, we stained HcRed-expressing embryos with Syto-16. Subsequently, these embryos were imaged as described, using fluorescent filters for HcRed and for Syto-16. The processed images were compared for each embryo. We found a high level of agreement between HcRed and Syto-16 images for blastocyst cell number and allocation (**Figure 2.5**).

## **DISCUSSION**

Microscopic imaging of live preimplantation embryos constitutes an excellent model for evaluating phototoxicity on cellular proliferation, differentiation, and morphogenesis — processes that are all well delineated in embryos. Moreover, these changes can be easily assessed in a short period of time using simple visualization tools. In the present studies, we chose to use the spinning-disk confocal microscope to image bovine and mouse embryos at their most sensitive stage of development, the time of embryonic genome activation, which occurs at the two-cell stage in mice and at the eight- to 16-cell stage in cattle. After this stage, surviving embryos undergo compaction at the morula stage and, later, cavitation and cell differentiation into the first two embryonic lineages (i.e., ICM and TE) to form a blastocyst. Comparison of the two models, side by side, allowed us to establish significant species differences in the sensitivity of embryos to fluorescent illumination.

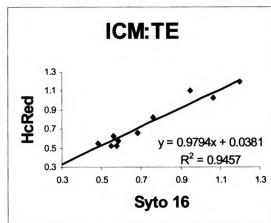
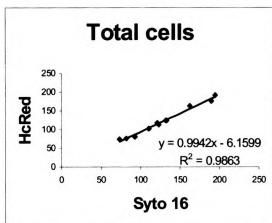
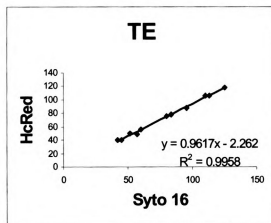
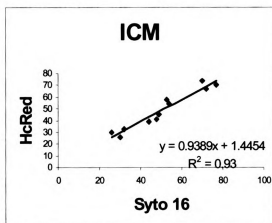
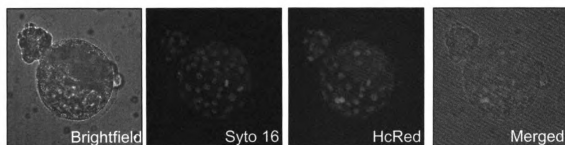


Figure 2.5: Comparison between HcRed and Syto 16 live imaging technique for counting ICM, TE, and total cells in transgenic SCNT embryos.

In general, bovine preimplantation embryos showed an amazing adaptability to stress conditions (e.g., long exposures to fluorescent illumination), which probably reflects the presence and effectiveness of stress protective mechanisms. Although far more sensitive than the bovine embryo, below certain levels of exposure mouse embryos developed and gave rise to live pups at approximately the same ratio as unexposed embryos. We therefore conclude that the spinning-disk confocal microscope is a suitable tool for imaging preimplantation embryos, provided that exposure is limited to a maximum of 20 exposures of 50 ms each.

It should be noted that in the present studies we utilized a spinning-disk confocal microscope that uses a Nipkow disk and standard fluorescent illumination; the spinning-disk confocal apparatus can be also equipped with laser illumination, but this light energy was not used in the present studies. Although we have not compared the two spinning-disk systems, we would expect a higher phototoxicity when imaging using a fluorescent source of higher energy (i.e., lasers). In our case, a mercury halide lamp was used; this source of illumination produces light in a similar spectrum to commonly used mercury arc lamps, but it has greater stability in both the short and long term, and a much longer working lifespan. Our illumination source was used at 100 percent intensity; however, the level of illumination received at the sample was reduced to 7 percent. This reduction is the result of passing the light through the spinning disk that, in this case, acts as a 93 percent ND filter.

Phototoxicity is not a well-understood phenomenon, although it occurs in

most forms of fluorescence microscopy and has been previously associated with ROS production [180]. Light-induced ROS production can occur as a consequence of fluorophores reacting with oxygen or following light-induced damage in cellular components. It has been reported that blue light (450-490 nm) stimulates H<sub>2</sub>O<sub>2</sub> (hydrogen peroxide) production in cultured cells by photoreduction of flavin, which in turn activates flavin-containing oxidases [181]. Both bovine and mouse embryos exposed to imaging significantly increased their ROS content as compared to nonimaged controls. However, only mouse embryos were negatively affected by high levels of cytoplasmic ROS. We speculate that bovine embryos are probably enriched with high levels of cytoplasmic antioxidants and ROS scavengers, allowing them to quickly bring down high cytoplasmic levels of ROS which otherwise could be detrimental for further embryo development.

As the negative effects of imaging on embryo development can be the consequence of both the fluorescent illumination and the excitation of fluorochromes in the sample, we assessed the effect of fluorescent illumination on embryos stained with MitoTracker Red, a mitochondrial probe known to be nontoxic for embryonic development. Here, we also found surprising and significant differences between the two species. While MitoTracker did not have any effect on bovine embryo development, mouse embryos stained with MitoTracker had a greater rate of development to blastocysts. However, the reasons for this remain unknown to us at this time.

Activation of caspases and DNA damage are two major events in

determining the fate of a cell towards apoptosis. However, in the present studies we found no evidence to indicate that the imaging technique affected the functionality of either one of these subcellular components. Therefore, activation of caspases and DNA damage do not appear to be an immediate consequence of exposure to the spinning-disk confocal imaging. The possibility exists, however, that activation of caspases, DNA damage, and apoptosis occur at a later time point or that a mechanism independent of caspases could be activated.

As a possible application of preimplantation embryonic screening, we investigated the possibility of determining cell number and their allocation to embryonic cell lineages at the blastocyst stage in bovine embryos. This characteristic is usually considered as an indication of embryo quality, although no data are yet available to associate cell number and allocation directly with developmental potential of blastocysts. Lack of these kinds of data is a consequence of a technical limitation that could be resolved by the use of the spinning-disk confocal microscopy. Differential staining of ICM and TE cells in mammalian blastocysts can only be performed using differential staining techniques, which can be achieved with a variety of different strategies [173]. However, all of these techniques require the destruction of the embryo and hence are incompatible with embryonic development. Our data indicate that it is possible to determine cell number and allocation in embryos expressing a fluorescent protein targeted to the nuclei. Cell number and allocation were determined by capturing 30 images of 150 ms each at different focal planes. This exposure level represents an exposure to fluorescent illumination well below (~

sixfold lower) the highest exposure level we tested, which resulted in no detrimental effect for *in vitro* bovine embryos stained with HcRed. Unfortunately, the transgenic approach of this methodology limits its application to nuclear-transfer-derived embryos. It would be desirable if a nontoxic, live nuclear staining were available — essentially making this technology amenable to nontransgenic embryos. To that end, we have tested some live nuclear staining alternatives (e.g., Syto16 and Draq5), but found that the staining itself was highly toxic (data not shown).

To our knowledge, this is the first report describing the use of spinning-disk confocal fluorescence microscopy for monitoring mammalian embryos and their development to term. Our results indicate that it is possible to image preimplantation embryos without compromising their developmental potential and functionality. Compared with mouse embryos, bovine embryos showed a greater tolerance to imaging when *in vitro* development was assessed. It remains to be determined whether these embryos are still capable of implanting and developing into healthy offspring when transferred into recipient cows. The use of this technology in embryological studies will enable us to correlate early preimplantation events with subsequent development in the same specimen.

## **ACKNOWLEDGMENTS**

We would like to thank Amy Iager, Zeki Beyhan and Jessica Armstrong for help with oocyte collections, Ricardo Felmer for help with nuclear transfer,

Kerrienne Cunniff for assistance with embryo transfers, and David Smith for technical assistance with the CARV system.

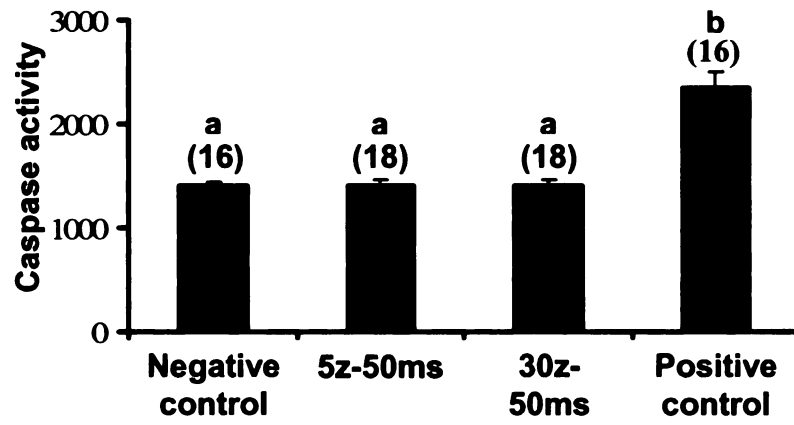
#### **COMPETING INTEREST STATEMENT**

The authors declare no competing interests.

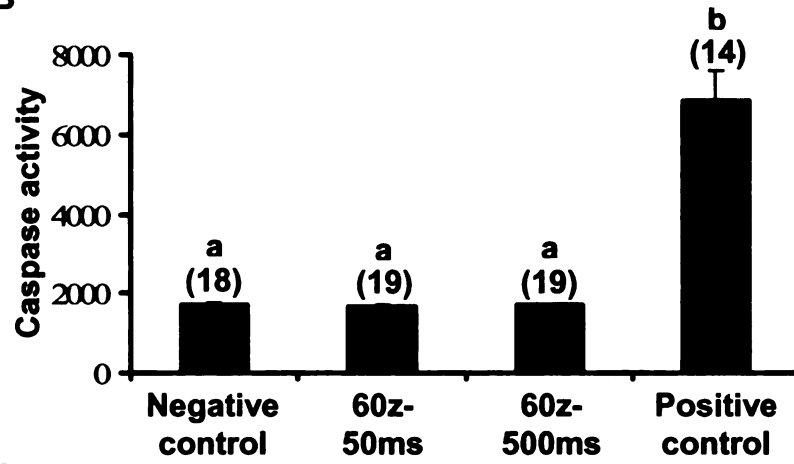
Supplementary Figure S1: Caspase 3 activity in bovine and mouse embryos following exposure to fluorescent imaging using the CARV system. Quantitation of caspase activity in (A) mouse and (B) bovine embryos (above bars, total number of embryos evaluated per group). Different letters indicate statistical differences between treatments ( $P < 0.05$ ). (C) Brightfield and fluorescent images of bovine and mouse embryos after imaging. Caspase 3 activity is determined by fluorescent intensity.



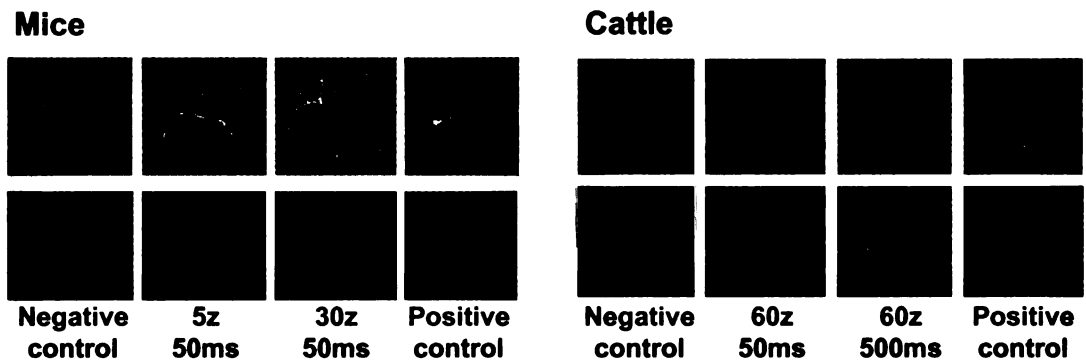
**A**



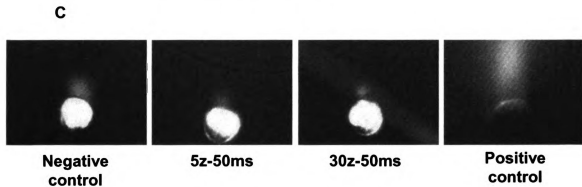
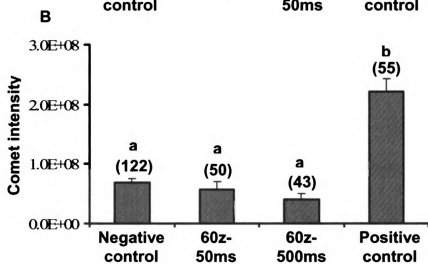
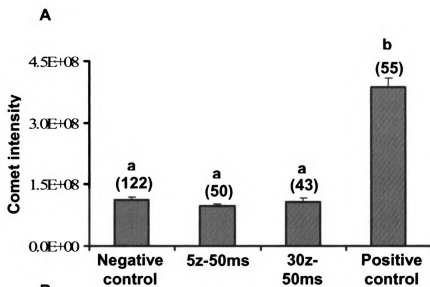
**B**



**C**



Supplementary Figure S2: DNA damage in imaged embryos determined by comet assay. Mean comet fluorescent intensity of individual (A) mouse and (B) bovine embryos measured 1.5 hours after imaging using the CARV system (above bars, total number of embryos evaluated per group). Different letters indicate statistical differences between treatments ( $P < 0.05$ ). (C) Representative images of comet tails observed after imaging mouse embryos using the CARV system. Positive control = incubation in 100 mM  $H_2O_2$  for 1 hour.



## CHAPTER 3

Pablo J Ross, Zeki Beyhan, Amy E Iager, Sook-Young Yoon, Christopher Malcuit, Karl Schellander, Rafael A Fissore, and Jose B Cibelli. Parthenogenetic Activation of Bovine Oocytes Using Bovine and Murine Phospholipase C Zeta.

Submitted for publication to BMC Developmental Biology.

## **CHAPTER 3**

### **PARTHENOGENETIC ACTIVATION OF BOVINE OOCYTES USING BOVINE AND MURINE PHOSPHOLIPASE C ZETA.**

## **ABSTRACT**

**Background:** During natural fertilization, sperm fusion with the oocyte induces long lasting intracellular calcium oscillations which in turn are responsible for oocyte activation. PLCZ has been identified as the factor that the sperm delivers into the egg to induce such a response. We tested the hypothesis that PLCZ cRNA injection can be used to activate bovine oocytes.

**Results:** Mouse and bovine PLCZ cRNAs were injected into matured bovine oocytes at different concentrations. Mouse PLCZ injection activated bovine oocytes at a maximum rate when the pipette concentration of cRNA ranged from 0.25 to 1  $\mu\text{g}/\mu\text{L}$ , while bovine PLCZ was optimal at 0.1  $\mu\text{g}/\mu\text{L}$ . At their most effective concentrations, PLCZ induced parthenogenetic development at rates similar to those observed using other activation stimuli such as Ionomycin/CHX and Ionomycin/DMAP. Injection of mouse and bovine PLCZ cRNA induced sperm-like calcium oscillations, whose frequency increased over time, and were dependent on the concentration of PLCZ cRNA injected. Injection of bovine and mouse PLCZ cRNA induced IP<sub>3</sub>R-1 degradation, although bovine PLCZ was more effective than mouse PLCZ.

**Conclusion:** PLCZ cRNA injection efficiently activated bovine oocytes by inducing a sperm-like calcium oscillatory pattern and IP<sub>3</sub>R-1 downregulation. Moreover, the rate of aneuploidy, usually high in embryos activated by chemical means, was not different from that of fertilized embryos.

## BACKGROUND

Ovulated mammalian oocytes are arrested at the metaphase II (MII) stage of meiosis and only complete meiosis after fertilization. Sperm is responsible for releasing the oocyte from its meiotic arrest and also for inducing other events that are collectively referred to as oocyte activation and include cortical granule exocytosis, reinitiation of meiosis, extrusion of the second polar body, formation of pronuclei, and recruitment of mRNA [13, 14]. In all mammalian species studied so far, activation of oocytes is triggered by repetitive rises in intracellular free- $\text{Ca}^{2+}$  concentration ( $[\text{Ca}^{2+}]_i$ ) [15], a sufficient and indispensable event [16]. The  $[\text{Ca}^{2+}]_i$  rises are generated by release of  $\text{Ca}^{2+}$  from intracellular stores mediated by the inositol 1,4,5-triphosphate ( $\text{IP}_3$ ) signaling pathway [182, 183].

It is hypothesized that upon fusion with the oocyte the sperm introduces a protein factor responsible for inducing production of  $\text{IP}_3$  and  $\text{Ca}^{2+}$  release. A growing body of evidence suggests that the factor the sperm delivers into the oocyte is phospholipase C-zeta (PLCZ) [111]. This PLC variant was sperm specific [17] and induced sperm-like  $[\text{Ca}^{2+}]_i$  oscillations when injected into mouse oocytes [19]. Injection of cRNA coding for PLCZ into mature mouse [17], human [20], and pig [21] oocytes induced  $[\text{Ca}^{2+}]_i$  oscillations and oocyte activation. In mouse sperm, PLCZ localized to the postacrosomal region [19], the area thought to first interact with the oocyte membrane [22]. Functional studies using RNAi to reduce the level of PLCZ in sperm showed that  $[\text{Ca}^{2+}]_i$  oscillations were reduced after intracytoplasmic sperm injection (ICSI) and a lower number of progeny was obtained after natural mating [23]. Finally, in fractionation studies, the presence

of immunoreactive PLCZ correlated with the ability of fractions to induce oocyte activation [19], and immunodepletion of PLCZ from sperm extracts suppressed its  $[Ca^{2+}]_i$  oscillation-inducing ability [17]. Altogether, this evidence indicates that PLCZ delivered into the oocyte upon sperm-oocyte fusion is the factor responsible for oocyte activation.

PLCZ, like other PLCs, catalyzes the hydrolysis of phosphatidyl 4,5-bisphosphate (PIP<sub>2</sub>), producing IP<sub>3</sub> and 1,2-diacylglycerol (DAG). The elevation in IP<sub>3</sub> concentration is responsible for inducing  $Ca^{2+}$  release from the endoplasmic reticulum (ER) upon IP<sub>3</sub> binding to the IP<sub>3</sub>R. The mechanism responsible for maintaining  $[Ca^{2+}]_i$  oscillations for long periods is not clear. However, IP<sub>3</sub>R-1 is believed to play an important role in controlling the duration of  $[Ca^{2+}]_i$  oscillations in mammalian oocytes [111, 130]. Following fertilization, IP<sub>3</sub>R-1 is degraded to about 50 percent the amount of the receptor present in a MII stage oocyte [128, 129]. IP<sub>3</sub>R-1 downregulation contributed to the decreased responsiveness to IP<sub>3</sub> observed after fertilization [131]. Moreover, post-translational modifications of IP<sub>3</sub>R-1 by cell-cycle-dependent kinases also played an important role in reducing IP<sub>3</sub>R-1 activity [132]. While PLCZ clearly triggered  $[Ca^{2+}]_i$  oscillations in the oocyte, its role in regulating IP<sub>3</sub>R-1 was not reported.

Parthenogenesis is the development of an embryo without paternal contribution [184]. When placed in the uterus of a surrogate mother, mammalian parthenogenetic embryos will develop to different stages depending on the species, but never to term [185]. Bovine oocytes can be parthenogenetically activated using ionomycin, ionophore, ethanol, or electric stimuli [29]. All of these



compounds will trigger a monotonic  $[Ca^{2+}]_i$  increase that, while necessary, is not sufficient to completely downregulate the synthesis of Maturation-Promoting Factor (MPF). To accomplish this goal, these  $[Ca^{2+}]_i$  releasing agents must be used in combination with a protein synthesis or protein kinase inhibitor such as cycloheximide or 6-dimethylaminopurine (DMAP), respectively [29]. Using these activation protocols, parthenotes reached the blastocyst stage at reasonable rates; however, the impact these treatments have on *in vivo* development has not been studied, mainly because parthenogenetic embryos are inherently limited in their developmental capacity.

In cattle, immunoreactive PLCZ was found in sperm, and injection of mouse PLCZ cRNA induced  $[Ca^{2+}]_i$  oscillation in oocytes [186]. However, the potential of bovine PLCZ cRNA to induce  $[Ca^{2+}]_i$  oscillations and parthenogenetic activation of bovine oocytes was not reported.

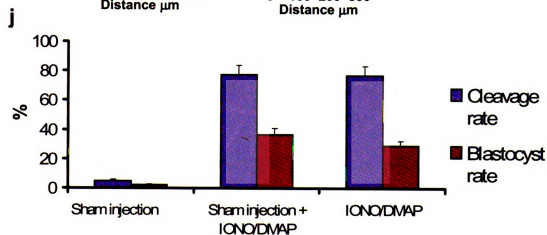
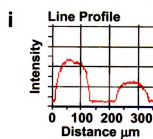
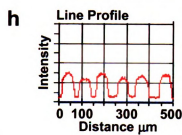
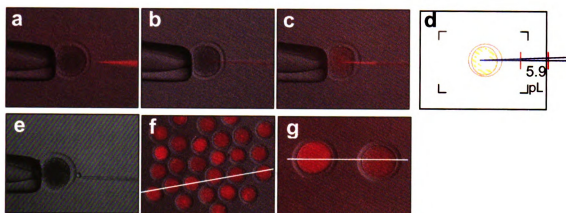
In this study, we report the calcium-oscillation-inducing activity of mouse and bovine PLCZ cRNA injected into bovine oocytes, as well as the effect of their injection on IP3R-1 concentration. We also compared the development of oocytes activated using mouse and bovine PLCZ cRNA to commonly used chemical activation stimuli and compared the effect of the activation protocol on embryo ploidy.

## RESULTS

### Validation of the intracytoplasmic injection technique for bovine oocytes

Intracytoplasmic injections into bovine oocytes represent a challenge because of the high elasticity of the plasma membrane and the opacity and darkness of the bovine oocyte. In this study, we adapted the technique used for ICSI to inject consistent volumes of PLCZ cRNA into bovine MII oocytes. Using this technique, we were able to inject a precise amount of media, confident of having penetrated the plasma membrane. To achieve this, a determined volume of media was loaded into a Fluorinert-filled pipette using a hydraulic microinjector. Then, the pipette was advanced into the oocyte up to about three-quarters of its diameter. By applying negative pressure, the oocyte cytoplasm was slowly aspirated. A well-defined meniscus was observed at the interface of the oocyte cytoplasm and the media when the plasma membrane was intact. When the plasma membrane was broken, the meniscus disappeared, and the flow of cytoplasm into the pipette was faster as a consequence of lower resistance. These indicators were used to determine that the membrane had been penetrated. Then, applying positive pressure, the cytoplasm was injected back into the oocyte, followed by the media containing cRNA (**Figure 3.1a-c**). The volume of media injected was controlled by observing the meniscus at the interface of media and Fluorinert, guided by the reticulum present in the microscope's field of view (**Figure 3.1d**). According to our measurements of the internal diameter of the pipette and the length of the injected column of media, we calculated that the injection volume would be ~ 6 pL.

Figure 3.1: Validation of intracytoplasmic injection technique. a, b, c: Sequence of injection. a) Pipette loaded with Texas Red dextran just before injection. b) Pipette advanced into the oocyte; cytoplasm is aspirated to break the plasma membrane. c) Aspirated cytoplasm and Texas Red dextran are injected into the oocyte. d) Schematic representation of the microscope reticulum used as guide to control the injected volume. The oocyte is represented in yellow and the pipette in blue. The red lines indicate the volume introduced into the oocyte which, calculated measuring the pipette internal diameters at both ends, is 5.9 pL. e) An oil drop of the same size as the injected volume is shown next to an oocyte. f) Oocytes injected using Texas Red dextran. g) From left to right, oocyte injected 2X and 1X the normal volume of Texas Red dextran. h) Fluorescent intensity profile of the line shown in f. i) Fluorescent intensity profile of the line shown in g. j) Developmental rates of injected and uninjected bovine oocytes after activation using ionomycin/DMAP.



Measuring the diameter of oil drops released in aqueous media, we calculated an injection volume of  $7 \pm 0.2$  pL (range 6 to 8.2 pL) (**Figure 3.1e**).

To corroborate the efficiency of the injection technique, we injected Texas Red dextran into the oocytes and then checked, under fluorescence excitation, the number of oocytes that had retained the dye. Out of 101 attempted injections, 99 resulted in successful injection of oocytes with clear red fluorescence in their cytoplasm (**Figure 3.1f**). Subsequent activation of these oocytes — using ionomycin/DMAP — induced parthenogenetic development at similar rates to noninjected controls (data not shown). Moreover, the fluorescence intensity observed in the oocytes was similar among injected oocytes, indicating that the volume of media injected was consistent from oocyte to oocyte (**Figure 3.1f-i**). Finally, parthenogenetically-activated (Ionomycin/DMAP) sham injected oocytes developed at similar rates than noninjected controls (**Figure 3.1j**).

### **Activation and parthenogenetic development of bovine oocytes injected with PLCZ cRNA**

We have previously shown that injection of mPLCZ cRNA into bovine oocytes induced long-lasting  $[Ca^{2+}]_i$  oscillations [186]. However, in those studies, we did not investigate the ability of mPLCZ to induce oocyte activation or parthenogenetic development. In addition, whether or not injection of bPLCZ cRNA could replicate the responses induced by bull sperm was not ascertained. To answer these pending questions, we first determined whether mPLCZ cRNA was able to induce oocyte activation, which was monitored by the extrusion of

the second polar body. When bovine oocytes were injected 22 hours after onset of maturation, extrusion of the second polar body was observed in 100 percent of the oocytes (n=13) within five hours of PLCZ cRNA injection. More importantly, rates of oocyte cleavage to the two-cell stage and pre-implantation embryo development to the blastocyst stage were comparable to those observed for oocytes activated by Ionomycin/DMAP (**Table 3.1**). We next examined whether injection of bPLCZ cRNA was able to induce activation and embryo development of bovine oocytes. As shown in **Table 3.2** (tenth dilutions), bPLCZ effectively induced activation and embryo development to the blastocyst stage. We then investigated whether an association could be established between cRNA concentrations and high rates of pre-implantation embryo development. We first examined tenth dilutions of our cRNA stock and then refined the concentrations to obtain maximum embryo development. Among the concentrations tested, mPLCZ cRNA was most effective when used at concentrations ranging from 0.25 to 1  $\mu\text{g}/\mu\text{L}$  (**Table 3.3**). Injection of bPLCZ cRNAs was effective at inducing bovine oocyte activation and embryo development at concentrations nearly 5-fold lower than those required for mPLCZ (**Tables 3.2 and 3.3**). Importantly, unlike mPLCZ, the highest concentrations of bPLCZ cRNA tested here had negative effects both on cleavage and blastocyst rates (**Table 3.2**).

With the optimal concentrations of m and bPLCZ cRNAs determined, we investigated whether PLCZ cRNAs induced pre-implantation embryo development to the blastocyst stage at rates comparable to those induced by IVF and by frequently used parthenogenetic procedures.

Table 3.1: Parthenogenetic embryo development induced by injection of mouse PLCZ cRNA into bovine oocytes (3 replicates).

	Ionomycin/DMAP	mPLCZ
Oocytes (n)	161	123
Cleavage rate <sup>1</sup>	81	88
Blastocyst rate <sup>1</sup>	18	23
Blastocyst cell number <sup>2</sup>	63 ± 16	75 ± 17

<sup>1</sup> Percentage from activated oocytes

<sup>2</sup> Mean ± standard error

Table 3.2: Optimization of bovine PLCZ cRNA concentration to activate bovine oocytes.

Experiment	bPLCZ cRNA concentration	Replicates	Oocytes injected	Cleavage Rate <sup>1</sup>	Blastocyst Rate <sup>1</sup>
Tenth dilutions	1 µg/ µL	3	110	49.1 <sup>a</sup>	12.7 <sup>a</sup>
	0.1 µg/ µL	3	118	87.3 <sup>b</sup>	29.7 <sup>b</sup>
	0.01 µg/ µL	3	112	69.6 <sup>a</sup>	15.2 <sup>a</sup>
Refined dilutions	0.5 µg/ µL	4	144	70.8 <sup>a</sup>	18.8 <sup>a</sup>
	0.1 µg/ µL	4	154	88.3 <sup>ab</sup>	29.9 <sup>a</sup>
	0.05 µg/ µL	4	145	89.0 <sup>b</sup>	22.8 <sup>a</sup>

<sup>a,b</sup>: Percentages not sharing a common letter within experiment are statistically different ( $P < 0.05$ , *Chi-square* test).

<sup>1</sup> Percentage from activated oocytes.

Table 3.3: Optimization of mouse PLCZ cRNA concentration to activate bovine oocytes.

Experiment	mPLCZ cRNA concentration	Replicates	Oocytes injected	Cleavage Rate <sup>1</sup>	Blastocyst Rate <sup>1</sup>
Tenth dilutions	0.5 µg/ µL	3	123	90.2 <sup>a</sup>	32.5 <sup>a</sup>
	0.05 µg/ µL	3	112	83.9 <sup>b</sup>	8.9 <sup>b</sup>
	0.005 µg/ µL	3	122	48.4 <sup>c</sup>	0.8 <sup>c</sup>
Refined dilutions	1 µg/ µL	3	107	79.4 <sup>a</sup>	33.6 <sup>a</sup>
	0.5 µg/ µL	3	112	92.0 <sup>a</sup>	33.9 <sup>a</sup>
	0.25 µg/ µL	3	110	85.5 <sup>a</sup>	33.6 <sup>a</sup>

a,b,c: Percentages not sharing a common letter within experiment are statistically different (P<0.05, *Chi-square* test).

<sup>1</sup> Percentage from activated oocytes



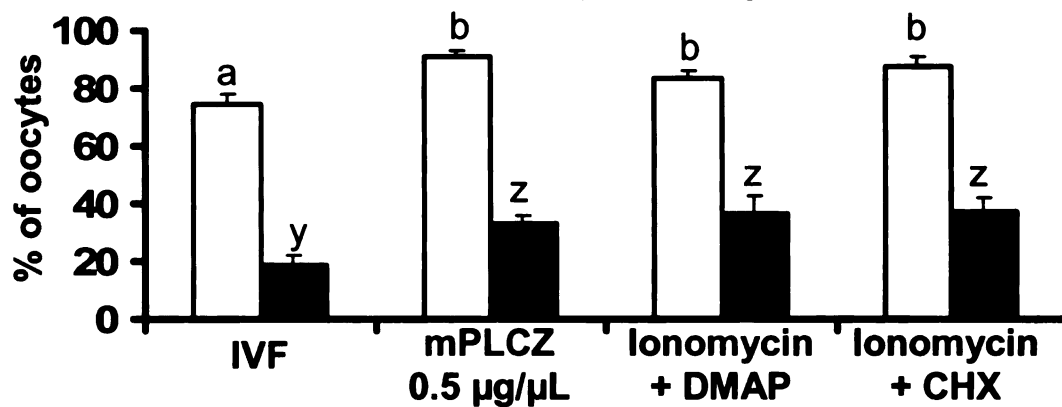
Cleavage and blastocyst rates were similar among parthenogenetic embryos regardless of the activation method (**Figure 3.2a**), and were higher than those achieved by IVF-derived embryos ( $P < 0.05$ ). Also, parthenogenetically activated zygotes consistently cleaved to the two-cell stage at earlier times than IVF embryos (**Figure 3.2b**). Among parthenotes, a higher proportion of DMAP-activated embryos had cleaved by 18 hours postactivation, but no differences were observed thereafter (**Figure 3.2b**). Collectively, our results show that injection of PLCZ cRNAs induces high rates of pre-implantation bovine embryo development.

### **Injection of PLCZ cRNAs induces $[Ca^{2+}]_i$ oscillations and IP<sub>3</sub>R-1 down regulation in bovine oocytes**

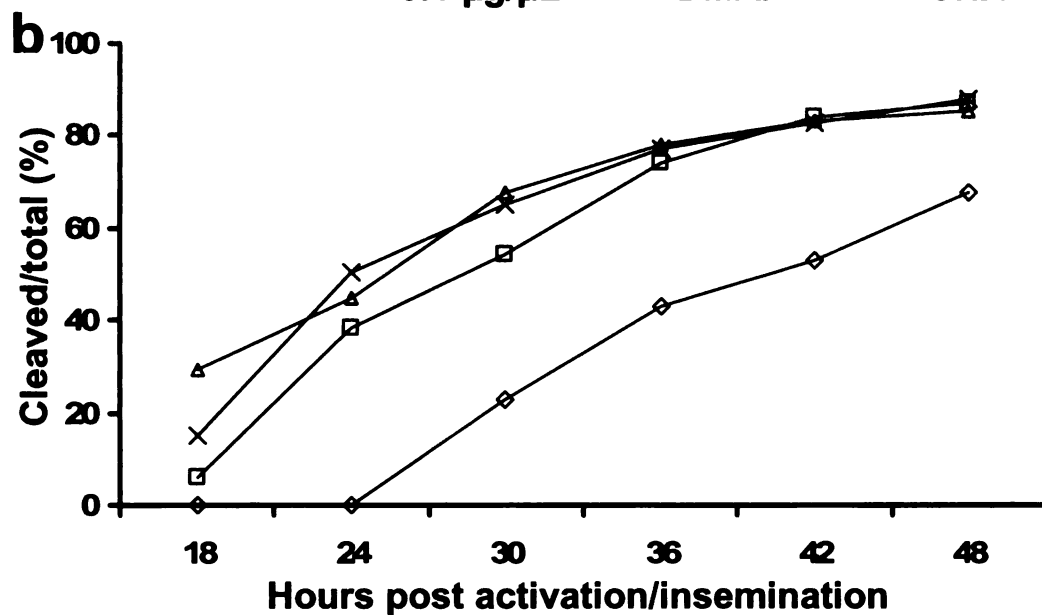
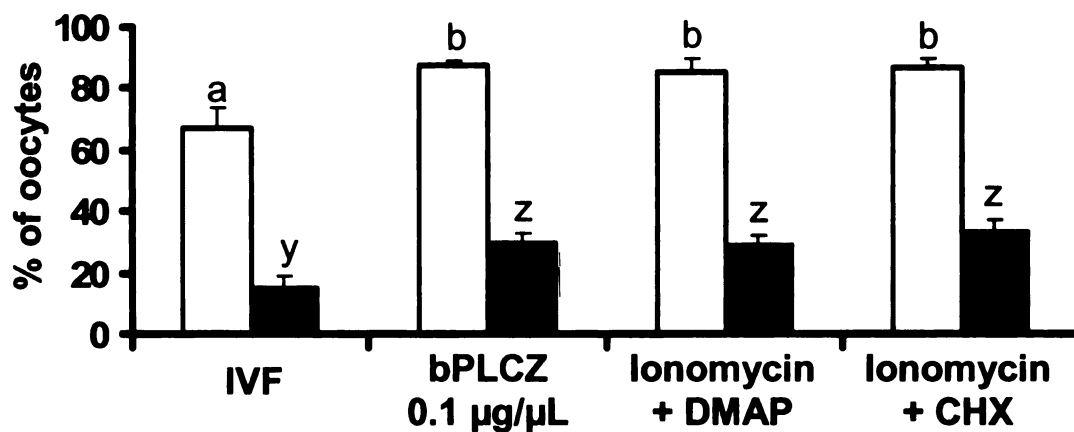
Our previous findings showing that concentration and PLCZ species-of-origin affected the ability of PLCZ cRNAs to induce embryo development suggested that the cRNAs under study were inducing specific  $[Ca^{2+}]_i$  responses, as it is well established that too low or excessive  $[Ca^{2+}]_i$  stimulation negatively impacts embryo development [13, 187]. Thus, we investigated the pattern of  $[Ca^{2+}]_i$  oscillations induced by the cRNA concentrations used to induce embryo development. Our results using mPLCZ extend our previous findings [186] and show that sperm-like oscillations are induced over the first few hours of injection and then transition to a higher frequency of  $[Ca^{2+}]_i$  oscillations, which likely reflects protein accumulation with increased translation time (**Figure 3.3a**). Regarding bPLCZ, the lower cRNA concentration tested (0.1  $\mu\text{g}/\mu\text{L}$ ), which

Figure 3.2: PLCZ cRNA injection induces bovine parthenogenetic development at similar rates to common chemical activation protocols. a) Mean cleavage (open bars) and blastocyst (black bars) rates after IVF or parthenogenetic activation using different methods. Error bar represents SEM. a, b or y, z: different superscripts represent  $P < 0.05$ . b) Cleavage of embryos after IVF or parthenogenetic activation using different methods. Iono = ionomycin; CHX = cycloheximide.

**a** Mouse PLCZ - 6 replicates (1028 oocytes)

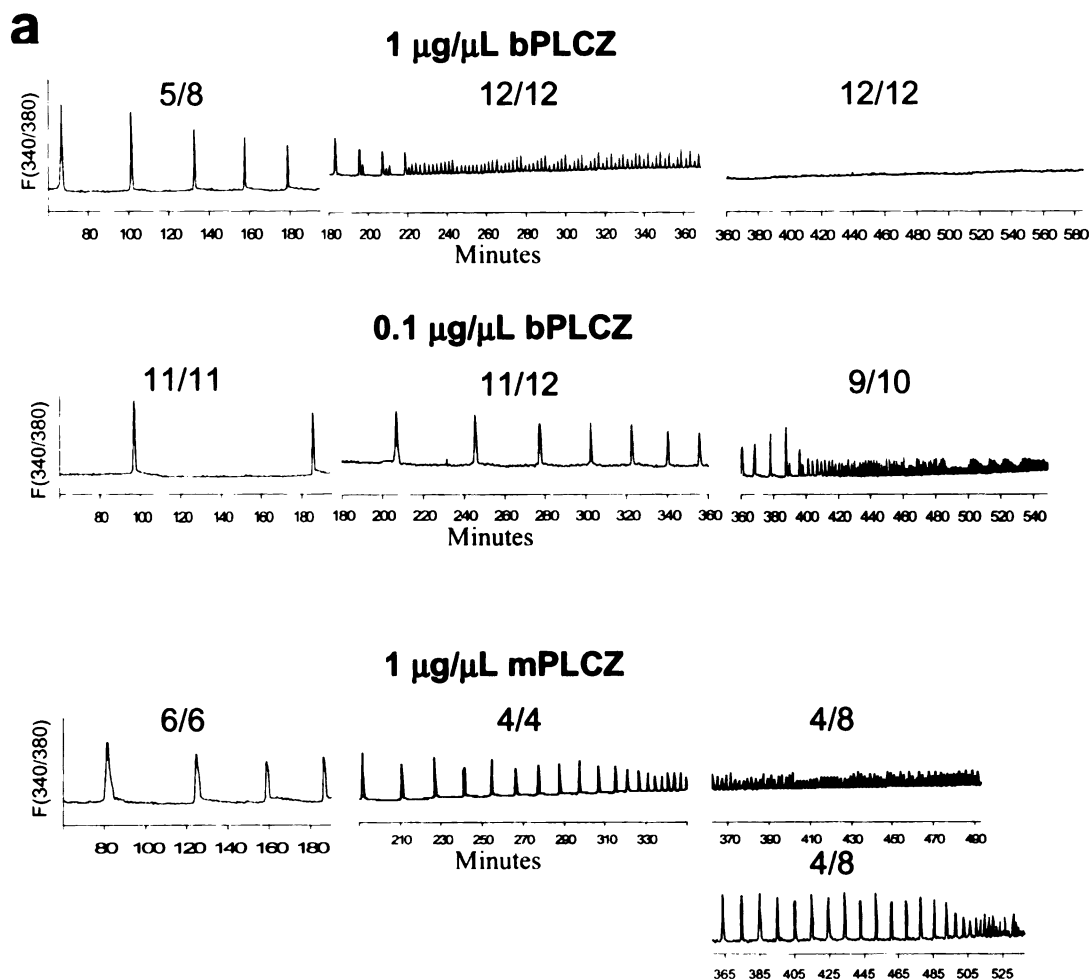


Bovine PLCZ - 7 replicates (1187 oocytes)

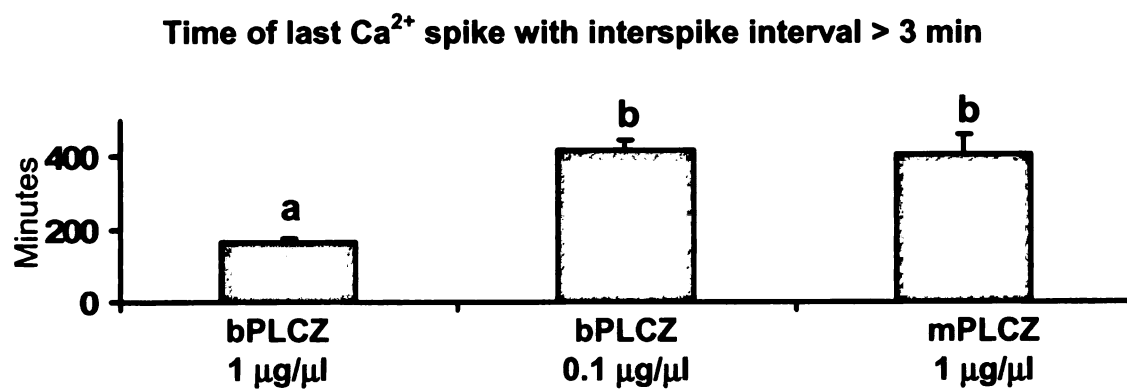


—◇— IVF —□— Iono/CHX —△— Iono/DMAP —×— bPLCZ

Figure 3.3: PLCZ cRNA injection induces sperm-like calcium oscillations. a) Representative  $[Ca^{2+}]_i$  profiles. The fluorescence intensity ratio at 340/380nm is plotted over time (minutes after PLCZ injection). The number above each graph represents the proportion of oocytes analyzed that displayed a similar pattern to that shown. b) Minutes after injection at which the  $[Ca^{2+}]_i$  pattern changed from interspike intervals of > 3 minutes to < 3 minutes for each treatment. Data represented as mean  $\pm$  SEM. Different letters indicate  $P < 0.05$ .



**b**



promoted high rates of embryo development, induced a pattern of oscillations similar to that induced by 1  $\mu\text{g}/\mu\text{L}$  of mPLCZ, and only transitioned to a high frequency of  $[\text{Ca}^{2+}]_i$  oscillations (less than three minute intervals) after 5 to 6 hours post-injection of the cRNA (**Figure 3.3b**). Injection of 1  $\mu\text{g}/\mu\text{L}$  of bPLCZ cRNA induced  $[\text{Ca}^{2+}]_i$  oscillations that transitioned into high frequency oscillations by  $\sim 3$  hours, and in all oocytes evaluated the oscillations ceased completely by 6 hours after injection (**Figure 3.3**). This complete cessation of  $[\text{Ca}^{2+}]_i$  oscillations was not observed during the timeframe analyzed in oocytes injected with 0.1  $\mu\text{g}/\mu\text{L}$  bPLCZ or with 1  $\mu\text{g}/\mu\text{L}$  mPLCZ cRNA.

Fertilization-associated  $[\text{Ca}^{2+}]_i$  oscillations are accompanied by a steady production of  $\text{IP}_3$  [188] that leads to down-regulation of  $\text{IP}_3\text{R-1}$  [128]. Accordingly, we evaluated whether the oscillations induced by injection of PLCZ cRNA resulted in  $\text{IP}_3\text{R-1}$  degradation, and whether the event of  $\text{IP}_3\text{R-1}$  down regulation was associated with PLCZ species-of-origin and concentration. We found that while injections of 0.1  $\mu\text{g}/\mu\text{L}$  bPLCZ or 1  $\mu\text{g}/\mu\text{L}$  mPLCZ cRNA induced fertilization-like loss of  $\text{IP}_3\text{R-1}$  protein (**Figure 3.4**), injection of 1  $\mu\text{g}/\mu\text{L}$  bPLCZ cRNA almost completely depleted  $\text{IP}_3\text{R-1}$  from oocytes (**Figure 3.4**). Together, these results demonstrate that PLCZ injection induced  $[\text{Ca}^{2+}]_i$  oscillations by stimulating  $\text{IP}_3$  production and suggest that, while highly conserved, there is species selectivity in terms of the potency of PLCZ molecules.

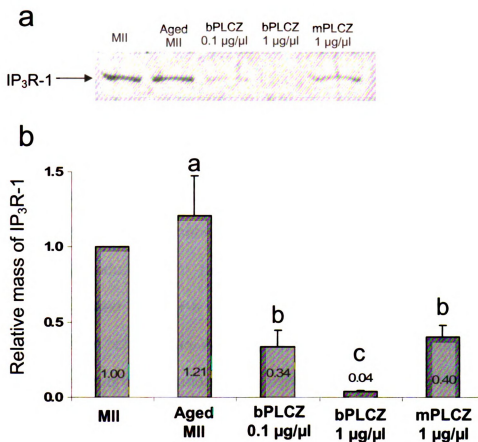


Figure 3.4: PLCZ cRNA injection induces IP<sub>3</sub>R-1 downregulation. a) Immunoblot. Five bovine oocytes were used per lane; samples were collected 12 hours after cRNA injection. MI I oocytes were collected at the time of cRNA injection. Aged MI I are noninjected oocytes that were left in culture the same amount of time as the injected ones. bPLCZ = bovine PLCZ; mPLCZ = mouse PLCZ b) Quantification of relative abundance of IP<sub>3</sub>R-1 versus the levels observed in MI I oocytes. The number in the bars indicates relative IP<sub>3</sub>R-1 mass. Data represented as mean  $\pm$  SEM of two replications. Different letters indicate  $P < 0.06$ .

### **PLCZ cRNA-activated bovine embryos exhibit high degree of normal chromosomal composition**

Activation of development in oocytes of large domestic species in the absence of fertilization requires the successive application of a  $\text{Ca}^{2+}$  ionophore followed by incubation for a few hours with a protein kinase or protein synthesis inhibitor [29]. While these treatments were highly effective at inducing pre-implantation embryo development, they caused high rates of chromosomal abnormalities [189-191]. Given that we have shown that injection of PLCZ cRNAs dose-dependently induce high rates of parthenogenetic pre-implantation development, we asked whether a higher proportion of these embryos showed normal chromosomal composition. Accordingly, we compared the chromosomal composition of eight-cell parthenogenetic embryos generated by injection of PLCZ cRNAs, versus that of embryos activated by two common chemical activation procedures, as well as of IVF-derived embryos (**Table 3.4; Figure 3.5**). Embryos generated using ionomycin/DMAP showed the highest proportion of abnormal ploidy (70%), while embryos activated using ionomycin/cycloheximide (33%) showed a modest amount of aneuploidy when compared to IVF-derived embryos (6 %). PLCZ cRNA-activated embryos exhibited the lowest percentage of aneuploid embryos among the parthenogenetic treatments, although it was not significantly different than CHX activated embryos. Moreover, the percentage of aneuploid embryos generated by PLCZ cRNA injection (25%) was not significantly different than that of IVF-derived embryos. These results



Table 3.4: Chromosomal composition of parthenogenetic 8-cell embryos activated using different protocols.

	Embryos		Informative				Mixoploid			Total	
	Evaluated	embryos	2n	3n	4n	(2n/4n)	Other	Abnormal			
IVF	22	17	16 (94%)	0	1 (6%)	0	0	1 (6%) <sup>a</sup>			
mPLCZ	28	16	12 (75%)	0	4 (25%)	0	0	4 (25%) <sup>ab</sup>			
Iono/DMAP	26	20	6 (30%)	0	10 (50%)	2 (10%)	2 (10%)	14 (70%) <sup>c</sup>			
Iono/CHX	28	18	12 (67%)	1 (5%)	5 (26%)	0	1	6 (33%) <sup>b</sup>			
Total	104	71									

<sup>a,b,c</sup>: Percentages not sharing a common letter within experiment are statistically different ( $P < 0.05$ , Chi-square test).

A total of 167 metaphases were evaluated (2.3 per informative embryo).

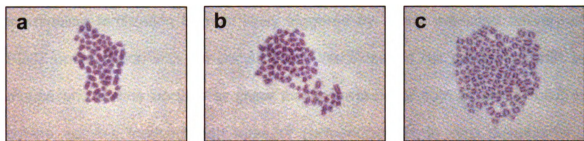


Figure 3.5: Representative chromosomal spreads from 8-cell stage bovine embryos (1000X). a) Diploid cell, b) triploid cell, and c) tetraploid cell.

demonstrated that injection of PLCZ cRNA was effective at inducing development of parthenogenetic embryos that exhibited normal chromosomal composition.

## **DISCUSSION**

A growing body of evidence indicates that oocyte activation during mammalian fertilization is most likely triggered by sperm mediated delivery of PLCZ upon fusion with the oocyte [111]. We extended our previous results in mouse and bovine oocytes to show that expression of both m and bPLCZ in bovine oocytes induced high rates of parthenogenetic in vitro development, consistent with our demonstration that expression of these cRNAs evoked fertilization-like  $[Ca^{2+}]_i$  oscillations in these oocytes. Importantly, significantly lower concentrations of bPLCZ cRNA were required to induce oscillations and parthenogenetic development than mPLCZ, suggesting that while the molecule is highly conserved among mammals, adaptations have occurred that confer higher specific activity within species. Lastly, given the higher proportion of normal chromosomal composition among embryos activated by injection of PLCZ cRNAs versus traditional chemical activation, this procedure might be more desirable for inducing oocyte activation in assisted reproductive techniques such as SCNT and ICSI.

## **PLCZ and parthenogenetic development**

Our results show that a single injection of m or bPLCZ cRNA into bovine oocytes induced high rates of oocyte activation and pre-implantation parthenogenetic development to the blastocyst stage. Notably, the rates of activation, embryonic cleavage, and development to the blastocyst stage were comparable to those observed after chemical activation. Unlike the latter procedures, where the  $[Ca^{2+}]_i$  rise induced by ionomycin was monotonic, and was therefore unable to persistently subdue MPF activity [192], requiring the use of protein synthesis or protein kinase inhibitors to attain complete activation, injection of PLCZ cRNA alone managed to induce all events of oocyte activation. It is worth noting that the effectiveness of PLCZ cRNA was dose-dependent, with either too low or too high of concentrations having detrimental effects on embryo development. Thus, while PLCZ cRNA injection may require dose optimization for the species of interest, it may serve as an advantageous alternative to chemical activation protocols to induce parthenogenetic and somatic cell nuclear transfer embryo development. Moreover, under the latter conditions, since the sperm  $[Ca^{2+}]_i$  pattern will be closely replicated, it would be possible to discern whether or not reprogramming defects commonly associated with nuclear transfer are at all due to aberrant  $[Ca^{2+}]_i$  signaling.

Embryo cleavage and development to blastocyst stage were higher in parthenotes than in IVF-derived embryos. The quality of oocytes utilized for these two procedures may explain these differences. For parthenogenetic activation, oocytes were denuded from the cumulus cells and only MII-stage oocytes (based

on the presence of a polar body) were used. Moreover, this procedure allowed for a stringent selection of good quality oocytes (with evenly granulated cytoplasm). In contrast, for IVF, less strict oocyte selection was performed, as the procedure utilizes cumulus-enclosed oocytes, resulting in insemination of a percentage of immature oocytes that had an inherently lower developmental potential.

IVF-derived embryos cleaved on average six to twelve hours later than those of parthenogenetic origin. During IVF, fertilization takes place within a period of 6 hours after insemination [193], while in the case of parthenotes, the time of activation was synchronized by ionomycin treatment or injection of PLCZ cRNA. Parthenogenetic embryos activated by using a combination of ionomycin/DMAP started to cleave earlier than those activated by ionomycin/cycloheximide treatment. The basis for this difference remains unclear, although a more rapid decline in MPF and MAPK was associated with this treatment [194].

Alterations of the chromosome composition of parthenogenetic bovine embryos are frequently reported [189-191]. Tetraploidy, the most common abnormality observed, may result from fusion of two blastomeres or from nuclear division without cytoplasmic division [195]. The basis for these abnormalities is not clear, but it is well established that the protocol used for oocyte activation affects the rate of aneuploidy [189]. The frequency of aneuploid embryos was greater when DMAP rather than cycloheximide was used in the activation protocol [189], and our study showed analogous results. Injection of PLCZ cRNA

activated bovine oocytes without causing a significant increase in the frequency of aneuploid embryos when compared to IVF-derived embryos. A quarter of PLCZ-activated embryos were tetraploid, which is within the range of chromosomal abnormalities found in bovine IVF embryos (15 to 30 percent) [196, 197]. Importantly, the slight increase in tetraploids observed among PLCZ cRNA-injected oocytes may be due to the use of cytochalasin, the application of which is required to obtain diploidization of parthenogenetically generated zygotes. Collectively, these results suggest that the chemicals commonly used for parthenogenetic activation may be responsible for the higher incidence of aneuploidy observed in bovine parthenotes and SCNT embryos.

### **PLCZ and $[Ca^{2+}]_i$ oscillations in bovine oocytes**

Here we show that injection of PLCZ cRNAs into bovine oocytes induced long-lasting  $[Ca^{2+}]_i$  oscillations that were similar to those induced by the sperm in this species. The injection of the PLCZ cRNAs was directly responsible for the  $[Ca^{2+}]_i$  responses, as  $[Ca^{2+}]_i$  oscillations were precluded when PLCZ cRNA injection took place in the presence of cycloheximide, which inhibited cRNA translation. Likewise,  $[Ca^{2+}]_i$  oscillations were not observed when bovine oocytes were injected with PLC $\delta$ 1 cRNA, a closely related family member (data not shown).

In bovine oocytes, fertilization-associated  $[Ca^{2+}]_i$  oscillations occurred approximately every 20 minutes [198], although variable  $[Ca^{2+}]_i$  oscillations patterns were observed, with one to five  $[Ca^{2+}]_i$  transients recorded during a 60-

minute period [199], possibly due to highly variable oocyte quality. Injection of PLCZ cRNA into bovine oocytes nearly replicated the sperm-induced  $[Ca^{2+}]_i$  oscillatory pattern, at least for the first few hours after injection. Inevitably, and regardless of concentration and species of origin, the frequency of PLCZ cRNA-induced oscillations increased, with oscillations occurring in less than three minute intervals. This change in the pattern of oscillations was likely to reflect protein accumulation as a result of translation of the cRNA and the time at which it occurs was influenced by cRNA concentration and species of origin. Under our conditions, high concentrations of bPLCZ cRNAs had the most dramatic effect, with oscillations ceasing completely by six hours after injection. The underlying mechanism responsible for the termination of the oscillations is not yet clear, although the almost complete downregulation of IP<sub>3</sub>R-1 observed in oocytes injected with 1 µg/µL of bPLCZ cRNA might be a contributing factor [128]. Other factors, such as IP<sub>3</sub>R-1 dephosphorylation [131, 132], or endoplasmic reticulum reorganization [200, 201] cannot be discounted.

It was interesting to note that cRNA concentrations that stimulated too low or too high  $[Ca^{2+}]_i$  of a response induced the lowest cleavage and developmental rates. These data are consistent with findings showing that the pattern of  $[Ca^{2+}]_i$  oscillations affected parthenogenetic oocyte activation events [13, 25, 26]. For example, it was demonstrated that a different number of  $[Ca^{2+}]_i$  transients was required to initiate each event of oocyte activation and that a greater number of transients was needed to complete these events [13]. It is reasonable to speculate that the shorter duration of the oscillatory  $[Ca^{2+}]_i$  transients we

observed with the injection of 1  $\mu\text{g}/\mu\text{L}$  of bPLCZ was not sufficient to initiate and/or complete certain physiological functions required for the development of parthenogenetic embryos to the blastocyst stage. Alternatively, the overwhelming stimulation of the phosphoinositide pathway may be detrimental to unknown cellular functions required for embryo development. Importantly, our observation that excessive  $[\text{Ca}^{2+}]_i$  oscillations induced by injection of PLCZ cRNA resulted in lower cleavage rates and embryo development agrees with previous reports indicating that high concentrations of PLCZ inhibited development of parthenogenetic embryos [20, 144].

The sperm factor is not species specific, as injection of sperm preparations from a variety of mammalian species were able to trigger fertilization-like  $[\text{Ca}^{2+}]_i$  oscillations in oocytes from different species [103, 202, 203]. Consistent with this view, injection of PLCZ cRNA coding for the human, simian, and mouse proteins induced  $[\text{Ca}^{2+}]_i$  oscillations and parthenogenetic development of oocytes from non-homologous species [144]. Here we extended those results and showed that mPLCZ was very efficient at inducing  $[\text{Ca}^{2+}]_i$  oscillations and parthenogenetic development in bovine oocytes. bPLCZ was seemingly much more active in bovine oocytes, as up to a 5-fold lower cRNA concentration was required to induce  $[\text{Ca}^{2+}]_i$  oscillations and activation responses comparable to those induced by mPLCZ. The opposite response was observed when m and b PLCZ cRNAs were injected in mouse oocytes (data not shown). While variations in the activity of PLCZs from different species have been described elsewhere, with human PLCZ being more effective at inducing



$[Ca^{2+}]_i$  oscillations in mouse oocytes than simian or mouse PLCZ [144], this was the first demonstration that a homologous form of the PLCZ protein was more effective within species than across species. Therefore, while the mechanism of initiation of  $[Ca^{2+}]_i$  oscillations in mammals is highly conserved, adaptations have occurred during evolution to carefully orchestrate the early events of oocyte activation, the appropriate conclusion of which will impact embryo development to term.

## CONCLUSIONS

We showed that injection of m and bPLCZ cRNA into bovine oocytes induced  $[Ca^{2+}]_i$  oscillations, IP<sub>3</sub>R-1 downregulation and parthenogenetic development up to the blastocyst stage in a dose-dependent manner. Also, at optimal concentrations, PLCZ cRNAs not only induced parthenogenetic development at rates comparable to those observed after using common chemical activation protocols, but also the generated embryos that exhibit lower levels of aneuploidy. Hence, PLCZ cRNA injection represents an effective tool to parthenogenetically activate oocytes and to decipher the impact of  $[Ca^{2+}]_i$  oscillations on mammalian development.

## METHODS

All chemicals were purchased from Sigma (St. Louis, MO) unless otherwise specified.

### **Oocyte collection and maturation**

Bovine ovaries were obtained from a slaughterhouse and transported in physiological saline solution in an insulated container. Upon arrival at the laboratory, the ovaries were rinsed first with warm tap water and then with physiological saline solution. Antral follicles (2 to 8 mm in diameter) were aspirated using an 18-gauge needle into a 50 mL conical tube by applying 60 mm Hg of negative pressure using a vacuum pump (Cook, Australia). Cumulus oocyte complexes (COCs), with evenly granulated oocyte cytoplasm surrounded by more than four compact layers of cumulus cells, were selected and washed three times in HEPES-buffered HECM medium [174] (HH; 114 mM NaCl, 3.2 mM KCl, 2 mM CaCl<sub>2</sub>, 0.5 mM MgCl<sub>2</sub>, 0.1 mM Na pyruvate, 2 mM NaHCO<sub>3</sub>, 10 mM HEPES, 17 mM Na lactate, 1X MEM nonessential amino acids, 100 IU/mL penicillin G, 100 µg/mL streptomycin, 3 mg/mL BSA). COCs were then matured in Medium 199 supplemented with 10 percent FBS (HyClone, Logan, UT), 1 µg/mL of FSH (Sioux Biochem, Sioux City, IA), 1 µg/mL of LH (Sioux Biochem, Sioux City, IA), 1 µg/mL 17β-estradiol, 2.3 mM of sodium pyruvate, and 25 µg/mL of gentamicin sulphate (Gibco, Grand Island, NY) .

### **PLCZ complementary RNA (cRNA) preparation**

A pBluescript vector containing the full-length coding sequence of murine PLCZ or pGEMT-easy vector of bovine PLCZ was linearized with EcoR1 for mouse PLCZ and Sal I for bovine PLCZ, and used as template for *in vitro* transcription by the T7 mMessage mMachine High Yield Capped RNA

Transcription Kit (Ambion, Austin, TX), following manufacturer instructions. Then, a poly-A tail was added to the cRNA using the Poly(A) Tailing Kit (Ambion). Finally, the cRNA was purified using the Mega Clear Kit (Ambion) and stored at -80°C in single-use aliquots.

Just before use, the cRNA was thawed on ice, heated to 85°C for three minutes, and centrifuged at 13,000 RPM at 4°C for five minutes. Then appropriate dilutions in RNase-/DNase-free water (Ambion) were prepared.

### **cRNA microinjection**

For cRNA injection, a Petri dish containing a 1 µL drop of cRNA and a 50 µL drop of HH under mineral oil was placed on an inverted microscope (TE2000-U, Nikon, Japan) equipped with micromanipulation equipment (Narishige, Japan) at room temperature. After removing the cumulus cells, MII oocytes were placed in the HH media and injected using a beveled micropipette (5 µm internal diameter, MIC-50-0, Humagen, Charlottesville, VA) loaded with Fluorinert, using hydraulic microinjection equipment (Eppendorf, Westbury, NY). cRNA was loaded from the tip of the pipette each time before microinjection. Then, the pipette was advanced into the oocytes and the cytoplasm was aspirated by applying negative pressure to ensure plasma membrane breakage. Finally, the aspirated cytoplasm, followed by the cRNA, was injected into the oocyte by applying positive pressure. The amount of PLCZ cRNA injected was controlled by observing the meniscus at the cRNA-Fluorinert interface.

### **Intracellular calcium monitoring**

Matured oocytes were injected with 0.5 mM Fura-2 dextran (MW 10,000, Molecular Probes, Eugene, OR) as described for PLCZ cRNA. Oocytes were monitored in groups in 100  $\mu$ L drops of protein-free TL-Hepes medium placed on a Petri dish with a glass bottom and covered with mineral oil. A 75 W Xenon arc lamp provided the excitation light and excitation wavelengths were of 340 and 380 nm. Wavelengths greater than 510 nm were collected through a 20X objective by Photometrics CCD SensSys camera (Roper Scientific; Tucson, AZ). Fluorescent intensity ratios (340/380 nm) were measured every twenty seconds for up to three hours using the software SimplePCI (C-Imaging System, Cramberry Township, PA).

### **Western blot of IP<sub>3</sub>R-1**

To assess the down-regulation of IP<sub>3</sub>R-1 protein, cell lysates from 5 bovine oocytes (without cumulus cells) were mixed with 15  $\mu$ L of 2X SB [204], as described previously [131], and stored at -80°C. Thawed samples were boiled for 3 min and loaded onto NuPAGE Novex 3-8% Tris-Acetate gels (Invitrogen, Carlsbad, CA). After electrophoresis, proteins were transferred onto nitrocellulose membranes (Micron Separations, Westboro, MA). The membranes were blocked by incubation in PBS containing 0.1% Tween (PBST) supplemented with 5% non-fat dry milk for 1.5 h at room temperature and then incubated overnight with a rabbit polyclonal antibody raised against the C-terminal amino acids 2735-2749 of mouse IP<sub>3</sub>R-1 (Rbt03) [205]. The

membranes were subsequently washed in PBST and incubated for 1 h with a goat anti-rabbit secondary antibody conjugated with horseradish peroxidase. Membranes were incubated for 1 minute in chemiluminescence reagent (NEN Life Science Products, Boston, MA) and developed according to manufacturer's instructions. The intensities of IP<sub>3</sub>R-1 bands were assessed using a Kodak 440 Image Station (Rochester, NY) and plotted using Sigma Plot (Jandel Scientific Software, San Rafael, CA). The intensity of the IP<sub>3</sub>R-1 band from bovine MII eggs was given the value of 1 and IP<sub>3</sub>R-1 abundance in other samples were expressed relative to abundance in MII oocytes.

### **In vitro fertilization**

COCs matured for 24 hours were co-incubated with sperm ( $10^6$  spermatozoa/mL) in a fertilization medium consisting of IVF-TALP (Tyrode's solution) [175] supplemented with 10 mM sodium lactate, 1 mM sodium pyruvate, 6 mg/ml BSA, 50 µg/mL heparin, 40 µM hypotaurine, 80 µM penicillamine, and 10 µM epinephrine) at 38.5°C in 5 % CO<sub>2</sub> in air for 20 hours. Presumptive zygotes were vortexed for two minutes to separate cumulus cells. Groups of 40 to 50 presumptive zygotes were cultured in 400 µL drops of KSOM (Chemicon, Temecula, CA) supplemented with 3 mg/mL BSA under mineral oil at 38.5°C, 5 % CO<sub>2</sub> in air, and humidity to saturation. Seventy-two hours after insemination, 5 % FBS was added to the culture media.

### **Parthenogenetic activation**

Oocytes that had matured for 20 to 22 hours were separated from the surrounding cumulus cells by vortexing in HH medium containing hyaluronidase (1 mg/mL) for 5 minutes. MII oocytes were selected based on the presence of a polar body. Twenty-two to 24 hours postmaturation, oocytes were injected with PLCZ and cultured 5 hours in KSOM containing 7.5 µg/mL cytochalasin B to generate diploid embryos. For chemical activation the oocytes were exposed to 5 µM ionomycin (Calbiochem, San Diego, CA) in HH medium for four minutes, then rinsed three times in HH medium and allocated to either four hours culture in 2 mM DMAP in KSOM or six hours culture in 10 µg/mL cycloheximide (CHX) and 5 µg/mL cytochalasin B in KSOM. After these treatments, oocytes were rinsed five times in HH media and cultured as described for IVF embryos.

### **Chromosomal Analysis**

Seventy-two hours after activation/fertilization, eight- to sixteen-cell embryos were cultured in KSOM-BSA plus 5 % FBS containing colcemid for 12 to 14 hours. Then, embryos were exposed to a hypotonic 1 % sodium citrate solution for three to five minutes to induce nuclear swelling. Subsequently, embryos were placed on a clean glass slide in a small volume of media. A methanol-acetic acid solution (1:1) was dropped on the embryos while gently blowing with the slides placed under the stereoscope. Then, just before the solution dried, another drop of methanol-acetic acid solution was placed on the embryos and allowed to dry for at least 24 hours at room temperature. After

drying, slides were stained with 5 % Giemsa solution (Invitrogen, Carlsbad, CA) for ten minutes. Chromosome spreads were evaluated at X1000 magnification with oil immersion optics (Nikon, Japan). Embryos were classified as being haploid, diploid, triploid, tetraploid, polyploid, and mixoploid.

### **Statistical analysis**

Cleavage and blastocyst rates were analyzed by chi-square tests when up to 4 replicates were available. When more than 4 replicates were performed, cleavage and blastocyst rate were analyzed using a one-way ANOVA approach in SAS (Carry, NC), with treatment as fixed effect. Similar approach was used also to analyze the continuous variables. Comparisons among treatments were performed using contrast statements. The proportion of embryos with abnormal ploidy was analyzed by a chi-square test.

### **ACKNOWLEDGMENTS**

The authors are extremely grateful to Kim Aebig, Alejandro Dindart, Jenna Kline, Jinni Riggs, and Lauren Stanko for assistance with ovary collections; to Jessica Armstrong for help with oocyte aspiration; and the Cellular Reprogramming Laboratory members for their support during the course of this study. This project was supported by the Michigan State University Experiment Station, The office of the Vice President for Research and Graduate Studies and the MSU foundation to JBC and by National Research Initiative Competitive Grant number 2007-35203-17840 from USDA Cooperative State Research,

Education, and Extension Service and by USDA/Hatch grant to RAF. RAF also received support from NIH/NICHD(#1R01HD051872).



## **CHPATER 4**

# **ACTIVATION OF BOVINE SOMATIC CELL NUCLEAR TRANSFER EMBRYOS BY PLCZ cRNA INJECTION**

## ABSTRACT

The production of cloned animals by the transfer of a differentiated somatic cell into an enucleated oocyte circumvents fertilization. Notably, during fertilization the sperm delivers a sperm-specific phospholipase C (PLCZ) that is responsible for triggering  $\text{Ca}^{2+}$  oscillations and oocyte activation. During bovine somatic cell nuclear transfer (SCNT), oocyte activation is artificially achieved by combined chemical treatments that induce a monotonic rise in intracellular  $\text{Ca}^{2+}$  and inhibit either phosphorylation or protein synthesis. In this study we tested the hypothesis that activation of bovine nuclear transfer embryos by PLCZ improves nuclear reprogramming. Injection of PLCZ cRNA into bovine oocytes reconstructed by SCNT induced  $\text{Ca}^{2+}$  oscillations similar to those observed after fertilization and supported high rates of blastocyst development that resembled embryos produced by IVF. Furthermore, gene expression analysis at the 8-cell and blastocyst stages revealed a similar expression pattern for a number of genes in both groups of embryos. Lastly, we analyzed chromatin modifications at the blastocyst stage and found that the levels of trimethylated lysine 27 at histone H3 were higher in bovine nuclear transfer embryos activated using CHX and DMAP than in those activated using PLCZ or derived from IVF. These results demonstrate that exogenous PLCZ can be used to activate bovine SCNT-derived embryos and supports the hypothesis that a fertilization-like activation response can enhance some aspects of nuclear reprogramming.

## INTRODUCTION

Generation of live offspring after somatic cell nuclear transfer (SCNT) was successfully achieved in numerous mammalian species [1]. However, the overall efficiency of the technology remains extremely low [171]. Failure to correctly reprogram the somatic cell genome following transfer into the oocyte cytoplasm was hypothesized to be a major cause of developmental abnormalities [206, 207]. Nuclear reprogramming is the process by which a specialized nucleus re-acquires developmental potential, adopting the role of a zygotic nucleus. This process involves the silencing of somatic-specific genes and activation of essential embryonic genes [12]. Although the process of nuclear reprogramming is not fully understood, it is becoming more and more evident that epigenetic modifications of chromatin (e.g. methylation and/or acetylation of DNA and histones) are fundamental for regulation of gene expression [9, 208].

In most mammalian species, oocytes are ovulated at the MII stage of meiosis and remain arrested until fertilized by sperm. Initiation of development is triggered by a series of long lasting intracellular free-calcium ( $[Ca^{2+}]_i$ ) oscillations. Several pieces of evidence support the hypothesis that the sperm, upon fusion with the oocyte, delivers a sperm-specific isoform of phospholipase C (PLC $\zeta$ ) [17, 18, 23, 109, 111, 209]. PLC $\zeta$  had the ability to function at basal  $Ca^{2+}$  concentrations [138], and thus, upon entering the oocyte's cytoplasm, induces hydrolysis of phosphatidylinositol-4,5-bisphosphate (PIP $_2$ ) generating 1,2-diacylglycerol (DAG) and inositol-1,4,5-tri-phosphate (IP $_3$ ). In turn, IP $_3$  binds to its receptor (IP $_3$ R), located on the endoplasmic reticulum (ER) membrane and

induces a conformational change that allows the free diffusion of  $\text{Ca}^{2+}$  into the oocyte's cytoplasm. By a yet uncharacterized mechanism,  $\text{Ca}^{2+}$  release and uptake are repeated, generating what is described as  $[\text{Ca}^{2+}]_i$  oscillations. The pattern of  $[\text{Ca}^{2+}]_i$  oscillations at fertilization is species-specific and observed over a relatively long period of time (3–4 hours in mice; 16–18 hours in cattle).

The importance of the  $[\text{Ca}^{2+}]_i$  oscillatory pattern was well-studied in mice and rabbits [24, 25]. Alterations in oocyte calcium signaling not only affected the early events of embryonic development [13, 26], but also gene expression in 8-cell [27] and blastocyst stage embryos [28], implantation [24, 28], and even development to term [28]. It is possible that the long-lasting effect of  $[\text{Ca}^{2+}]_i$  oscillations was mediated by alterations in chromatin structure and reprogramming of gene expression that occur after fertilization [24, 27, 28]. These observations suggest that improper oocyte activation may affect the level of nuclear reprogramming following SCNT.

Most activation protocols commonly used during SCNT rely on chemicals that not only induce a non-physiological  $\text{Ca}^{2+}$ -transient pattern, but also affect other cellular processes, with possible negative consequences for embryonic development [29, 156]. For example, cycloheximide use during activation of bovine SCNT embryos was associated with delayed DNA synthesis [156], and the use of 6-DMAP as the activating agent often resulted in a high proportion of aneuploid embryos [189–191].

We have previously shown that PLCZ cRNA injection into bovine oocyte was able to induce long lasting  $[\text{Ca}^{2+}]_i$  oscillations, IP<sub>3</sub>R-1 downregulation, and

supported high rates of parthenogenetic development to the blastocyst stage (Chapter 3 of this dissertation). In the present study we compared the *in vitro* development, gene expression patterns and epigenetic modifications in SCNT embryos activated by PLCZ cRNA injection with embryos activated by chemical methods or produced by IVF. Although all activation protocols supported oocyte activation and embryo development, embryos activated by PLCZ displayed gene expression profiles and levels of trimethylated lysine 27 at histone H3 that closely resembled IVF embryos.

## **MATERIALS AND METHODS**

All chemicals were purchased from Sigma (St. Louis, MO) unless stated otherwise.

### **PLCZ complementary RNA (cRNA) preparation**

A pBluescript vector containing the full-length coding sequence of murine PLCZ was linearized with EcoR1, and used as template for *in vitro* transcription by the T7 mMessage mMachine High Yield Capped RNA Transcription Kit (Ambion, Austin, TX), following manufacturer instructions. A poly-A tail was then added to the cRNA using a Poly(A) Tailing Kit (Ambion). The cRNA was purified using the Mega Clear Kit (Ambion) and stored at -80°C in single-use aliquots. Just before use, the cRNA was thawed on ice, heated to 85°C for three minutes, and centrifuged at 13,000 RPM at 4°C for five minutes.

## **Somatic Cell Nuclear Transfer**

Oocytes were obtained from abattoir-derived ovaries and matured in vitro as previously described [210]. SCNT was performed as described [210]. Briefly, cumulus cells were removed by vortex agitation in media containing 1 mg/mL hyaluronidase 16-18 hours after oocyte maturation. Oocyte enucleation was performed by aspirating the metaphase II chromosomes in a small volume of surrounding cytoplasm. Donor cells were dissociated by treatment with 10 IU/mL of pronase in HECM-Hepes (HH) media [174] for 5 minutes. A single cell was inserted into the perivitelline space of the enucleated oocyte and fused in calcium-free sorbitol fusion medium by applying a single direct current pulse of 234 volts/mm for 22  $\mu$ s.

## **Activation and embryo culture**

Activation of fused NT units was performed 2 hours after fusion. Three different activation protocols were implemented: 1) Ionomycin/DMAP, 2) Ionomycin/CHX, and 3) PLCZ. In groups 1 and 2, the embryos were treated with 5  $\mu$ M ionomycin (Calbiochem, San Diego, CA) for 4 minutes followed by incubation in KSOM medium containing either 10  $\mu$ g/mL cycloheximide and 5  $\mu$ g/mL cytochalasin B for 5 hours (Ionomycin/CHX), or 2 mM 6-DMAP from 4 hours (Ionomycin/DMAP). Activation using PLCZ was performed by intracytoplasmic injection of ~6-8 pL of 1  $\mu$ g/ $\mu$ L mPLCZ cRNA as previously described (Chapter 3). Then the embryos were cultured in potassium simplex optimized medium (KSOM) containing 7.5  $\mu$ g/ $\mu$ L cytochalasin B for 5 hours to

prevent the extrusion of the second polar body. After activation, the NT units were rinsed several times in hepes buffered-HECM (HH) medium and cultured in 400  $\mu$ L drops of KSOM medium supplemented with 3 mg/mL of bovine serum albumin (BSA) under mineral oil at 38.5°C and 5% CO<sub>2</sub> in air. On day 3 (NT=day 0), the embryo culture drops were supplemented with 10% fetal bovine serum (FBS) and cultured under the same conditions until day 7. Eight-cell and blastocyst stage embryos were collected 50 and 180 h after activation respectively.

Fertilized control embryos were produce by in vitro fertilization using tyrodes albumin lactate pyruvate (TALP)-based medium [175].

### **Intracellular calcium monitoring**

Intracellular  $\text{Ca}^{2+}$  concentration was measured using Fura red. After PLCZ injection, the zygotes were loaded in HH medium containing 2  $\mu$ M Fura red-AM (Invitrogen), 0.02 % Pluronic F-127 (Invitrogen) and 0.5 M sulfinpyrazone for 10 min at 38.5°C. After loading, oocytes were placed in 50  $\mu$ L drops of protein-free HH medium containing 0.5 M sulfinpyrazone on a Petri dish with a glass bottom and covered with mineral oil. During the first 5 hours after PLCZ injection the medium was also supplemented with 7.5  $\mu$ g/mL of cytochalasin B. The Petri dish was placed on a heated stage on a Nikon TE2000-U microscope (Nikon, Tokio, Japan). A 120W metal halide lamp (X-Cite 120) provided the excitation light through fiber optics and excitation wavelengths were of 440 and 490 nm. Wavelengths greater than 600 nm were collected through a 20X

objective by an EMCCD camera fitted with on-chip multiplication gain (Cascade 512B, Roper Scientific). Fluorescent intensity ratios (440/490 nm) were measured every twenty seconds using Metamorph software (Universal Imaging Corp., Downingtown, PA).

### **Blastocysts differential staining and TUNEL assay**

The zona pellucida of each blastocyst was removed by incubation in 10 IU/mL pronase for 2 min. After thoroughly rinsing the embryos in HH medium, they were exposed for 10 seconds to 0.2 % Triton X-100 in PBS containing 2 mg/mL BSA. The embryos were then incubated 15 minutes in PBS-BSA containing 10 µg/mL bisbenzimidazole and 30 µg/mL propidium iodide. After staining, the embryos were fixed in 4 % paraformaldehyde for 15 minutes and stored at 4°C for no more than 7 days until terminal deoxynucleotidyl transferase-mediated dUTP nick-end labeling (TUNEL) assay was performed. TUNEL labeling was performed using the In Situ Cell Death Detection Kit (Roche Applied Science) following manufacturer indications. Briefly, the embryos were exposed to the labeling solution, containing the terminal deoxynucleotidyl transferase and fluorescein-labeled nucleotide mixture, for 1 hour at 37°C in a humid chamber. The embryos were then treated with RNase A (50 IU/mL) for 30 min at 37°C. RQ1-DNase (10 IU/mL)-treated embryos were used as a positive control and negative controls were incubated in labeling solution omitting the enzyme. After intensive washing in PBS-BSA, the embryos were mounted in a small drop of ProLong Gold antifade solution (Invitrogen) and evaluated under epifluorescence



microscopy. Trophectoderm cells were observed as red nuclei, inner cell mass cells as blue nuclei, and TUNEL positive cells as green nuclei.

### **Blastocyst chromosomal analysis**

Embryos were incubated for 12 to 14 hours in KSOM-BSA plus 5 % FBS containing 0.05 µg/mL demecolcine. Then, embryos were exposed to a hypotonic 0.075M KCl solution for five minutes to induce nuclear swelling. Subsequently, embryos were placed on a clean glass slide in a small volume of media. A methanol-acetic acid solution (1:1) was dropped on top of embryos while gently blowing with the slides placed under the stereoscope. Just before the solution dried the slide was submerged in a 3:1 methanol-acetic acid solution for 1 hour, and then allowed to dry at room temperature for 24 hours. After drying, samples were mounted using Prolong Gold antifade solution with diamidino-2-phenylindole (DAPI; Invitrogen). Chromosome spreads were evaluated under epifluorescence at 1000X magnification with oil immersion optics (Nikon, Japan). Embryos were classified as being haploid, diploid, triploid, tetraploid, polyploid, and mixoploid.

### **Cell number determination of live embryos**

The total number of cells in the blastocysts used for gene expression analysis was determined by live confocal microscopy as previously described [210]. Briefly, the nuclei were stained by incubation in HH medium containing 5 µM Syto 16 (Molecular Probes, Eugene, Oregon) for 15 min. Then, the embryos

were placed with the ICM facing the objective lens in between two coverslips separated from each other by 150  $\mu\text{m}$  and imaged using a spinning-disk confocal system (CARV, Atto Bioscience Inc. Rockville, MD) mounted on a Nikon TE2000-U microscope. A Z-stack of the embryo was acquired every 5  $\mu\text{m}$  and the images were processed for 3-D deconvolution using Autoquant and analyzed using Metamorph software. All nuclei were marked by drawing a contour on the image for each focal plane and counted.

### **Quantitative RT-PCR**

Groups of 5 8-cell embryos and individual blastocysts were lysed in 20  $\mu\text{L}$  of extraction buffer, and then incubated at 42°C for 30 min followed by centrifugation at 3000g for 2 minutes and stored at -80°C. Before RNA extraction, each sample was spiked with 2  $\mu\text{L}$  of 250 fg/ $\mu\text{L}$  of HcRed1 cRNA, used as an exogenous control [91], and 50  $\mu\text{g}$  of tRNA as a carrier. Total RNA was extracted from each sample using the PicoPure RNA Isolation Kit (Arcturus) according to the manufacturer's instructions. Residual genomic DNA was removed by DNase I digestion using an RNase-Free DNase Set (Quiagen). RNA was eluted from the purification column using 11  $\mu\text{L}$  of nuclease-free water (Ambion). RNA was then primed with oligo-dT (Invitrogen) and converted into cDNA using Superscript II (Invitrogen) following manufacturer's instructions. Each reverse transcription reaction (RT) was finally diluted with nuclease free water to a final volume of 60  $\mu\text{L}$ .

The quantification of all gene transcripts was done by real-time quantitative RT-PCR using SYBR Green PCR Master Mix (Applied Biosystems, Foster City, CA). Absolute quantification using this method is described elsewhere (Li and Wang, 2000; Whelan et al., 2003). Primer sequences for all the genes are shown in **Table 4.1**.

Each reaction mixture consisted of 2  $\mu$ L of cDNA, 5  $\mu$ mol of each forward and reverse primers, 7.5  $\mu$ L of nuclease free water, and 12.5  $\mu$ L of SYBR Green PCR Master Mix in a total reaction volume of 25  $\mu$ L. Reactions were performed in duplicate for each sample in an ABI Prism 7000 Sequence Detection System (Applied Biosystems). Dissociation curves were performed after each PCR run to ensure that a single PCR product had been amplified.

The copy number of HcRed1 cRNA was determined for each sample using a standard curve constructed from the plasmid pHc-Red1-Nuc. For HcRed, GAPDH, OCT-4, NANOG, SOX2, CDX2 and FGFr2 plasmids containing the partial cDNAs were used to construct standard curves using tenfold serial dilutions. For TRYP8, GLUT1, DSC2 and U2AF1L2 a relative standard curve was used to determine abundance in arbitrary units using serial dilutions of amplified cDNA from a pool of bovine IVF and SCNT blastocysts and fibroblasts.

For each measurement, threshold lines were adjusted to intersect amplification lines in exponential portion of amplification curve using the automatic setting of the thermocycler program. HcRed1 (external control) abundance was determined in each sample and used to normalize for differences in RNA extraction and RT efficiency.

Table 4.1: Primers used for quantitative real time RT-PCR.

Gene	GenBank accession number	Primer sequence	Amplicon size
HcRed [91]		F: 5'-GCCCCGGCTTCACCTTCA-3'	79 bp
		R: 5'-GGCCTCGTACAGCTCGAAGTA-3'	
CDX2	XM_871005	F: 5'-GCAAAGGAAAGGAAATCAACAA-3'	84 bp
		R: 5'-GGGCTCTGGGACGCTTCT-3'	
DSC2	XM_615164	F: 5'-TGTTGCAGCGAACGACAAAG-3'	75 bp
		F: 5'-CCGCAAGTGTCTTAAATTTGG-3'	
FGFr2	XM_880481	R: 5'-CTGGCAGCTAAATCTCGATGAA-3'	86 bp
		R: 5'-GACCTGGTGTGCTGTACCTACCA-3'	
GAPDH [91]	BG691477	F: 5'-GCCATCAATGACCCCTTCAT-3'	70 bp
		R: 5'-TGCCGTGGTGGAATCA-3'	
GLUT1	NM_174602	F: 5'-TCCGGCAGGAGGAGCAAGT-3'	177 bp
		R: 5'-TGCTGAGATCTATCAGTTTGAG-3'	
NANOG	DQ069776	F: 5'-CGTGTCCTTGCAAACGTCAT-3'	66 bp
		R: 5'-CTGTCTCTCCTCTTCCCTCCTC-3'	
OCT4	NM_174580	F: 5'-CCACCCTGCAGCAAAATTAGC-3'	68 bp
		R: 5'-CCACACTCGGACCACGTCCT-3'	
SOX2	NM_001105463	F: 5'-GGTTGACATCGTTGGTAATTTATAATAGC-3'	88 bp
		R: 5'-CACAGTAATTTTCATGTTGGTTTTTCA-3'	
TRYP8	NM_174690	F: 5'-CCACACTCGGACCACGTCCT-3'	83 bp
		R: 5'-AGCCAGCGCAGATCATGTT-3'	
U2AF1L2 [80]	XR_028361	F: 5'-GGAGTAGTCATGAGGCGAGAA-3'	78 bp
		R: 5'-TTCCGCTGCTTTGAGAACTGT-3'	

Blastocyst embryo samples were further normalized to the total cell number of each individual embryo.

### **Immunostaining of embryos**

Embryos were washed in PBS containing 1 mg/mL of PVA, fixed with 4% paraformaldehyde for 15 min in PBS (GIBCO) and stored at 4°C in PBS containing 1 mg/mL of polyvinyl alcohol (PVA) for no longer than 3 weeks. Embryos were permeabilized in 1% Triton X-100 for 30 min at room temperature, then incubated with Image-iT FX signal enhancer (Invitrogen) for 30 min, and blocked with 10% normal goat serum for 2 hours. Embryos were incubated overnight at 4°C in 1% BSA and primary antibodies against trimethylated lysine 27 of histone H3 (H3K27me3; Abcam, ab6002) and acetylated lysine 5 of histone H4 (H4K5Ac; Upstate, 07-327). After 6 h washing in PBS containing 0.1% Triton X-100, embryos were incubated with secondary antibodies conjugated with Alexa 488 and Alexa 594 (Invitrogen) for 1 hour at room temperature. DNA was visualized by bisbenzimidazole staining. For imaging, embryos were mounted in 11 µL of anti-fading solution and compressed with a coverslip. Imaging was performed using a spinning disk confocal system mounted on a Nikon TE-2000 microscope at 40X (numerical aperture (NA) 1.3) and 100X (NA 1.3) magnifications. Optical sections every 1 µm were acquired for each embryo. Metamorph software was used for image acquisition and analysis. All sections were combined by a maximum projection and each nucleus delineated under the blue channel (nuclear staining). Also, two different cytoplasmic areas were

delineated to use as background fluorescence. The regions were then transferred to the red and green channels and the average pixel intensity calculated by the software for each region. For analysis, each region's fluorescence intensity was divided by the average of the two cytoplasmic regions.

### **Statistical analysis**

Continuous response variables were analyzed by ANOVA using the MIXED procedure of SAS (Carry, NC). The models included treatment as fixed effect and a random effect of manipulation day. Rates of embryonic development to cleavage and blastocyst stage were evaluated using a generalized linear model methodology, including the fixed effect of treatment and the random effect of replicate. The analyses were implemented using the GLIMMIX procedure of SAS, assuming a binomial distribution of the response variables and a logit link function.

## **RESULTS AND DISCUSSION**

### **PLCZ triggers fertilization-like $[Ca^{2+}]_i$ oscillations in bovine oocyte reconstructed by SCNT**

We have previously shown that injection of PLCZ cRNA into bovine oocytes induced long lasting  $[Ca^{2+}]_i$  oscillations, downregulation of the IP<sub>3</sub>R-1 and supported parthenogenetic development to the blastocyst stage. In the present study we wanted to extend these findings and confirm whether PLCZ

triggers fertilization-like  $[Ca^{2+}]_i$  oscillations in oocytes reconstructed by SCNT (**Figure 4.1**). During the first 3 hours after injection, a series of  $[Ca^{2+}]_i$  oscillations were observed with intervals of 28 minutes, and then their frequency increased to one oscillation every 8 minutes from 5 to 9 hours after PLCZ injection (**Table 4.2**).

Some oocytes (5/10) stopped oscillating during the recorded period at 9, 10.5, 11, 12, and 13 hours post injection of PLCZ. For those in which oscillations continued, the frequency started to decrease with oscillations occurring every 26 minutes from 11-14 hours post-activation. The initial pattern of oscillations (1-5 hours) was similar to that elicited by fertilization [198, 199]; however, the increased frequency of  $[Ca^{2+}]_i$  oscillations in SCNT embryos between 5 and 9 hours after PLCZ injection is not observed after IVF and likely reflects protein accumulation with increased translation time. The frequency subsequently decreased to a fertilization-like rate, with oscillations lasting for more than 12 hours in most of the embryos.

The ability of PLCZ cRNA injection to induce repetitive  $[Ca^{2+}]_i$  rises provided a method to mimic the sperm-induced oocyte activation stimulus and to test the hypothesis that a more physiological oocyte activation stimulus can improve reprogramming after SCNT. Injection of boar sperm extract into bovine eggs also induced sperm-like  $[Ca^{2+}]_i$  oscillations and was used to activate bovine SCNT embryos. However, the oscillations ceased 5 hours after the injection and IP<sub>3</sub>R-1 downregulation was not observed [158]. In mice,  $[Ca^{2+}]_i$  oscillations and oocyte activation are usually achieved by strontium chloride treatment, which is

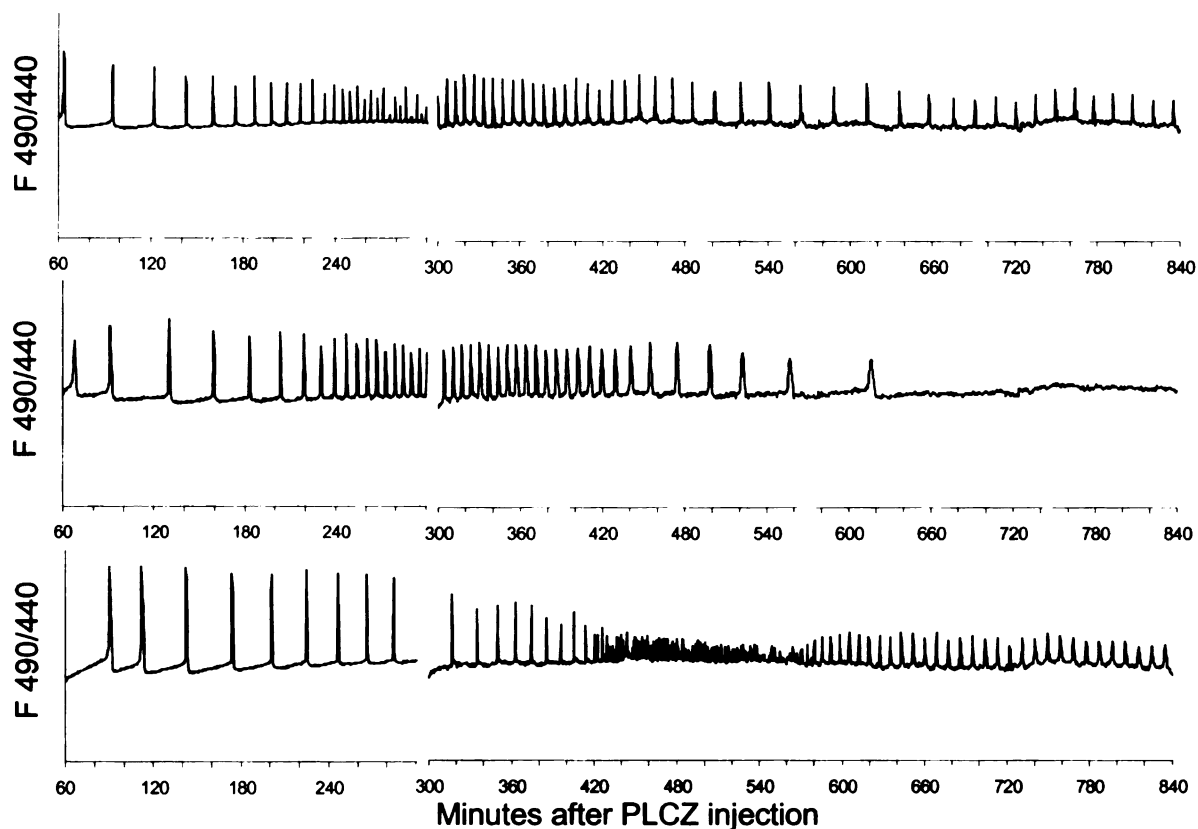


Figure 4.1: Representative  $[Ca^{2+}]_i$  profiles observed in SCNT embryos from 1 to 14 hours after mPLCZ cRNA injection.

Table 4.2: Time interval between  $[Ca^{2+}]_i$  oscillations in SCNT embryos activated using PLCZ cRNA injection.

Time after PLCZ injection	Oscillating oocytes (n)	Mean $\pm$ SEM interval between $[Ca^{2+}]_i$ increases (min)
1 to 3 h:	10/10	28.4 $\pm$ 1.6
3 to 5 h:	10/10	13.2 $\pm$ 2.6
5 to 7 h:	10/10	8.1 $\pm$ 1.3
7 to 9 h:	10/10	8.1 $\pm$ 2.1
9 to 11 h:	9/10	19.8 $\pm$ 5.3
11 to 14 h:	5/10	25.7 $\pm$ 6.3



believed to act by sensitizing IP<sub>3</sub>R to low IP<sub>3</sub> concentrations, causing the gating of IP<sub>3</sub>R and Ca<sup>2+</sup> release. In bovine oocytes however, strontium chloride did not induce [Ca<sup>2+</sup>]<sub>i</sub> oscillations [98]. Moreover, in mice, strontium chloride did not downregulate IP<sub>3</sub>R, suggesting that the PI pathway was not completely activated [128].

Along with our previous observations that PLCZ cRNA induced [Ca<sup>2+</sup>]<sub>i</sub> oscillations, IP<sub>3</sub>R-1 downregulation and parthenogenetic development when injected into MII oocytes (Chapter 3), these data suggest that injection of PLCZ cRNA into oocytes reconstructed by SCNT can be used as an activation stimulus that mimics sperm-induced activation.

### **Embryonic development of cloned embryos activated by PLCZ cRNA injection**

To evaluate whether PLCZ mRNA injection supports activation and in vitro development of bovine SCNT embryos, we injected mPLCZ cRNA into oocytes reconstructed by nuclear transfer and compared cleavage and development rates induced by this treatment with those induced by chemical activation and by in vitro fertilization. Results are presented in **Table 4.3** and representative figures of blastocysts obtained with the different activation protocols are shown in **Figure 4.2**. A total of 769 bovine SCNT embryos were produced in 9 replicates. Equivalent cleavage rates were observed among SCNT groups, ranging from 75.4% to 79.2% (P>0.05). The cleavage rate of IVF (87.0%) embryos was higher

Table 4.3: Preimplantation development of IVF and SCNT derived embryos activated using different protocols.

Treatment	Embryos cultured	Cleaved (%)	Blastocysts (%)
IVF	492	428 (87.0) <sup>a</sup>	125 (25.4) <sup>a</sup>
PLCZ	332	262 (78.9) <sup>b</sup>	92 (27.7) <sup>ab</sup>
Iono/DMAP	327	259 (79.2) <sup>b</sup>	109 (33.3) <sup>bc</sup>
Iono/CHX	329	248 (75.4) <sup>b</sup>	118 (35.9) <sup>c</sup>

a, b, c: Percentages not sharing a common letter are statistically different ( $P < 0.05$ , Chi-square test).

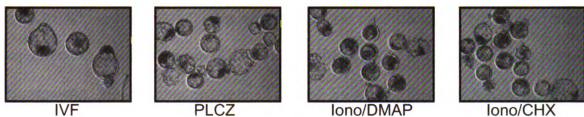


Figure 4.2: Representative pictures of blastocysts generated by IVF and SCNT using different activation protocols.

than those of SCNT embryos ( $P<0.05$ ). Development of the embryos to blastocyst stage was highest for SCNT embryos activated with Iono/CHX and lowest for embryos produced by IVF ( $P<0.05$ ). Although statistically different, all groups produced blastocysts at rates of 25-36% which were comparable to those reported in the literature for IVF and SCNT embryos [6, 48, 155, 211]. Moreover, blastocysts morphology was generally *excellent* and consistent across all treatment groups, according to the international embryo transfer society (IETS) guidelines for evaluation of bovine embryos [212].

Total cell number and number of cells allocated to the TE and ICM were regarded as valuable indicators of cattle embryo quality [173, 213]. A higher total cell number in the embryo correlated with developmental potential of IVF [213] and SCNT embryos [214]. We determined the total number of cells and their allocation to inner cell mass (ICM) and trophectoderm (TE) of expanded/hatched blastocysts. No differences were observed in total, TE, or ICM cell numbers (**Figure 4.3**); however, the ratio of ICM:TE cells was higher in SCNT embryos activated using DMAP than in those activated by using CHX or derived from IVF ( $P<0.05$ ). PLCZ activated embryos did not differ from IVF or SCNT groups. It was suggested that aberrant allocation of ICM and TE cells to the blastocyst stage may be responsible for the abnormalities observed after transfer of SCNT embryos [215]. Similar to our observation, SCNT embryos activated using Ionomycin/DMAP presented a significantly higher ratio of ICM:total cells when compared to IVF and in vivo produced embryos [215]. On the other hand, we observed no differences between embryos activated using Ionomycin/CHX or

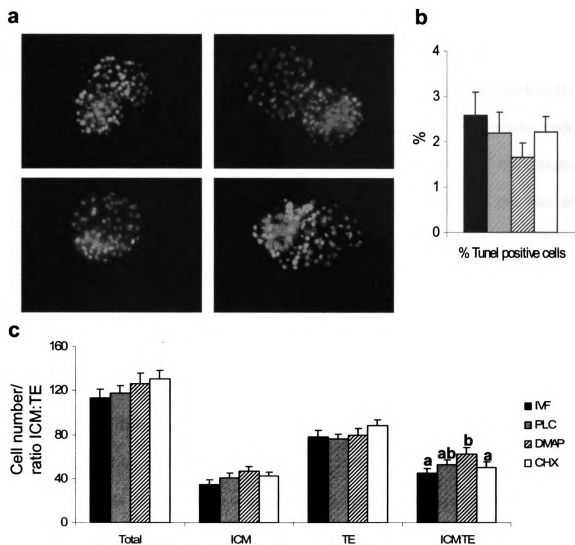


Figure 4.3: Cell number, allocation, and apoptosis in IVF and SCNT embryos produced using different activation methods. a) Representative images of analyzed embryos; ICM (blue), TE (red), and TUNEL positive nuclei (Green). b) Quantification of TUNEL positive cells per embryo. c) Comparison of cell number and allocation among groups. <sup>a,b</sup>: bars not sharing a common letter are statistically different ( $P < 0.05$ ).

PLCZ cRNA injection and IVF controls, which could indicate that SCNT embryos activated by these means may have a better developmental potential.

We also determined the incidence of apoptosis among blastocysts produced with the different activation strategies. The proportion of apoptotic cells in blastocysts, as assessed by TUNEL staining, was similar among all the groups analyzed ( $P>0.05$ ; **Figure 4.3**). Finally, we performed chromosomal analysis at the blastocyst stage because maintenance of normal ploidy is a prerequisite for embryos to develop to term. The fibroblast donor cell line used in this study had a normal diploid chromosomal composition (**Appendix Figure A1**). After SCNT we observed that 86% of the embryos were diploid at the blastocyst stage irrespective of the activation protocol, and similar to IVF-derived embryos (**Figure 4.4; Table 4.4**). This is in contrast to our observations of embryo ploidy at 8-cell stage after parthenogenetic activation. When oocytes were parthenogenetically activated, the rate of aneuploidy was influenced by the activation treatment with a higher incidence of polyploidy in embryos activated using ionomycin/DMAP than with PLCZ cRNA injection (Chapter 3). A similar difference between parthenogenetic and SCNT embryos was previously reported [189], while the basis for this remains unclear.

Taken together these results indicate that PLCZ mRNA injection was an effective method to induce activation of embryonic development after SCNT and that the embryos generated by this method presented similar characteristics to embryos produced by IVF in terms of cell number and allocation, apoptosis and embryo ploidy.

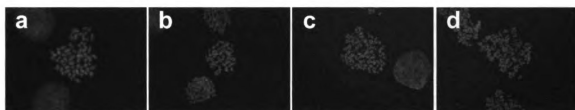


Figure 4.4: Representative blastocyst chromosomal spreads. a, b: diploid chromosome complements, c, d: tetraploid chromosome complements.

Table 4.4: Chromosomal composition of blastocysts activated using different protocols

Treatment	n	Diploid	Tetraploid	Mixoploid	Total abnormal
IVF	15	13	2		2 (13.3%)
PLCZ	12	10	1	1*	2 (16.7%)
Iono/DMAP	12	11	1		1 (8.3%)
Iono/CHX	20	17	2	1#	3 (15.0%)

\* diploid/triploid; # diploid/tetraploid

## **Effect of oocyte activation method on nuclear reprogramming after somatic cell nuclear transfer**

Reprogramming of gene expression involves reactivation of important embryonic genes as well as the repression of somatic cell-specific genes. To test whether the type of activation stimulus has an effect on the reactivation of embryonic genes, we first evaluated the abundance of select transcripts at the 8-cell stage that have been shown to become transcriptionally active during embryonic genome activation. Expression levels in 8-cell embryos were normalized to an external control to account for differences in RNA extraction and RT efficiency.

Gene expression analysis at the 8-cell stage revealed that cloned embryos were able to express desmocollin 2 (DSC2) and glucose transporter 1 (GLUT1) at levels similar to IVF embryos ( $P > 0.05$ ; **Figure 4.5**). Although, GLUT1 expression was affected by the type of SCNT activation protocol, with embryos activated using CHX presenting a higher level of transcripts than those activated by PLCZ cRNA injection ( $P < 0.05$ ). On the other hand, OCT4 (Oct-3, POU5F1) transcript abundance was significantly lower in DMAP-activated SCNT embryos compared to IVF derived embryos. Albeit OCT4 transcripts may be provided by the maternal pool supplied with the oocyte, OCT4 was shown to be expressed at the 8-cell stage in bovine embryos. Thus, a lower level of OCT4 in Ionomycin/DMAP activated-SCNT embryos could represent failure or incomplete initiation of OCT4 transcription.

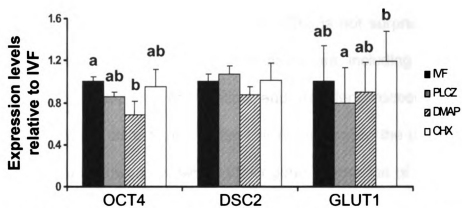


Figure 4.5: Quantification of mRNA abundance in 8-cell embryos generated by IVF or SCNT using different activation protocols. <sup>a,b</sup>: bars not sharing a common letter are statistically different ( $P < 0.05$ ).



We also performed gene expression analysis at the blastocyst stage to compare the level of reprogramming between the embryos activated with the different stimuli. Blastocyst gene expression was compared among IVF and SCNT embryos using RT-PCR [84-87], quantitative real time PCR [88-90], and microarrays [79-82, 216]. However, no clear picture of which genes are consistently misexpressed has yet emerged. This is not surprising considering that several aspects of the nuclear transfer procedure, including donor cell type, type of recipient cytoplasm, enucleation and transfer procedures, activation method, and embryo culture environment diverged among the different studies. Some of these factors were shown to affect gene expression of cloned embryos [80, 84, 86, 87, 89, 216].

We evaluated the expression of genes that are characteristic of the two cell lineages that comprise the blastocyst. OCT4, NANOG and SOX2 have been characterized as important for pluripotency and ICM formation, while the transcription factor CDX2 and the FGF receptor type 2 (FGFR2) have been shown to be expressed specifically in the TE of mouse embryos. We also determined the expression of TRYP8, a gene expressed by the somatic cell but not during preimplantation development of fertilized embryos, and of U2AF1L2, a gene found to discriminate between IVF and SCNT embryos in a previous study [217]. Blastocyst gene expression was normalized to the exogenous control and then to the total cell number in the embryo, as determined just before embryo lysis. We found that GAPDH, OCT4 and CDX2 were expressed at significantly lower levels in CHX activated SCNT embryos than in the other groups (**Figure 4.6**).

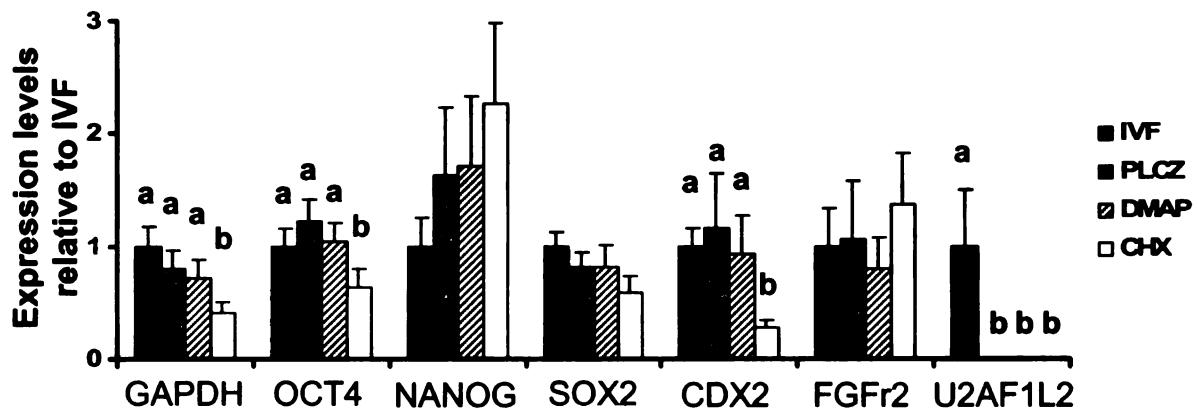


Figure 4.6: Quantification of mRNA abundance in blastocysts generated by IVF or SCNT using different activation protocols. <sup>a,b</sup>: bars with different superscripts indicate significant differences (P<0.05)

It is interesting that the expression of a housekeeping gene (GAPDH), a transcription factor important for ICM development (OCT4), and a transcription factor important for TE development (CDX2) were expressed at lower levels in SCNT embryos activated by ionomycin/CHX compared to the other groups. However, blastocysts activated using Iono/DMAP showed a pattern of gene expression similar to those activated by PLCZ. Thus, this difference can only be attributed to the use of CHX, given that the ionomycin and CB treatment are also included in Ionomycin/DMAP and PLCZ activation protocols, respectively. Moreover, in agreement with our previous report [80], U2AF1L2, a gene involved in RNA splicing, was only detected in IVF embryos, indicating that reprogramming of this locus failed in SCNT embryos irrespective of the activation protocol. Although the role of U2AF1L2 in embryonic development was not investigated, the intrinsic capacity of this gene to affect several cellular processes could lead to potentially serious alterations in the ability of cloned embryos to develop normally. Finally, TRYP8, which was expressed at high levels in the donor cells, was amplified in a higher proportion ( $P < 0.05$ ) of SCNT embryos activated by CHX and DMAP (60% and 62.5%, respectively) than in IVF and SCNT embryos activated using PLCZ (11% and 33% respectively). Expression of donor cell-specific genes was previously observed in cloned mice, suggesting that nuclear reprogramming may be incomplete after nuclear transfer [218]. This epigenetic memory can have adverse consequence for embryonic development, as demonstrated by mouse cloning experiments in which nuclear transfer embryos developed better in donor cell culture medium than in embryo culture

medium [218]. Our finding that a more physiological activation stimulus (PLCZ) resulted in a reduction of somatic gene expression abnormalities provides evidence that oocyte activation may play a role in reprogramming the embryonic genome leading to erasure of somatic cell epigenetic memory. Similarly, it was shown that a more physiological pattern of  $[Ca^{2+}]_i$  oscillations affected gene expression at the blastocyst stage [28] and that the  $Ca^{2+}$  signal was required at an appropriate level to induce translation of maternally stored mRNA in the early zygote [13], potentially affecting the reprogramming of the zygotic chromatin.

Our observation that GAPDH abundance was different between IVF embryos and SCNT embryos activated with ionomycin/CHX raised caution on the use of this gene as a control to normalize gene expression levels in studies comparing fertilized and cloned embryos. This was an interesting result given the fact that in several publications on gene expression analysis in embryos, GAPDH was the only reference gene used. If the employed reference gene fluctuates between samples, the subsequent normalization will produce erroneous results. In our study, the use of an external control gene added before RNA extraction accounted for variability in RNA extraction and RT efficiency. Nonetheless, it must be recognized that differences in sample quality or degradation during storage are not controlled by the exogenous control strategy. Also, the amount of sample material has to be carefully controlled for the external control to be effective. In the case of preimplantation embryos, the number of embryos allocated to each sample can be precisely determined; however, at the blastocyst stage, differences in embryo cell number can alter the initial total RNA input.

Therefore, in our blastocyst samples we normalized gene expression levels to the total cell number of the embryos determined just before RNA extraction. The imaging methodology used for determining the number of cells in live embryos did not compromise the viability of mouse and bovine preimplantation embryos [210]. We have also determined that neither staining with Syto16 nor staining and imaging of the embryos affected the expression of GAPDH of bovine parthenogenetic embryos (**Appendix Figure A2**). Coupled with the use of an external control, our method for cell number determination, although technically demanding, offered a reliable way to normalize gene expression levels, thus allowing the proper interpretation of blastocyst gene expression data.

Although the precise mechanism of nuclear reprogramming after SCNT has not been elucidated, it is known that chromatin remodeling plays a fundamental role. Chromatin remodeling involves changes in acetylation and methylation of histone tails, among other chromatin modifications. In the present study we evaluated genome-wide histone methylation at histone H3 lysine 27 (H3K27me3), associated with gene silencing, and histone acetylation at histone H4 lysine 5 (H4K5Ac), associated with transcriptional activation, by immunofluorescence (**Figure 4.7**). We found that the levels of acetylated histone did not differ among groups; however, the levels of H3K27me3 were higher in bovine SCNT embryos activated using CHX or DMAP compared to those activated using PLCZ or derived from IVF ( $P < 0.05$ ; **Figure 4.7**). Tri-methylation of histone H3 at lysine 27 is catalyzed by polycomb group complexes and is associated with stable and heritable gene silencing [219].

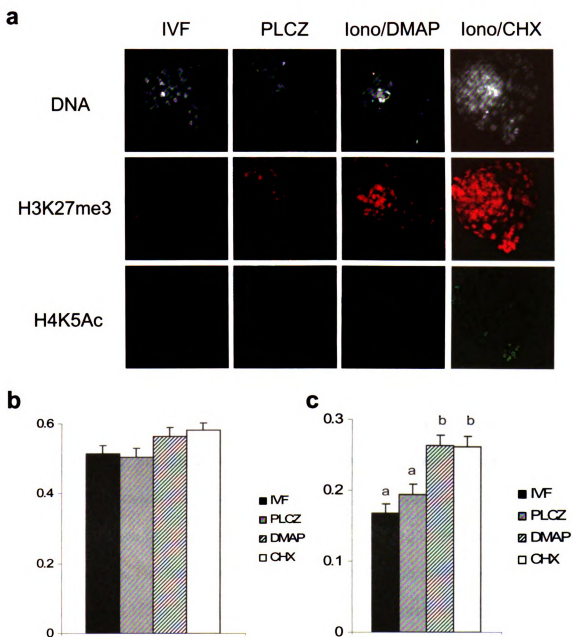


Figure 4.7: Immunofluorescence analyses of IVF and SCNT embryos activated by using different protocols. a) Representative pictures of immunostained blastocyst stage embryos. Semi-quantitative evaluation of b) H4K5Ac and c) H3K27me3 immunostaining. <sup>a,b</sup>: bars with different superscripts indicate significant differences ( $P < 0.05$ ).

We have previously analyzed the levels of H3K27me3 through preimplantation development of bovine IVF, parthenogenetic, and chemically activated SCNT embryos, and found that the levels of H3K27me3 decreased from the PN stage, reaching a minimum at the 8-cell stage, and then increasing at the blastocyst stage in all groups (**Appendix Figure A3 and A4**). In SCNT embryos activated by ionomycin/CHX, the levels reached at the blastocyst stage were significantly higher than those attained by IVF and parthenogenetically derived embryos. Also, donor somatic cell nuclei were stained for H3K27me3 at higher levels than embryonic nuclei (**Appendix Figure A4**). In the present study, we found that the levels of H3K27me3 were similar to IVF embryos when SCNT embryos were activated by a sperm-like stimulus (PLCZ), but higher when we used chemical activation. This observation was in agreement with our gene expression data where chemically activated embryos showed higher levels of somatic gene expression, suggesting that embryos activated by chemical means may retain a somatic-like pattern of epigenetic arrangement compared to PLC activated and fertilized embryos. The mechanism by which the activation system influenced the reprogramming of H3K27me3 represents an interesting area for future research. Moreover, given the importance of H3K27me3 in conferring stem cell identity to embryonic stem cells [220-222], it is tempting to speculate that aberrant H3K27me3 in cloned embryos activated by chemical means may lead to abnormal cell differentiation thus resulting in developmental abnormalities and embryonic lethality.

In summary, we have utilized an oocyte activation treatment (PLCZ cRNA injection) that closely recapitulated the calcium oscillation patterns observed after fertilization. We demonstrate that this treatment supported activation and in vitro development of bovine nuclear transfer embryos at rates comparable to those induced by chemical activation and by fertilization. Also, the embryos activated using this protocol had similar characteristics in terms of cell number, ploidy, apoptosis, and chromatin modifications to in vitro fertilized embryos. Conversely, U2AF1L1 expression was not detected in any of the SCNT groups, indicating that some abnormalities common to SCNT embryos persisted in clones activated by PLCZ cRNA injection. However, most gene expression alterations observed in chemically activated embryos were not evident in embryos activated by PLCZ cRNA injection. Determining the postimplantation developmental potential of SCNT embryos activated by PLCZ cRNA injection will be the subject of future research.



## **CHAPTER 5**

### **SUMMARY AND FUTURE DIRECTIONS**

Somatic cell nuclear transfer remains an inefficient technique in spite of 10 years of research since the first mammal was cloned [1]. This inefficiency was attributed to incomplete reprogramming of the somatic cell nucleus [9, 11, 208]. Nuclear reprogramming is initiated by the recipient oocyte and likely continues through early embryonic development [11]. Alterations of the signaling mechanism leading to oocyte activation and initiation of embryonic development was shown to affect early events of oocyte activation, like mRNA translation [13, 25], as well as fetal and term development [28]; probably by affecting the reprogramming of the zygotic genome. In all mammals studied so far, oocyte activation is characterized by long lasting  $[Ca^{2+}]_i$  oscillations, which persist for several hours [111]. During bovine SCNT, oocytes are usually activated using chemicals that induce a single increase in  $[Ca^{2+}]_i$ , supplemented with broad-spectrum protein synthesis inhibitors or kinase inhibitors [29, 98, 146]. These treatments, which do not recapitulate the signaling events triggered by the fertilizing sperm, may have adverse consequences for nuclear reprogramming and for development of the cloned embryos [29, 98]. We hypothesized that activating bovine SCNT embryos with a system that closely mimics the activation mechanism brought about by the sperm would result in a more efficient nuclear reprogramming. To address this hypothesis we first investigated the nature of the activation signal in the bovine model (Chapter 3), and then implemented a sperm-like activation protocol to induce activation of SCNT embryos (Chapter 4).

PLCZ, which was characterized in mice, humans, and pigs, is believed to be the activation factor the sperm delivers upon fusion with the oocyte at

fertilization. We determined that bovine oocytes responded with  $[Ca^{2+}]_i$  oscillations similar to those induced by fertilization when injected with bovine and mouse derived PLCZ cRNA. Also, injection of PLCZ cRNA induced IP<sub>3</sub>R downregulation, confirming that PLCZ acts through the production of IP<sub>3</sub>. Moreover, we showed that injection of PLCZ cRNA induced parthenogenetic preimplantation development at rates similar to fertilized embryos and parthenogenetic embryos activated by chemical means. We have also determined the most efficient concentrations of the cRNAs to induce oocyte activation. Moreover, by adjusting the concentration of cRNA injected, the  $[Ca^{2+}]_i$  response could be modulated; for example, the duration of  $[Ca^{2+}]_i$  oscillations ceased by 6 hours when 1 µg/µL bPLCZ was used, while it continued for a longer period of time when 0.1 µg/µL of bPLCZ was injected. This system of oocyte activation represents the first long-lasting  $[Ca^{2+}]_i$ -oscillation inducing treatment that can efficiently activate bovine oocytes. This model will be useful to test the effect of  $[Ca^{2+}]_i$  oscillations in early events of bovine oocyte activation. Moreover, because bovine ICSI does not results in oocyte activation, using PLCZ to activate ICSI-derived embryos can potentially improve the development of these embryos, and represents an important model to test the long-term effects of oocyte activation systems and of  $[Ca^{2+}]_i$  oscillation regimens, including embryonic and fetal viability, and even susceptibility of offspring to adult diseases.

Of interest to us was the fact that mouse and bovine PLCZ had a higher activity when introduced into oocytes of the respective species, compared with

cross-species injections. It will be interesting to determine how this molecule interacts with their partners and whether the gene sequence differences among them, which are mainly at the inter-domain regions, play any role in this specificity. The presence of oocyte-specific modulators/activators of PLCZ has been recently suggested, as transgenic mice expressing an ectopic PLCZ gene under a constitutive promoter only showed abnormalities at the ovary characterized by parthenogenetic activation of MII oocytes and development of ovarian tumors of germ cell origin, indicating that only the oocyte has the machinery to translate the PLCZ signal [223]. A stretch of positively-charged amino acids within the X-Y linker region, which also acts as a nuclear localization signal, has been suggested as the possible site of interaction with PLCZ substrate [140]. Importantly, the presence of this region was required to attain maximal enzymatic activity [224], and incubation of PLCZ with a blocking peptide that most likely binds to this region resulted in decreased enzymatic activity [142]. Moreover, the X-Y linker region was recently identified to be a site for proteolysis, generating two fragments which in combination retained high PLC activity [142]. These fragments were detected in sperm and sperm fractions that contain PLC activity, and even in fractions devoid of full length PLCZ [142]. Altogether, these studies suggest that the inter-domain regions and more specifically the X-Y linker region has important regulatory functions for PLCZ activity and it is probably responsible for its specificity. More studies are needed to better characterize the function of this region and to establish the mechanism of its actions.

Having established a protocol of oocyte activation that mimicked sperm induced activation, we set out to test our hypothesis by comparing different characteristics of cloned embryos activated by PLCZ cRNA injection or standard chemical systems and IVF derived embryos. The ultimate measure of nuclear reprogramming is the generation of live offspring; however, embryo transfer in cattle is time consuming and expensive. Consequently, providing in vitro evidence is a necessary step to justify such endeavor. In this study we established that PLCZ cRNA injection led to the efficient preimplantation development of cloned bovine embryos of high quality, as judged by in vitro development, cell number and allocation, incidence of apoptosis and karyotyping. When we looked at reactivation of embryonic genes in cloned embryos, PLCZ presented a similar pattern of gene expression to IVF controls, while Ionomycin/CHX- and Ionomycin/DMAP-activated embryos showed some divergences compared to IVF embryos. These abnormalities in gene expression were in all cases observed for only one of the chemical treatments. This led us to speculate that they were a consequence of the inhibition of protein synthesis (CHX) or protein phosphorylation (DMAP), but not because of the abnormal  $[Ca^{2+}]_i$  regimen. On the other hand, a somatic-specific gene was inactivated more efficiently in PLCZ-activated embryos than in the chemically-activated embryos, likely indicating that the  $[Ca^{2+}]_i$  oscillations induced by PLCZ were important to induce silencing of somatic specific genes. More somatic-specific genes will need to be analyzed to substantiate this hypothesis. Nevertheless, we also found that an epigenetic mark (H3K27me3) associated with stable silencing

of gene transcription was reprogrammed to a fertilized-embryo level in clones activated using PLCZ cRNA injection but not in clones chemically activated. Altogether these data provide evidence that a more physiological oocyte activation signal (PLCZ) can lead to a more efficient nuclear reprogramming.

The mechanism of reprogramming for the H3K27me3 epigenetic mark has not been investigated in preimplantation embryos, which has stimulated efforts in our laboratory toward characterizing the dynamics of this histone methylation mark during preimplantation development of bovine fertilized, parthenogenetic and cloned embryos. Also, the expression of the genes responsible for catalyzing this histone modification is being studied. Moreover, in light of the recent discovery of two enzymes that have the capacity to remove this specific histone methylation mark [225-229], it would be interesting to investigate if they play a role in chromatin reprogramming after somatic cell nuclear transfer.

A gene that was shown to be expressed by fertilized embryos but not by cloned embryos activated by chemical means also was not activated in PLCZ activated embryos, suggesting that some abnormalities associated with SCNT are not rescued by activation with PLCZ. Activation with PLCZ required treatment with CB to avoid the segregation of a second polar body containing part of the somatic cell chromosomes (**Appendix Figure A4**). CB is an actin-polymerization inhibitor which may have detrimental effects for embryonic development or for nuclear reprogramming by not allowing the movement of molecules to their required site of action. It is also possible that a different  $[Ca^{2+}]_i$  oscillatory pattern is necessary to induce reprogramming of a somatic cell nucleus than to

reprogram the gametes' chromatin, i.e. during fertilization. Moreover, other components of the sperm, which are not provided by the somatic cell, may be required to initiate normal embryonic development. For instance, the sperm protein PAWP, which resides in the perinuclear theca, was required for meiotic resumption and pronuclear development following fertilization [230]. Also, mature sperm carried full length mRNAs which were delivered into the oocyte upon fertilization giving credence to the notion that they may indeed play a role in development [231], but the functional relevance of these molecules to fertilization and embryonic development was not determined [96]. Testing the requirements of these sperm components in SCNT models will provide information about their function, as well as potentially improving cloning efficiency.

Taken together our experiments provide evidence that the oocyte activation system can affect gene expression at 8-cell and blastocyst stage, as well as chromatin modifications, implying that the activation stimulus has a role in nuclear reprogramming. SCNT embryos activated with PLCZ showed great similarities to embryos generated by IVF, possibly indicating a more efficient nuclear reprogramming.

Allowing the development of SCNT embryos activated with PLCZ to further stages, and even to term, will likely provide more conclusive evidence on the involvement of the activation stimulus during nuclear reprogramming.

## **APPENDIX**





Figure A1: Cytogenetic analysis of donor cell line used for SCNT. The analysis was performed on G-banded cells by Cell Line Genetics (Madison, WI) resulting in an apparently normal Female Bovine Karyotype (60,XX).

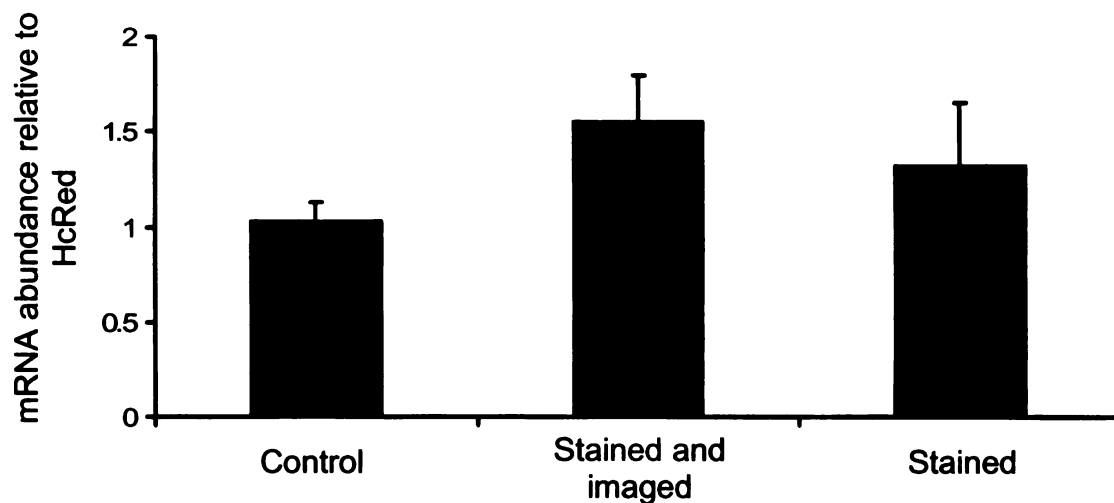
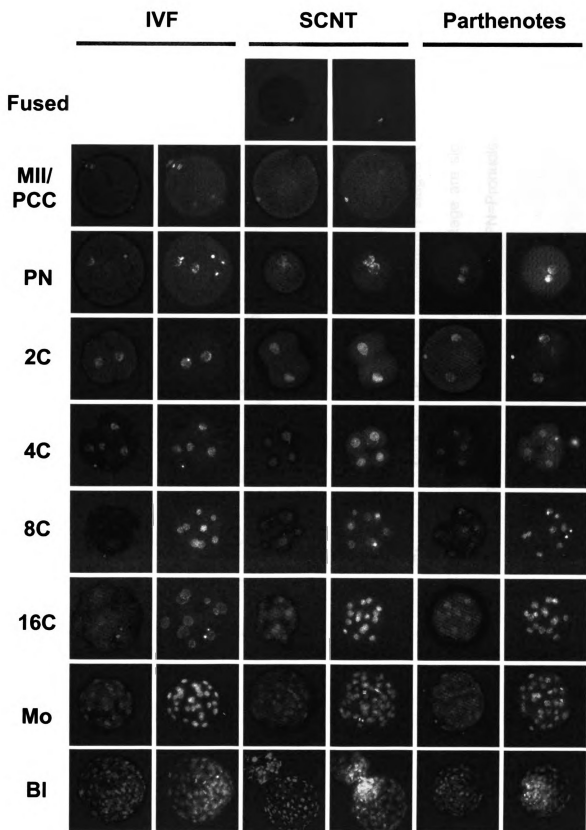


Figure A2: Confocal imaging of bovine embryos does not affect the level of GAPDH transcript abundance. GAPDH mRNA abundance was analyzed by quantitative real-time RT-PCR in groups of five 8-cell embryos that were stained with Syto 16 (5  $\mu$ M for 15 minutes, Stained, n=4); stained and imaged using a spinning-disc confocal microscope (Stained and imaged, n=4); or left untreated (Control, n=4). HcRed cRNA was added to the sample before RNA extraction as an external control. No significant differences were observed among the groups (P=0.43).

Figure A3: Immunofluorescence staining for trimethylated Histone 3 lysine 27 (H3K27me3) of bovine embryos of different origins at different stages of preimplantation development. Shown are images of H3K27me3 (red) and nuclear staining with bisbenzimidazole (white) of representative embryos (400X). IVF: in vitro fertilized embryo; SCNT: somatic cell nuclear transfer; Fused: SCNT reconstructed embryo right after fusion of somatic cell and oocyte; MII: metaphase II stage oocyte (IVF group); PCC: premature chromosome condensation (SCNT group); PN: pronuclear stage embryo; 2C: 2-cell stage embryo; 4C: 4-cell stage embryo; 8C: 8-cell stage embryo; 16C: 16-cell stage embryo; Mo: Morula; Bl: Blastocyst.



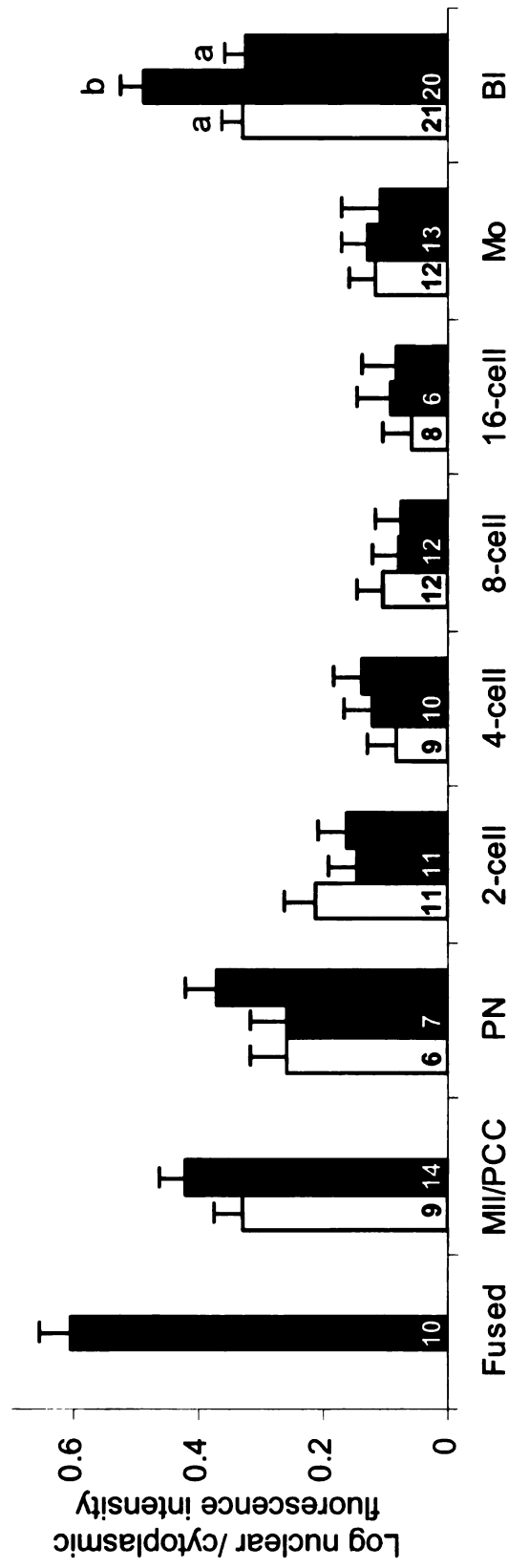


Figure A4: Level of Histone H3 lysine 27 trimethylation (H3K27me3) in embryos derived from in vitro fertilization (open bars), SCNT (black bars), and parthenogenesis (grey bars) at different stages of preimplantation development. Data shown as  $\text{ls-mean} \pm \text{SEM}$ . <sup>a,b</sup> Bars with different letters within stage are significantly different ( $P < 0.05$ ). MII=Metaphase II oocyte; PCC=premature chromosome condensation; PN=Pronuclear stage embryo; Mo=Morula; BI=blastocyst.

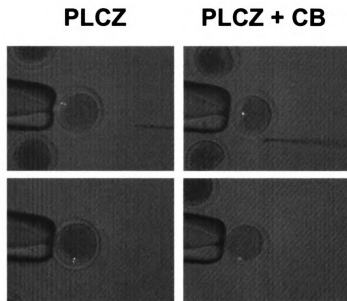


Figure A4: Cytochalasin B (CB) is required to avoid extrusion of a polar body after injection of PLCZ cRNA into bovine SCNT oocytes. Bovine reconstructed oocytes were incubated in the presence or absence of 7.5  $\mu\text{g/mL}$  of CB for 5 hours after PLCZ cRNA injection. DNA was labeled using bisbenzimidazole and embryos analyzed under epifluorescence microscopy. A polar body was extruded in 14 of 22 embryos activated with PLCZ in the absence of CB, while only 1 of 23 embryos cultured in the presence of CB extruded a polar body. Representative images are shown (200X).

## REFERENCES

1. Cibelli J. Developmental biology. A decade of cloning mystique. *Science* 2007; 316: 990-992.
2. Trounson AO. Future and applications of cloning. *Methods Mol Biol* 2006; 348: 319-332.
3. Wilmut I, Beaujean N, de Sousa PA, Dinnyes A, King TJ, Paterson LA, Wells DN, Young LE. Somatic cell nuclear transfer. *Nature* 2002; 419: 583-586.
4. Kuroiwa Y, Kasinathan P, Matsushita H, Sathiyaselan J, Sullivan EJ, Kakitani M, Tomizuka K, Ishida I, Robl JM. Sequential targeting of the genes encoding immunoglobulin-mu and prion protein in cattle. *Nat Genet* 2004; 36: 775-780.
5. Hill JR, Burghardt RC, Jones K, Long CR, Looney CR, Shin T, Spencer TE, Thompson JA, Winger QA, Westhusin ME. Evidence for placental abnormality as the major cause of mortality in first-trimester somatic cell cloned bovine fetuses. *Biol Reprod* 2000; 63: 1787-1794.
6. Heyman Y, Chavatte-Palmer P, LeBourhis D, Camous S, Vignon X, Renard JP. Frequency and occurrence of late-gestation losses from cattle cloned embryos. *Biol Reprod* 2002; 66: 6-13.
7. Zakhartchenko V, Mueller S, Alberio R, Schernthaner W, Stojkovic M, Wenigerkind H, Wanke R, Lassnig C, Mueller M, Wolf E, Brem G. Nuclear transfer in cattle with non-transfected and transfected fetal or cloned transgenic fetal and postnatal fibroblasts. *Mol Reprod Dev* 2001; 60: 362-369.
8. Cibelli JB, Campbell KH, Seidel GE, West MD, Lanza RP. The health profile of cloned animals. *Nat Biotechnol* 2002; 20: 13-14.
9. Rideout WM, III, Eggan K, Jaenisch R. Nuclear Cloning and Epigenetic Reprogramming of the Genome. *Science* 2001; 293: 1093-1098.
10. Reik W, Dean W, Walter J. Epigenetic reprogramming in mammalian development. *Science* 2001; 293: 1089-1093.
11. Latham KE. Cloning: questions answered and unsolved. *Differentiation* 2004; 72: 11-22.
12. Latham KE. Early and delayed aspects of nuclear reprogramming during cloning. *Biol Cell* 2005; 97: 119-132.



13. Ducibella T, Huneau D, Angelichio E, Xu Z, Schultz RM, Kopf GS, Fissore R, Madoux S, Ozil JP. Egg-to-embryo transition is driven by differential responses to  $\text{Ca}(2+)$  oscillation number. *Dev Biol* 2002; 250: 280-291.
14. Schultz RM, Kopf GS. Molecular basis of mammalian egg activation. *Curr Top Dev Biol* 1995; 30: 21-62.
15. Miyazaki S, Shirakawa H, Nakada K, Honda Y. Essential role of the inositol 1,4,5-trisphosphate receptor/ $\text{Ca}^{2+}$  release channel in  $\text{Ca}^{2+}$  waves and  $\text{Ca}^{2+}$  oscillations at fertilization of mammalian eggs. *Dev Biol* 1993; 158: 62-78.
16. Jones KT.  $\text{Ca}^{2+}$  oscillations in the activation of the egg and development of the embryo in mammals. *Int J Dev Biol* 1998; 42: 1-10.
17. Saunders CM, Larman MG, Parrington J, Cox LJ, Royse J, Blayney LM, Swann K, Lai FA. PLC zeta: a sperm-specific trigger of  $\text{Ca}(2+)$  oscillations in eggs and embryo development. *Development* 2002; 129: 3533-3544.
18. Swann K, Saunders CM, Rogers NT, Lai FA. PLCzeta(zeta): a sperm protein that triggers  $\text{Ca}^{2+}$  oscillations and egg activation in mammals. *Semin Cell Dev Biol* 2006; 17: 264-273.
19. Fujimoto S, Yoshida N, Fukui T, Amanai M, Isobe T, Itagaki C, Izumi T, Perry AC. Mammalian phospholipase Czeta induces oocyte activation from the sperm perinuclear matrix. *Dev Biol* 2004; 274: 370-383.
20. Rogers NT, Hobson E, Pickering S, Lai FA, Braude P, Swann K. Phospholipase Czeta causes  $\text{Ca}^{2+}$  oscillations and parthenogenetic activation of human oocytes. *Reproduction* 2004; 128: 697-702.
21. Yoneda A, Kashima M, Yoshida S, Terada K, Nakagawa S, Sakamoto A, Hayakawa K, Suzuki K, Ueda J, Watanabe T. Molecular cloning, testicular postnatal expression, and oocyte-activating potential of porcine phospholipase Czeta. *Reproduction* 2006; 132: 393-401.
22. Sutovsky P, Manandhar G, Wu A, Oko R. Interactions of sperm perinuclear theca with the oocyte: implications for oocyte activation, anti-polyspermy defense, and assisted reproduction. *Microsc Res Tech* 2003; 61: 362-378.
23. Knott JG, Kurokawa M, Fissore RA, Schultz RM, Williams CJ. Transgenic RNA interference reveals role for mouse sperm phospholipase Czeta in triggering  $\text{Ca}^{2+}$  oscillations during fertilization. *Biol Reprod* 2005; 72: 992-996.

24. Ozil JP, Huneau D. Activation of rabbit oocytes: the impact of the Ca<sup>2+</sup> signal regime on development. *Development* 2001; 128: 917-928.
25. Ducibella T, Schultz RM, Ozil JP. Role of calcium signals in early development. *Semin Cell Dev Biol* 2006; 17: 324-332.
26. Ozil JP, Markoulaki S, Toth S, Matson S, Banrezes B, Knott JG, Schultz RM, Huneau D, Ducibella T. Egg activation events are regulated by the duration of a sustained [Ca<sup>2+</sup>]<sub>cyt</sub> signal in the mouse. *Dev Biol* 2005; 282: 39-54.
27. Rogers NT, Halet G, Piao Y, Carroll J, Ko MS, Swann K. The absence of a Ca(2+) signal during mouse egg activation can affect parthenogenetic preimplantation development, gene expression patterns, and blastocyst quality. *Reproduction* 2006; 132: 45-57.
28. Ozil JP, Banrezes B, Toth S, Pan H, Schultz RM. Ca<sup>2+</sup> oscillatory pattern in fertilized mouse eggs affects gene expression and development to term. *Dev Biol* 2006; 300: 534-544.
29. Alberio R, Zakhartchenko V, Motlik J, Wolf E. Mammalian oocyte activation: lessons from the sperm and implications for nuclear transfer. *Int J Dev Biol* 2001; 45: 797-809.
30. Spemann H. *Ver. Deutsch. Zool. Ges. Leipzig (Freiburg)* 1914; 24: 216-221.
31. Spemann H. *Embryonic development and induction*. New Haven, London: Yale University Press; H. Milford, Oxford University Press; 1938.
32. Briggs R, King T. Transplantation of living nuclei from blastula cells into enucleated frogs' eggs. *Proc Natl Acad Sci U S A* 1952; 38: 455-463.
33. McKinnell RG. *Proceedings: Genetics and the cancer cell: nuclear transplantation*. *Proc Natl Cancer Conf* 1972; 7: 65-72.
34. DiBernardino MA. *Genomic Potential of Differentiated Cells*. New York: Columbia University Press; 1997.
35. Illmensee K, Hoppe PC. Nuclear transplantation in *Mus musculus*: developmental potential of nuclei from preimplantation embryos. *Cell* 1981; 23: 9-18.
36. McGrath J, Solter D. Nuclear transplantation in mouse embryos. *J Exp Zool* 1983; 228: 355-362.

37. McGrath J, Solter D. Inability of mouse blastomere nuclei transferred to enucleated zygotes to support development in vitro. *Science* 1984; 226: 1317-1319.
38. Willadsen SM. Nuclear transplantation in sheep embryos. *Nature* 1986; 320: 63-65.
39. Prather RS, Barnes FL, Sims MM, Robl JM, Eyestone WH, First NL. Nuclear transplantation in the bovine embryo: assessment of donor nuclei and recipient oocyte. *Biol Reprod* 1987; 37: 859-866.
40. Stice SL, Robl JM. Nuclear Reprogramming in Nuclear Transplant Rabbit Embryos. *Biol Reprod* 1988; 39: 657-664.
41. Prather RS, Sims MM, First NL. Nuclear transplantation in early pig embryos. *Biol Reprod* 1989; 41: 414-418.
42. Kono T, Tsunoda Y, Nakahara T. Production of identical twin and triplet mice by nuclear transplantation. *J Exp Zool* 1991; 257: 214-219.
43. Meng L, Ely JJ, Stouffer RL, Wolf DP. Rhesus monkeys produced by nuclear transfer. *Biol Reprod* 1997; 57: 454-459.
44. Yang X, Jiang S, Kovacs A, Foote RH. Nuclear totipotency of cultured rabbit morulae to support full-term development following nuclear transfer. *Biol Reprod* 1992; 47: 636-643.
45. Keefer CL, Stice SL, Matthews DL. Bovine inner cell mass cells as donor nuclei in the production of nuclear transfer embryos and calves. *Biol Reprod* 1994; 50: 935-939.
46. Campbell KHS, McWhir J, Ritchie WA, Wilmut I. Sheep cloned by nuclear transfer from a cultured cell line. *Nature* 1996; 380: 64-66.
47. Wilmut I, Schnieke AE, McWhir J, Kind AJ, Campbell KHS. Viable offspring derived from fetal and adult mammalian cells. *Nature* 1997; 385: 810-813.
48. Cibelli JB, Stice SL, Golueke PJ, Kane JJ, Jerry J, Blackwell C, Ponce de Leon FA, Robl JM. Cloned transgenic calves produced from nonquiescent fetal fibroblasts. *Science* 1998; 280: 1256-1258.
49. Wakayama T, Perry AC, Zuccotti M, Johnson KR, Yanagimachi R. Full-term development of mice from enucleated oocytes injected with cumulus cell nuclei. *Nature* 1998; 394: 369-374.

50. Baguisi A, Behboodi E, Melican DT, Pollock JS, Destrempes MM, Cammuso C, Williams JL, Nims SD, Porter CA, Midura P, Palacios MJ, Ayres SL, Denniston RS, Hayes ML, Ziomek CA, Meade HM, Godke RA, Gavin WG, Overstrom EW, Echelard Y. Production of goats by somatic cell nuclear transfer. *Nat Biotechnol* 1999; 17: 456-461.
51. Onishi A, Iwamoto M, Akita T, Mikawa S, Takeda K, Awata T, Hanada H, Perry AC. Pig cloning by microinjection of fetal fibroblast nuclei. *Science* 2000; 289: 1188-1190.
52. Lanza RP, Cibelli JB, Diaz F, Moraes CT, Farin PW, Farin CE, Hammer CJ, West MD, Damiani P. Cloning of an Endangered Species (*Bos gaurus*) Using Interspecies Nuclear Transfer. *Cloning* 2000; 2: 79-90.
53. Loi P, Ptak G, Barboni B, Fulka J, Jr., Cappai P, Clinton M. Genetic rescue of an endangered mammal by cross-species nuclear transfer using post-mortem somatic cells. *Nat Biotechnol* 2001; 19: 962-964.
54. Chesne P, Adenot PG, Viglietta C, Baratte M, Boulanger L, Renard JP. Cloned rabbits produced by nuclear transfer from adult somatic cells. *Nat Biotechnol* 2002; 20: 366-369.
55. Shin T, Kraemer D, Pryor J, Liu L, Rugila J, Howe L, Buck S, Murphy K, Lyons L, Westhusin M. A cat cloned by nuclear transplantation. *Nature* 2002; 415: 859.
56. Zhou Q, Renard JP, Le Friec G, Brochard V, Beaujean N, Cherifi Y, Fraichard A, Cozzi J. Generation of fertile cloned rats by regulating oocyte activation. *Science* 2003; 302: 1179.
57. Woods GL, White KL, Vanderwall DK, Li GP, Aston KI, Bunch TD, Meerdo LN, Pate BJ. A mule cloned from fetal cells by nuclear transfer. *Science* 2003; 301: 1063.
58. Galli C, Lagutina I, Crotti G, Colleoni S, Turini P, Ponderato N, Duchi R, Lazzari G. Pregnancy: a cloned horse born to its dam twin. *Nature* 2003; 424: 635.
59. Gomez MC, Pope CE, Giraldo A, Lyons LA, Harris RF, King AL, Cole A, Godke RA, Dresser BL. Birth of African Wildcat cloned kittens born from domestic cats. *Cloning Stem Cells* 2004; 6: 247-258.
60. Lee BC, Kim MK, Jang G, Oh HJ, Yuda F, Kim HJ, Hossein MS, Kim JJ, Kang SK, Schatten G, Hwang WS. Dogs cloned from adult somatic cells. *Nature* 2005; 436: 641.

61. Li Z, Sun X, Chen J, Liu X, Wisely SM, Zhou Q, Renard JP, Leno GH, Engelhardt JF. Cloned ferrets produced by somatic cell nuclear transfer. *Dev Biol* 2006; 293: 439-448.
62. Kim MK, Jang G, Oh HJ, Yuda F, Kim HJ, Hwang WS, Hossein MS, Kim JJ, Shin NS, Kang SK, Lee BC. Endangered wolves cloned from adult somatic cells. *Cloning Stem Cells* 2007; 9: 130-137.
63. Shi D, Lu F, Wei Y, Cui K, Yang S, Wei J, Liu Q. Buffalos (*Bubalus bubalis*) cloned by nuclear transfer of somatic cells. *Biol Reprod* 2007; 77: 285-291.
64. Berg DK, Li C, Asher G, Wells DN, Oback B. Red deer cloned from antler stem cells and their differentiated progeny. *Biol Reprod* 2007; 77: 384-394.
65. Polejaeva IA, Chen SH, Vaught TD, Page RL, Mullins J, Ball S, Dai Y, Boone J, Walker S, Ayares DL, Colman A, Campbell KH. Cloned pigs produced by nuclear transfer from adult somatic cells. *Nature* 2000; 407: 86-90.
66. Wheeler MB. Production of transgenic livestock: Promise fulfilled. *J. Anim Sci.* 2003; 81: 32-37.
67. Kuroiwa Y, Kasinathan P, Matsushita H, Sathiyaselan J, Sullivan EJ, Kakitani M, Tomizuka K, Ishida I, Robl JM. Sequential targeting of the genes encoding immunoglobulin-[mu] and prion protein in cattle. *Nat Genet* 2004; 36: 775-780.
68. McCreath KJ, Howcroft J, Campbell KH, Colman A, Schnieke AE, Kind AJ. Production of gene-targeted sheep by nuclear transfer from cultured somatic cells. *Nature* 2000; 405: 1066-1069.
69. Lai L, Kolber-Simonds D, Park KW, Cheong HT, Greenstein JL, Im GS, Samuel M, Bonk A, Rieke A, Day BN, Murphy CN, Carter DB, Hawley RJ, Prather RS. Production of alpha-1,3-galactosyltransferase knockout pigs by nuclear transfer cloning. *Science* 2002; 295: 1089-1092.
70. Wells DN, Misica PM, Tervit HR, Vivanco WH. Adult somatic cell nuclear transfer is used to preserve the last surviving cow of the Enderby Island cattle breed. *Reprod Fertil Dev* 1998; 10: 369-378.
71. Lanza RP, Dresser BL, Damiani P. Cloning Noah's Ark. *Scientific American* 2000; 283: 84-89.

72. Jenuwein T, Allis CD. Translating the Histone Code. *Science* 2001; 293: 1074-1080.
73. Dean W, Santos F, Stojkovic M, Zakhartchenko V, Walter J, Wolf E, Reik W. Conservation of methylation reprogramming in mammalian development: aberrant reprogramming in cloned embryos. *Proc Natl Acad Sci U S A* 2001; 98: 13734-13738.
74. Santos F, Zakhartchenko V, Stojkovic M, Peters A, Jenuwein T, Wolf E, Reik W, Dean W. Epigenetic marking correlates with developmental potential in cloned bovine preimplantation embryos. *Curr Biol* 2003; 13: 1116-1121.
75. Morgan HD, Santos F, Green K, Dean W, Reik W. Epigenetic reprogramming in mammals. *Hum Mol Genet* 2005; 14: R47-58.
76. Wee G, Koo D-B, Song B-S, Kim J-S, Kang M-J, Moon S-J, Kang Y-K, Lee K-K, Han Y-M. Inheritable Histone H4 Acetylation of Somatic Chromatins in Cloned Embryos. *J. Biol. Chem.* 2006; 281: 6048-6057.
77. Enright BP, Sung LY, Chang CC, Yang X, Tian XC. Methylation and Acetylation Characteristics of Cloned Bovine Embryos from Donor Cells Treated with 5-aza-2'-Deoxycytidine. *Biol Reprod* 2005; 72: 944-948.
78. Yeo S, Lee KK, Han YM, Kang YK. Methylation changes of lysine 9 of histone H3 during preimplantation mouse development. *Mol Cells* 2005; 20: 423-428.
79. Pfister-Genskow M, Myers C, Childs LA, Lacson JC, Patterson T, Betthausen JM, Goueleke PJ, Koppang RW, Lange G, Fisher P, Watt SR, Forsberg EJ, Zheng Y, Leno GH, Schultz RM, Liu B, Chetia C, Yang X, Hoeschele I, Eilertsen KJ. Identification of differentially expressed genes in individual bovine preimplantation embryos produced by nuclear transfer: improper reprogramming of genes required for development. *Biol Reprod* 2005; 72: 546-555.
80. Beyhan Z, Ross PJ, Lager AE, Kocabas AM, Cunniff K, Rosa GJ, Cibelli JB. Transcriptional reprogramming of somatic cell nuclei during preimplantation development of cloned bovine embryos. *Dev Biol* 2007; 305: 637-649.
81. Smith SL, Everts RE, Tian XC, Du F, Sung LY, Rodriguez-Zas SL, Jeong BS, Renard JP, Lewin HA, Yang X. Global gene expression profiles reveal significant nuclear reprogramming by the blastocyst stage after cloning. *Proc Natl Acad Sci U S A* 2005; 102: 17582-17587.

82. Somers J, Smith C, Donnison M, Wells DN, Henderson H, McLeay L, Pfeffer PL. Gene expression profiling of individual bovine nuclear transfer blastocysts. *Reproduction* 2006; 131: 1073-1084.
83. Zhou W, Xiang T, Walker S, Farrar V, Hwang E, Findeisen B, Sadeghieh S, Arenivas F, Abruzzese RV, Polejaeva I. Global gene expression analysis of bovine blastocysts produced by multiple methods. *Mol Reprod Dev* 2007; doi: 10.1002/mrd.20797.
84. Daniels R, Hall VJ, French AJ, Korfiatis NA, Trounson AO. Comparison of gene transcription in cloned bovine embryos produced by different nuclear transfer techniques. *Mol Reprod Dev* 2001; 60: 281-288.
85. Daniels R, Hall V, Trounson AO. Analysis of gene transcription in bovine nuclear transfer embryos reconstructed with granulosa cell nuclei. *Biol Reprod* 2000; 63: 1034-1040.
86. Wrenzycki C, Wells D, Herrmann D, Miller A, Oliver J, Tervit R, Niemann H. Nuclear transfer protocol affects messenger RNA expression patterns in cloned bovine blastocysts. *Biol Reprod* 2001; 65: 309-317.
87. Jang G, Jeon HY, Ko KH, Park HJ, Kang SK, Lee BC, Hwang WS. Developmental competence and gene expression in preimplantation bovine embryos derived from somatic cell nuclear transfer using different donor cells. *Zygote* 2005; 13: 187-195.
88. Smith C, Berg D, Beaumont S, Standley NT, Wells DN, Pfeffer PL. Simultaneous gene quantitation of multiple genes in individual bovine nuclear transfer blastocysts. *Reproduction* 2007; 133: 231-242.
89. Beyhan Z, Forsberg EJ, Eilertsen KJ, Kent-First M, First NL. Gene expression in bovine nuclear transfer embryos in relation to donor cell efficiency in producing live offspring. *Mol Reprod Dev* 2007; 74: 18-27.
90. de ACLS, Powell AM, do Vale Filho VR, Wall RJ. Comparison of gene expression in individual preimplantation bovine embryos produced by in vitro fertilisation or somatic cell nuclear transfer. *Reprod Fertil Dev* 2005; 17: 487-496.
91. Bettegowda A, Patel OV, Ireland JJ, Smith GW. Quantitative analysis of messenger RNA abundance for ribosomal protein L-15, cyclophilin-A, phosphoglycerokinase, beta-glucuronidase, glyceraldehyde 3-phosphate dehydrogenase, beta-actin, and histone H2A during bovine oocyte maturation and early embryogenesis in vitro. *Mol Reprod Dev* 2006; 73: 267-278.

92. Kopecny V, Flechon JE, Camous S, Fulka J, Jr. Nucleogenesis and the onset of transcription in the eight-cell bovine embryo: fine-structural autoradiographic study. *Mol Reprod Dev* 1989; 1: 79-90.
93. Schultz RM. The molecular foundations of the maternal to zygotic transition in the preimplantation embryo. *Hum Reprod Update* 2002; 8: 323-331.
94. Eichenlaub-Ritter U, Peschke M. Expression in in-vivo and in-vitro growing and maturing oocytes: focus on regulation of expression at the translational level. *Hum Reprod Update* 2002; 8: 21-41.
95. Wassarman PM, Jovine L, Litscher ES. A profile of fertilization in mammals. *Nat Cell Biol* 2001; 3: E59-64.
96. Krawetz SA. Paternal contribution: new insights and future challenges. *Nat Rev Genet* 2005; 6: 633-642.
97. Sun QY, Schatten H. Centrosome inheritance after fertilization and nuclear transfer in mammals. *Adv Exp Med Biol* 2007; 591: 58-71.
98. Malcuit C, Fissore RA. Activation of fertilized and nuclear transfer eggs. *Adv Exp Med Biol* 2007; 591: 117-131.
99. Parrington J, Swann K, Shevchenko VI, Sesay AK, Lai FA. Calcium oscillations in mammalian eggs triggered by a soluble sperm protein. *Nature* 1996; 379: 364-368.
100. Kimura Y, Yanagimachi R. Intracytoplasmic sperm injection in the mouse. *Biol Reprod* 1995; 52: 709-720.
101. Swann K. A cytosolic sperm factor stimulates repetitive calcium increases and mimics fertilization in hamster eggs. *Development* 1990; 110: 1295-1302.
102. Homa ST, Swann K. A cytosolic sperm factor triggers calcium oscillations and membrane hyperpolarizations in human oocytes. *Hum Reprod* 1994; 9: 2356-2361.
103. Wu H, He CL, Fissore RA. Injection of a porcine sperm factor triggers calcium oscillations in mouse oocytes and bovine eggs. *Mol Reprod Dev* 1997; 46: 176-189.



104. Jones KT, Nixon VL. Sperm-induced  $\text{Ca}^{2+}$  oscillations in mouse oocytes and eggs can be mimicked by photolysis of caged inositol 1,4,5-trisphosphate: evidence to support a continuous low level production of inositol 1, 4,5-trisphosphate during mammalian fertilization. *Dev Biol* 2000; 225: 1-12.
105. Stice SL, Robl JM. Activation of mammalian oocytes by a factor obtained from rabbit sperm. *Mol Reprod Dev* 1990; 25: 272-280.
106. Miyazaki S, Ito M. Calcium signals for egg activation in mammals. *J Pharmacol Sci* 2006; 100: 545-552.
107. Steinhardt RA, Epel D, Carroll EJ, Jr., Yanagimachi R. Is calcium ionophore a universal activator for unfertilised eggs? *Nature* 1974; 252: 41-43.
108. Miyazaki S, Igusa Y. Fertilization potential in golden hamster eggs consists of recurring hyperpolarizations. *Nature* 1981; 290: 702-704.
109. Kurokawa M, Sato K, Fissore RA. Mammalian fertilization: from sperm factor to phospholipase C $\zeta$ . *Biol Cell* 2004; 96: 37-45.
110. Stricker SA. Comparative biology of calcium signaling during fertilization and egg activation in animals. *Dev Biol* 1999; 211: 157-176.
111. Malcuit C, Kurokawa M, Fissore RA. Calcium oscillations and mammalian egg activation. *J Cell Physiol* 2006; 206: 565-573.
112. Markoulaki S, Matson S, Abbott AL, Ducibella T. Oscillatory CaMKII activity in mouse egg activation. *Dev Biol* 2003; 258: 464-474.
113. Knott JG, Gardner AJ, Madgwick S, Jones KT, Williams CJ, Schultz RM. Calmodulin-dependent protein kinase II triggers mouse egg activation and embryo development in the absence of  $\text{Ca}^{2+}$  oscillations. *Dev Biol* 2006; 296: 388-395.
114. Madgwick S, Levasseur M, Jones KT. Calmodulin-dependent protein kinase II, and not protein kinase C, is sufficient for triggering cell-cycle resumption in mammalian eggs. *J Cell Sci* 2005; 118: 3849-3859.
115. Gardner AJ, Knott JG, Jones KT, Evans JP. CaMKII can participate in but is not sufficient for the establishment of the membrane block to polyspermy in mouse eggs. *J Cell Physiol* 2007; 212: 275-280.

116. Reimann JD, Gardner BE, Margottin-Goguet F, Jackson PK. Emi1 regulates the anaphase-promoting complex by a different mechanism than Mad2 proteins. *Genes Dev* 2001; 15: 3278-3285.
117. Reimann JD, Freed E, Hsu JY, Kramer ER, Peters JM, Jackson PK. Emi1 is a mitotic regulator that interacts with Cdc20 and inhibits the anaphase promoting complex. *Cell* 2001; 105: 645-655.
118. Rauh NR, Schmidt A, Bormann J, Nigg EA, Mayer TU. Calcium triggers exit from meiosis II by targeting the APC/C inhibitor XErp1 for degradation. *Nature* 2005; 437: 1048-1052.
119. Hansen DV, Tung JJ, Jackson PK. CaMKII and polo-like kinase 1 sequentially phosphorylate the cytostatic factor Emi2/XErp1 to trigger its destruction and meiotic exit. *Proc Natl Acad Sci U S A* 2006; 103: 608-613.
120. Liu J, Maller JL. Calcium elevation at fertilization coordinates phosphorylation of XErp1/Emi2 by Plx1 and CaMK II to release metaphase arrest by cytostatic factor. *Curr Biol* 2005; 15: 1458-1468.
121. Shoji S, Yoshida N, Amanai M, Ohgishi M, Fukui T, Fujimoto S, Nakano Y, Kajikawa E, Perry AC. Mammalian Emi2 mediates cytostatic arrest and transduces the signal for meiotic exit via Cdc20. *Embo J* 2006; 25: 834-845.
122. Madgwick S, Hansen DV, Levasseur M, Jackson PK, Jones KT. Mouse Emi2 is required to enter meiosis II by reestablishing cyclin B1 during interkinesis. *J Cell Biol* 2006; 174: 791-801.
123. Atkins CM, Nozaki N, Shigeri Y, Soderling TR. Cytoplasmic polyadenylation element binding protein-dependent protein synthesis is regulated by calcium/calmodulin-dependent protein kinase II. *J Neurosci* 2004; 24: 5193-5201.
124. Racki WJ, Richter JD. CPEB controls oocyte growth and follicle development in the mouse. *Development* 2006; 133: 4527-4537.
125. Mochida S, Hunt T. Calcineurin is required to release *Xenopus* egg extracts from meiotic M phase. *Nature* 2007; 449: 336-340.
126. Nishiyama T, Yoshizaki N, Kishimoto T, Ohsumi K. Transient activation of calcineurin is essential to initiate embryonic development in *Xenopus laevis*. *Nature* 2007; 449: 341-345.

127. Halet G, Tunwell R, Parkinson SJ, Carroll J. Conventional PKCs regulate the temporal pattern of  $\text{Ca}^{2+}$  oscillations at fertilization in mouse eggs. *J Cell Biol* 2004; 164: 1033-1044.
128. Jellerette T, He CL, Wu H, Parys JB, Fissore RA. Down-regulation of the inositol 1,4,5-trisphosphate receptor in mouse eggs following fertilization or parthenogenetic activation. *Dev Biol* 2000; 223: 238-250.
129. Brind S, Swann K, Carroll J. Inositol 1,4,5-trisphosphate receptors are downregulated in mouse oocytes in response to sperm or adenophostin A but not to increases in intracellular  $\text{Ca}^{2+}$  or egg activation. *Dev Biol* 2000; 223: 251-265.
130. Lee B, Yoon SY, Fissore RA. Regulation of fertilization-initiated  $[\text{Ca}^{2+}]_i$  oscillations in mammalian eggs: a multi-pronged approach. *Semin Cell Dev Biol* 2006; 17: 274-284.
131. Jellerette T, Kurokawa M, Lee B, Malcuit C, Yoon SY, Smyth J, Vermassen E, De Smedt H, Parys JB, Fissore RA. Cell cycle-coupled  $[\text{Ca}^{2+}]_i$  oscillations in mouse zygotes and function of the inositol 1,4,5-trisphosphate receptor-1. *Dev Biol* 2004; 274: 94-109.
132. Lee B, Vermassen E, Yoon SY, Vanderheyden V, Ito J, Alfandari D, De Smedt H, Parys JB, Fissore RA. Phosphorylation of IP3R1 and the regulation of  $[\text{Ca}^{2+}]_i$  responses at fertilization: a role for the MAP kinase pathway. *Development* 2006; 133: 4355-4365.
133. Jones KT, Cruttwell C, Parrington J, Swann K. A mammalian sperm cytosolic phospholipase C activity generates inositol trisphosphate and causes  $\text{Ca}^{2+}$  release in sea urchin egg homogenates. *FEBS Lett* 1998; 437: 297-300.
134. Rice A, Parrington J, Jones KT, Swann K. Mammalian sperm contain a  $\text{Ca}^{2+}$ -sensitive phospholipase C activity that can generate  $\text{InsP}(3)$  from  $\text{PIP}(2)$  associated with intracellular organelles. *Dev Biol* 2000; 228: 125-135.
135. Parrington J, Jones ML, Tunwell R, Devader C, Katan M, Swann K. Phospholipase C isoforms in mammalian spermatozoa: potential components of the sperm factor that causes  $\text{Ca}^{2+}$  release in eggs. *Reproduction* 2002; 123: 31-39.
136. Jones KT, Matsuda M, Parrington J, Katan M, Swann K. Different  $\text{Ca}^{2+}$ -releasing abilities of sperm extracts compared with tissue extracts and phospholipase C isoforms in sea urchin egg homogenate and mouse eggs. *Biochem J* 2000; 346 Pt 3: 743-749.

137. Mehlmann LM, Chattopadhyay A, Carpenter G, Jaffe LA. Evidence that phospholipase C from the sperm is not responsible for initiating  $\text{Ca}^{2+}$  release at fertilization in mouse eggs. *Dev Biol* 2001; 236: 492-501.
138. Kouchi Z, Fukami K, Shikano T, Oda S, Nakamura Y, Takenawa T, Miyazaki S. Recombinant phospholipase C $\zeta$  has high  $\text{Ca}^{2+}$  sensitivity and induces  $\text{Ca}^{2+}$  oscillations in mouse eggs. *J Biol Chem* 2004; 279: 10408-10412.
139. Yoon S-Y, Fissore RA. Release of phospholipase C { $\zeta$ } and  $[\text{Ca}^{2+}]_i$  oscillation-inducing activity during mammalian fertilization. *Reproduction* 2007; 134: 695-704.
140. Nomikos M, Mulgrew-Nesbitt A, Pallavi P, Mihalyne G, Zaitseva I, Swann K, Lai FA, Murray D, McLaughlin S. Binding of phosphoinositide-specific phospholipase C- $\zeta$  (PLC- $\zeta$ ) to phospholipid membranes: potential role of an unstructured cluster of basic residues. *J Biol Chem* 2007; 282: 16644-16653.
141. Kouchi Z, Shikano T, Nakamura Y, Shirakawa H, Fukami K, Miyazaki S. The role of EF-hand domains and C2 domain in regulation of enzymatic activity of phospholipase C $\zeta$ . *J Biol Chem* 2005; 280: 21015-21021.
142. Kurokawa M, Yoon S-Y, Alfandari D, Fukami K, Sato K, Fissore RA. Proteolytic processing of phospholipase C $\zeta$  and  $[\text{Ca}^{2+}]_i$  oscillations during mammalian fertilization. *Dev Biol* 2007; doi: 10.1016/j.ydbio.2007.09.040.
143. Saunders CM, Swann K, Lai FA. PLC $\zeta$ , a sperm-specific PLC and its potential role in fertilization. *Biochem Soc Symp* 2007: 23-36.
144. Cox LJ, Larman MG, Saunders CM, Hashimoto K, Swann K, Lai FA. Sperm phospholipase C $\zeta$  from humans and cynomolgus monkeys triggers  $\text{Ca}^{2+}$  oscillations, activation and development of mouse oocytes. *Reproduction* 2002; 124: 611-623.
145. Igarashi H, Knott JG, Schultz RM, Williams CJ. Alterations of PLC $\beta$ 1 in mouse eggs change calcium oscillatory behavior following fertilization. *Dev Biol* 2007; doi:10.1016/j.ydbio.2007.09.028.
146. Machaty Z. Activation of oocytes after nuclear transfer. *Methods Mol Biol* 2006; 348: 43-58.
147. Fissore RA, Robl JM. Mechanism of calcium oscillations in fertilized rabbit eggs. *Dev Biol* 1994; 166: 634-642.

148. Nakada K, Mizuno J. Intracellular calcium responses in bovine oocytes induced by spermatozoa and by reagents. *Theriogenology* 1998; 50: 269-282.
149. Susko-Parrish JL, Leibfried-Rutledge ML, Northey DL, Schutkus V, First NL. Inhibition of protein kinases after an induced calcium transient causes transition of bovine oocytes to embryonic cycles without meiotic completion. *Dev Biol* 1994; 166: 729-739.
150. De La Fuente R, King WA. Developmental consequences of karyokinesis without cytokinesis during the first mitotic cell cycle of bovine parthenotes. *Biol Reprod* 1998; 58: 952-962.
151. Hill J, Winger Q, Jones K, Keller D, King WA, Westhusin M. The effect of donor cell serum starvation and oocyte activation compounds on the development of somatic cell cloned embryos. *Cloning* 1999; 1: 201-208.
152. Vesely J, Havlicek L, Strnad M, Blow JJ, Donella-Deana A, Pinna L, Letham DS, Kato J, Detivaud L, Leclerc S, et al. Inhibition of cyclin-dependent kinases by purine analogues. *Eur J Biochem* 1994; 224: 771-786.
153. Alberio R, Kubelka M, Zakhartchenko V, Hajdich M, Wolf E, Motlik J. Activation of bovine oocytes by specific inhibition of cyclin-dependent kinases. *Mol Reprod Dev* 2000; 55: 422-432.
154. Motlik J, Alberio R, Zakhartchenko V, Stojkovic M, Kubelka M, Wolf E. The effect of activation of Mammalian oocytes on remodeling of donor nuclei after nuclear transfer. *Cloning Stem Cells* 2002; 4: 245-252.
155. Zakhartchenko V, Durcova-Hills G, Stojkovic M, Schernthaner W, Prella K, Steinborn R, Muller M, Brem G, Wolf E. Effects of serum starvation and re-cloning on the efficiency of nuclear transfer using bovine fetal fibroblasts. *J Reprod Fertil* 1999; 115: 325-331.
156. Alberio R, Brero A, Motlik J, Cremer T, Wolf E, Zakhartchenko V. Remodeling of donor nuclei, DNA-synthesis, and ploidy of bovine cumulus cell nuclear transfer embryos: effect of activation protocol. *Mol Reprod Dev* 2001; 59: 371-379.
157. Zhang D, Pan L, Yang LH, He XK, Huang XY, Sun FZ. Strontium promotes calcium oscillations in mouse meiotic oocytes and early embryos through InsP3 receptors, and requires activation of phospholipase and the synergistic action of InsP3. *Hum Reprod* 2005; 20: 3053-3061.

158. Knott JG, Poothapillai K, Wu H, He CL, Fissore RA, Robl JM. Porcine Sperm Factor Supports Activation and Development of Bovine Nuclear Transfer Embryos. *Biol Reprod* 2002; 66: 1095-1103.
159. Squirrell JM, Wokosin DL, White JG, Bavister BD. Long-term two-photon fluorescence imaging of mammalian embryos without compromising viability. *Nat Biotechnol* 1999; 17: 763-767.
160. Wang E, Babbey CM, Dunn KW. Performance comparison between the high-speed Yokogawa spinning disc confocal system and single-point scanning confocal systems. *J Microsc* 2005; 218: 148-159.
161. Nakano A. Spinning-disk confocal microscopy – a cutting-edge tool for imaging of membrane traffic. *Cell Struct Funct* 2002; 27: 349-355.
162. Nipkow P. Elektrisches teleskop (Electric telescope). Berlin, Germany. Kaiserliches patentamt, Patent No. 30, 105. 1884.
163. Petran M, Hadravsky M, Egger MD, Galambos R. Tandem-scanning reflected-light microscope. *J Opt Soc. Am.* 1968; 58: 661–664.
164. Bement WM, Benink HA, von Dassow G. A microtubule-dependent zone of active RhoA during cleavage plane specification. *J Cell Biol.* 2005; 170: 91-101.
165. Moore AT, Rankin KE, von Dassow G, Peris L, Wagenbach M, Ovechkina Y, Andrieux A, Job D, Wordeman L. MCAK associates with the tips of polymerizing microtubules. *J Cell Biol.* 2005; 169: 391-397.
166. Landa LR, Jr., Harbeck M, Kaihara K, Chepurny O, Kitiphongspattana K, Graf O, Nikolaev VO, Lohse MJ, Holz GG, Roe MW. Interplay of Ca<sup>2+</sup> and cAMP Signaling in the Insulin-secreting MIN6 {beta}-Cell Line. *J Biol. Chem.* 2005; 280: 31294-31302.
167. Hara M, Bindokas V, Lopez JP, Kaihara K, Landa LR, Jr., Harbeck M, Roe MW. Imaging endoplasmic reticulum calcium with a fluorescent biosensor in transgenic mice. *Am J Physiol Cell Physiol* 2004; 287: C932-938.
168. Galliera E, Jala VR, Trent JO, Bonecchi R, Signorelli P, Lefkowitz RJ, Mantovani A, Locati M, Haribabu B. {beta}-Arrestin-dependent Constitutive Internalization of the Human Chemokine Decoy Receptor D6. *J Biol. Chem.* 2004; 279: 25590-25597.

169. Marrelli SP, Eckmann MS, Hunte MS. Role of endothelial intermediate conductance K<sub>Ca</sub> channels in cerebral EDHF-mediated dilations. *Am J Physiol Heart Circ Physiol* 2003; 285: H1590-1599.
170. Faber DC, Molina JA, Ohlrichs CL, Vander Zwaag DF, Ferre LB. Commercialization of animal biotechnology. *Theriogenology* 2003; 59: 125-138.
171. Wilmut I, Beaujean N, de Sousa PA, Dinnyes A, King TJ, Paterson LA, Wells DN, Young LE. Somatic cell nuclear transfer. *Nature* 2002; 419: 583-587.
172. Boiani M, Eckardt S, Scholer HR, McLaughlin KJ. Oct4 distribution and level in mouse clones: consequences for pluripotency. *Genes Dev.* 2002; 16: 1209-1219.
173. Van Soom A, Vanroose G, de Kruif A. Blastocyst evaluation by means of differential staining: a practical approach. *Reprod Domest Anim* 2001; 36: 29-35.
174. Seshagiri P, Bavister B. Phosphate is required for inhibition by glucose of development of hamster 8-cell embryos in vitro. *Biol Reprod* 1989; 40: 607-614.
175. Parrish JJ, Susko-Parrish JL, Leibfried-Rutledge ML, Critser ES, Eyestone WH, First NL. Bovine in vitro fertilization with frozen-thawed semen. *Theriogenology* 1986; 25: 591-600.
176. Niwa H, Yamamura K-i, Miyazaki J-i. Efficient selection for high-expression transfectants with a novel eukaryotic vector. *Gene* 1991; 108: 193-199.
177. Singh NP, McCoy MT, Tice RR, Schneider EL. A simple technique for quantitation of low levels of DNA damage in individual cells. *Exp Cell Res* 1988; 175: 184-191.
178. Morita Y, Perez GI, Paris F, Miranda SR, Ehleiter D, Haimovitz-Friedman A, Fuks Z, Xie ZH, Reed JC, Schuchman EH, Kolesnick RN, Tilly JL. Oocyte apoptosis is suppressed by disruption of the acid sphingomyelinase gene or by sphingosine-1-phosphate therapy. *Nature Medicine* 2000; 6: 1109-1114.
179. Van Soom A, Boerjan M, Ysebaert M-T, de Kruif A. Cell allocation to the inner cell mass and the trophectoderm in bovine embryos cultured in two different media. *Mol Reprod Dev* 1996; 45: 171-182.

180. Jou MJ, Jou SB, Guo MJ, Wu HY, Peng TI. Mitochondrial reactive oxygen species generation and calcium increase induced by visible light in astrocytes. *Ann N Y Acad Sci* 2004; 1011: 45-56.
181. Hockberger PE, Skimina TA, Centonze VE, Lavin C, Chu S, Dadras S, Reddy JK, White JG. Activation of flavin-containing oxidases underlies light-induced production of H<sub>2</sub>O<sub>2</sub> in mammalian cells. *Proc Natl Acad Sci U S A* 1999; 96: 6255-6260.
182. Stith BJ, Espinoza R, Roberts D, Smart T. Sperm increase inositol 1,4,5-trisphosphate mass in *Xenopus laevis* eggs preinjected with calcium buffers or heparin. *Dev Biol* 1994; 165: 206-215.
183. Turner PR, Sheetz MP, Jaffe LA. Fertilization increases the polyphosphoinositide content of sea urchin eggs. *Nature* 1984; 310: 414-415.
184. Kaufman MH, Huberman E, Sachs L. Genetic control of haploid parthenogenetic development in mammalian embryos. *Nature* 1975; 254: 694-695.
185. Kono T. Genomic imprinting is a barrier to parthenogenesis in mammals. *Cytogenet Genome Res* 2006; 113: 31-35.
186. Malcuit C, Knott JG, He C, Wainwright T, Parys JB, Robl JM, Fissore RA. Fertilization and inositol 1,4,5-trisphosphate (IP<sub>3</sub>)-induced calcium release in type-1 inositol 1,4,5-trisphosphate receptor down-regulated bovine eggs. *Biol Reprod* 2005; 73: 2-13.
187. Gordo AC, Wu H, He CL, Fissore RA. Injection of sperm cytosolic factor into mouse metaphase II oocytes induces different developmental fates according to the frequency of [Ca<sup>2+</sup>]<sub>i</sub> oscillations and oocyte age. *Biol Reprod* 2000; 62: 1370-1379.
188. Jones KT, Nixon VL. Sperm-Induced Ca<sup>2+</sup> Oscillations in Mouse Oocytes and Eggs Can Be Mimicked by Photolysis of Caged Inositol 1,4,5-Trisphosphate: Evidence to Support a Continuous Low Level Production of Inositol 1,4,5-Trisphosphate during Mammalian Fertilization. *Dev Biol* 2000; 225: 1-12.
189. Bhak JS, Lee SL, Ock SA, Mohana Kumar B, Choe SY, Rho GJ. Developmental rate and ploidy of embryos produced by nuclear transfer with different activation treatments in cattle. *Anim Reprod Sci* 2006; 92: 37-49.



190. Van De Velde A, Liu L, Bols PE, Ysebaert MT, Yang X. Cell allocation and chromosomal complement of parthenogenetic and IVF bovine embryos. *Mol Reprod Dev* 1999; 54: 57-62.
191. Winger QA, De La Fuente R, King WA, Armstrong DT, Watson AJ. Bovine parthenogenesis is characterized by abnormal chromosomal complements: implications for maternal and paternal co-dependence during early bovine development. *Dev Genet* 1997; 21: 160-166.
192. Kubiak JZ, Weber M, de Pennart H, Winston NJ, Maro B. The metaphase II arrest in mouse oocytes is controlled through microtubule-dependent destruction of cyclin B in the presence of CSF. *Embo J* 1993; 12: 3773-3778.
193. Xu KP, Greve T. A detailed analysis of early events during in-vitro fertilization of bovine follicular oocytes. *J Reprod Fertil* 1988; 82: 127-134.
194. Liu L, Yang X. Interplay of maturation-promoting factor and mitogen-activated protein kinase inactivation during metaphase-to-interphase transition of activated bovine oocytes. *Biol Reprod* 1999; 61: 1-7.
195. Hare WC, Singh EL, Betteridge KJ, Eaglesome MD, Randall GC, Mitchell D, Bilton RJ, Trounson AO. Chromosomal analysis of 159 bovine embryos collected 12 to 18 days after estrus. *Can J Genet Cytol* 1980; 22: 615-626.
196. Kawarsky SJ, Basrur PK, Stubbings RB, Hansen PJ, King WA. Chromosomal abnormalities in bovine embryos and their influence on development. *Biol Reprod* 1996; 54: 53-59.
197. Viuff D, Palsgaard A, Rickords L, Lawson LG, Greve T, Schmidt M, Avery B, Hyttel P, Thomsen PD. Bovine embryos contain a higher proportion of polyploid cells in the trophectoderm than in the embryonic disc. *Mol Reprod Dev* 2002; 62: 483-488.
198. Nakada K, Mizuno J, Shiraishi K, Endo K, Miyazaki S. Initiation, persistence, and cessation of the series of intracellular  $Ca^{2+}$  responses during fertilization of bovine eggs. *J Reprod Dev* 1995; 41: 77-84.
199. Fissore RA, Dobrinsky JR, Balise JJ, Duby RT, Robl JM. Patterns of intracellular  $Ca^{2+}$  concentrations in fertilized bovine eggs. *Biol Reprod* 1992; 47: 960-969.
200. FitzHarris G, Marangos P, Carroll J. Cell cycle-dependent regulation of structure of endoplasmic reticulum and inositol 1,4,5-trisphosphate-induced  $Ca^{2+}$  release in mouse oocytes and embryos. *Mol Biol Cell* 2003; 14: 288-301.

201. Fitzharris G, Marangos P, Carroll J. Changes in endoplasmic reticulum structure during mouse oocyte maturation are controlled by the cytoskeleton and cytoplasmic dynein. *Dev Biol* 2007.
202. Palermo GD, Avrech OM, Colombero LT, Wu H, Wolny YM, Fissore RA, Rosenwaks Z. Human sperm cytosolic factor triggers  $Ca^{2+}$  oscillations and overcomes activation failure of mammalian oocytes. *Mol Hum Reprod* 1997; 3: 367-374.
203. Wu H, He CL, Fissore RA. Injection of a porcine sperm factor induces activation of mouse eggs. *Mol Reprod Dev* 1998; 49: 37-47.
204. Laemmli UK. Cleavage of structural proteins during the assembly of the head of bacteriophage T4. *Nature* 1970; 227: 680-685.
205. Parys JB, de Smedt H, Missiaen L, Bootman MD, Sienaert I, Casteels R. Rat basophilic leukemia cells as model system for inositol 1,4,5-trisphosphate receptor IV, a receptor of the type II family: functional comparison and immunological detection. *Cell Calcium* 1995; 17: 239-249.
206. Hochedlinger K, Jaenisch R. Nuclear reprogramming and pluripotency. *Nature* 2006; 441: 1061-1067.
207. Shi W, Zakhartchenko V, Wolf E. Epigenetic reprogramming in mammalian nuclear transfer. *Differentiation* 2003; 71: 91-113.
208. Reik W, Dean W, Walter J. Epigenetic Reprogramming in Mammalian Development. *Science* 2001; 293: 1089-1093.
209. Swann K, Larman MG, Saunders CM, Lai FA. The cytosolic sperm factor that triggers  $Ca^{2+}$  oscillations and egg activation in mammals is a novel phospholipase C: PLCzeta. *Reproduction* 2004; 127: 431-439.
210. Ross PJ, Perez GI, Ko T, Yoo MS, Cibelli JB. Full developmental potential of mammalian preimplantation embryos is maintained after imaging using a spinning-disk confocal microscope. *Biotechniques* 2006; 41: 741-750.
211. Kane MT. A review of in vitro gamete maturation and embryo culture and potential impact on future animal biotechnology. *Anim Reprod Sci* 2003; 79: 171-190.
212. Wright JM. Photographic illustrations of embryo developmental stage and quality codes. In: Stringfellow DA, Seidel SM (eds.), *Manual of the International Embryo Transfer Society* (third ed.). Savoy, IL: IETS; 1998: 167-170.

213. van Soom A, Ysebaert MT, de Kruif A. Relationship between timing of development, morula morphology, and cell allocation to inner cell mass and trophoctoderm in in vitro-produced bovine embryos. *Mol Reprod Dev* 1997; 47: 47-56.
214. Renard JP, Maruotti J, Jouneau A, Vignon X. Nuclear reprogramming and pluripotency of embryonic cells: Application to the isolation of embryonic stem cells in farm animals. *Theriogenology* 2007; 68 Suppl 1: S196-205.
215. Koo D-B, Kang Y-K, Choi Y-H, Park JS, Kim H-N, Oh KB, Son D-S, Park H, Lee K-K, Han Y-M. Aberrant Allocations of Inner Cell Mass and Trophoctoderm Cells in Bovine Nuclear Transfer Blastocysts. *Biol Reprod* 2002; 67: 487-492.
216. Zhou W, Xiang T, Walker S, Farrar V, Hwang E, Findeisen B, Sadeghieh S, Arenivas F, Abruzzese RV, Polejaeva I. Global gene expression analysis of bovine blastocysts produced by multiple methods. *Mol Reprod Dev* 2007; DOI: 10.1002/mrd.20797.
217. Beyhan Z, Ross PJ, Lager AE, Kocabas AM, Cuniff K, Rosa GJ, Cibelli JB. Transcriptional reprogramming of somatic cell nuclei during preimplantation development of cloned bovine embryos. *Dev Biol* 2007.
218. Gao S, Chung YG, Williams JW, Riley J, Moley K, Latham KE. Somatic cell-like features of cloned mouse embryos prepared with cultured myoblast nuclei. *Biol Reprod* 2003; 69: 48-56.
219. Schuettengruber B, Chourrout D, Vervoort M, Leblanc B, Cavalli G. Genome regulation by polycomb and trithorax proteins. *Cell* 2007; 128: 735-745.
220. Azuara V, Perry P, Sauer S, Spivakov M, Jorgensen HF, John RM, Gouti M, Casanova M, Warnes G, Merckenschlager M, Fisher AG. Chromatin signatures of pluripotent cell lines. *Nat Cell Biol* 2006; 8: 532-538.
221. Boyer LA, Plath K, Zeitlinger J, Brambrink T, Medeiros LA, Lee TI, Levine SS, Wernig M, Tajonar A, Ray MK, Bell GW, Otte AP, Vidal M, Gifford DK, Young RA, Jaenisch R. Polycomb complexes repress developmental regulators in murine embryonic stem cells. *Nature* 2006; 441: 349-353.
222. Lee TI, Jenner RG, Boyer LA, Guenther MG, Levine SS, Kumar RM, Chevalier B, Johnstone SE, Cole MF, Isono K, Koseki H, Fuchikami T, Abe K, Murray HL, Zucker JP, Yuan B, Bell GW, Herbolzheimer E, Hannett NM, Sun K, Odom DT, Otte AP, Volkert TL, Bartel DP, Melton DA, Gifford DK, Jaenisch R, Young RA. Control of developmental

- regulators by Polycomb in human embryonic stem cells. *Cell* 2006; 125: 301-313.
223. Yoshida N, Amanai M, Fukui T, Kajikawa E, Brahmajosyula M, Iwahori A, Nakano Y, Shoji S, Diebold J, Hessel H, Huss R, Perry AC. Broad, ectopic expression of the sperm protein PLCZ1 induces parthenogenesis and ovarian tumours in mice. *Development* 2007; 134: 3941-3952.
  224. Kuroda K, Ito M, Shikano T, Awaji T, Yoda A, Takeuchi H, Kinoshita K, Miyazaki S. The role of X/Y linker region and N-terminal EF-hand domain in nuclear translocation and Ca<sup>2+</sup> oscillation-inducing activities of phospholipase C $\zeta$ , a mammalian egg-activating factor. *J Biol Chem* 2006; 281: 27794-27805.
  225. Agger K, Cloos PA, Christensen J, Pasini D, Rose S, Rappsilber J, Issaeva I, Canaani E, Salcini AE, Helin K. UTX and JMJD3 are histone H3K27 demethylases involved in HOX gene regulation and development. *Nature* 2007; 449: 731-734.
  226. Lan F, Bayliss PE, Rinn JL, Whetstine JR, Wang JK, Chen S, Iwase S, Alpatov R, Issaeva I, Canaani E, Roberts TM, Chang HY, Shi Y. A histone H3 lysine 27 demethylase regulates animal posterior development. *Nature* 2007; 449: 689-694.
  227. Swigut T, Wysocka J. H3K27 Demethylases, at Long Last. *Cell* 2007; 131: 29-32.
  228. De Santa F, Totaro MG, Prosperini E, Notarbartolo S, Testa G, Natoli G. The histone H3 lysine-27 demethylase Jmjd3 links inflammation to inhibition of polycomb-mediated gene silencing. *Cell* 2007; 130: 1083-1094.
  229. Xiang Y, Zhu Z, Han G, Lin H, Xu L, Chen CD. JMJD3 is a histone H3K27 demethylase. *Cell Res* 2007; 17: 850-857.
  230. Wu AT, Sutovsky P, Manandhar G, Xu W, Katayama M, Day BN, Park KW, Yi YJ, Xi YW, Prather RS, Oko R. PAWP, a sperm-specific WW domain-binding protein, promotes meiotic resumption and pronuclear development during fertilization. *J Biol Chem* 2007; 282: 12164-12175.
  231. Ostermeier GC, Miller D, Huntriss JD, Diamond MP, Krawetz SA. Reproductive biology: delivering spermatozoan RNA to the oocyte. *Nature* 2004; 429: 154.

MICHIGAN STATE UNIVERSITY LIBRARIES



3 1293 02956 3024